Journal of Medicinal Chemistry

pubs.acs.org/jmc Article

Evaluation of the Structure−Activity Relationship of Microtubule-Targeting 1,2,4-Triazolo[1,5-*a*]pyrimidines Identifies New Candidates for Neurodegenerative Tauopathies

Killian Oukoloff, Goodwell Nzou, Carmine Varricchio, Bobby Lucero, Thibault Alle, Jane Kovalevich, Ludovica Monti, Anne-Sophie Cornec, Yuemang Yao, Michael J. James, John Q. Trojanowski, Virginia M.-Y. Lee, Amos B. Smith, III, Andrea Brancale, Kurt R. Brunden,* and Carlo Ballatore*

Cite This: *J. Med. Chem.* 2021, 64, 1073−1102 Read Online

ACCESS | Metrics & More | Article Recommendations | Supporting Information

ABSTRACT: Studies in tau and Aβ plaque transgenic mouse models demonstrated that brain-penetrant microtubule (MT)-stabilizing compounds, including the 1,2,4-triazolo[1,5-*a*]-pyrimidines, hold promise as candidate treatments for Alzheimer's disease and related neurodegenerative tauopathies. Triazolopyrimidines have already been investigated as anticancer agents; however, the antimitotic activity of these compounds does not always correlate with stabilization of MTs in cells. Indeed, previous studies from our laboratories identified a critical role for the fragment linked at C6 in determining whether triazolopyrimidines promote MT stabilization or, conversely, disrupt MT integrity in cells. To further elucidate the structure−activity relationship (SAR) and to identify potentially improved MT-stabilizing candidates for neurodegenerative disease, a comprehensive set of 68 triazolopyrimidine congeners bearing structural modifications at C6 and/or C7 was designed, synthesized, and evaluated. These studies expand upon prior understanding of triazolopyrimidine SAR and enabled the identification of novel analogues that, relative to the existing lead, exhibit improved physicochemical properties, MT-stabilizing activity, and pharmacokinetics.

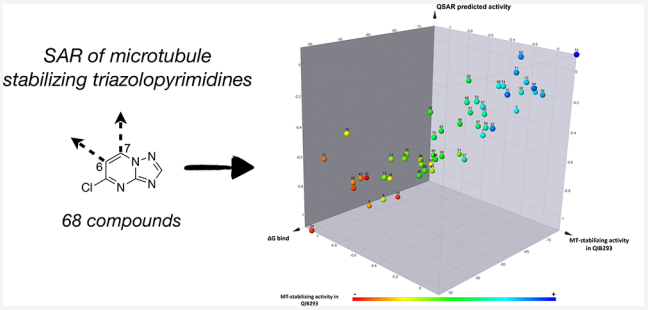

INTRODUCTION

In Alzheimer's disease (AD) and related neurodegenerative tauopathies,[1] the hyperphosphorylation of the microtubule (MT)-associated protein tau promotes its dissociation from MTs and eventual deposition into insoluble aggregates, which are commonly referred to as neurofibrillary tangles (NFTs) and neuropil threads (NTs). Reduced tau binding to MTs is believed to trigger alterations in the normal structure and dynamics of MTs in the axons of neurons that ultimately cause or contribute to impaired axonal transport and resulting axonal dystrophy.[2] Given the evidence of neuronal MT abnormalities in AD patients and in tau and Aβ plaque transgenic (Tg) mouse models,[3] CNS-active MT-stabilizing agents have been proposed as molecules that may provide therapeutic benefits in AD and related tauopathies.[4] Multiple preclinical studies[5−8] in tau Tg mice have shown that relatively low and infrequent doses of CNS-active MT-stabilizing natural products, such as epothilone D (**1**, Figure 1) and dictyostatin (**2**, Figure 1), can lead to significant improvements in several endpoints including an increase in MT density, a reduction in axonal dystrophy, and a significant lowering of both tau pathology and neuron loss.[5−7] More recently, brain-penetrant MT-stabilizing 1,2,4-triazolo[1,5-*a*]pyrimidines that are structurally simpler and are endowed with generally more favorable drug-like absorption, distribution, metabolism, and excretion-pharmacokinetics (ADME-PK) properties than MT-stabilizing natural products[9] have also shown promising results both *in vitro* and *in vivo*.[10−12] Although the MT binding site of the triazolopyrimidines is known to be different than that of taxol, epothilone D, and other taxane site binders,[13] evaluation of a selected prototype (**3**, Figure 1) in a mouse model of tauopathy revealed that this compound could exert similar beneficial effects to those previously observed with **1**, indicating that triazolopyrimidines hold promise as candidate treatments for neurodegenerative tauopathies.[12] More recently, **3** has also been shown to decrease axonal dystrophy, with a resulting reduction of Aβ peptide and Aβ plaque deposition in a Tg mouse model of senile plaque formation.[14]

Received: September 28, 2020
Published: January 7, 2021

https://dx.doi.org/10.1021/acs.jmedchem.0c01605
J. Med. Chem. 2021, 64, 1073−1102

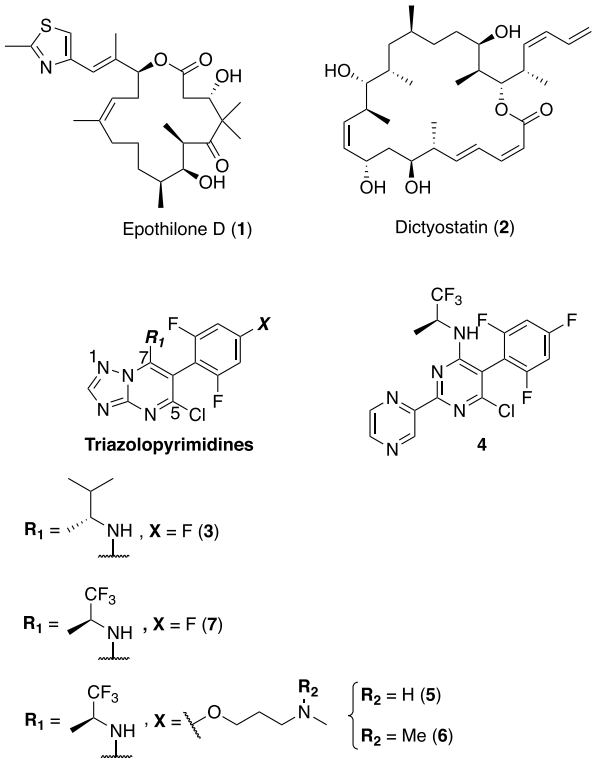

Figure 1. Structure of MT-stabilizing natural products, epothilone D and dictyostatin, and selected examples of MT-binding triazolopyrimidines and phenylpyrimidines.

MT-active triazolopyrimidines and structurally related phenylpyrimidines (*e.g.*, **4**) have already been evaluated as candidate treatments for cancer chemotherapy.[15,16] This effort, which culminated in the identification of cevipabulin (**5**) as a clinical candidate,[17,18] included a comprehensive assessment of the structure−activity relationship (SAR) in cytotoxicity assays that used rapidly dividing cancer cell-lines.[15] More recent studies from our laboratories suggested that the antimitotic activity of these compounds may not always correlate with stabilization of MTs in cells. Indeed, evaluation of representative examples of triazolopyrimidines and related phenylpyrimidines in cell-based assays of MT stabilization revealed that varying the scaffold (*i.e.*, triazolopyrimidine or phenylpyrimidine) or substitution pattern results in molecules that can either promote MT stabilization or, conversely, disrupt MT integrity.[11] For example, an evaluation of a selected set of triazolopyrimidines and phenylpyrimidines for their ability to produce elevations in known cellular markers of stable MTs,[19] such as acetylated and de-tyrosinated α-tubulin (AcTub and GluTub, respectively), revealed that typically the phenylpyrimidines, such as **4**, produce an unusual bell-shaped concentration−response curve in these assays. In addition, these compounds cause a concentration-dependent decrease in total cellular α- and β-tubulin resulting from proteasome-mediated degradation, with a visible reduction of MT networks. Interestingly, although similar observations were made for some triazolopyrimidines, including **5** and its brain-penetrant[10] congener **6** (Figure 1), replacement of the alkoxide side-chain of these molecules with a fluorine atom, as in **7** (Figure 1) or **3**, had a dramatic impact on the MT-stabilizing properties of the compounds as demonstrated by the fact that the latter molecules caused the desired linear concentration-dependent increase in MT stabilization and MT mass in cells over the tested concentrations without decreased cellular tubulin levels or changing MT morphology.[11] These findings, combined with the observation that the amine fragment linked at C7 of lead compound, **3**, is likely to be the primary site of metabolism,[12] led to a more systematic exploration of the SAR of triazolopyrimidines modified at C6 and C7. The results from these studies led to the identification of selected congeners that, relative to the existing lead, **3**, exhibit improved physicochemical properties, MT-stabilizing activity, and pharmacokinetics.

Scheme 1[a]

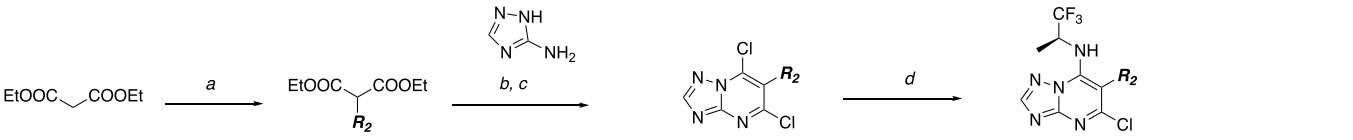

R_2 = phenyl (**76**)
R_2 = 4-fluorophenyl (**77**)
R_2 = 2-fluorophenyl (**78**)
R_2 = 2,4-difluorophenyl (**79**)
R_2 = 2,6-difluorophenyl (**80**)
R_2 = 3,5-difluorophenyl (**81**)
R_2 = 2,5-difluorophenyl (**82**)
R_2 = 3,4-difluorophenyl (**83**)
R_2 = 2,3,4-trifluorophenyl (**84**)
R_2 = 2,4,6-trifluorophenyl (**85**)
R_2 = 2,4,6-trifluorobenzyl (**86**)
R_2 = 2,6-difluoro-4-methylphenyl (**87**)
R_2 = 2,6,-difluoro-4-trifluoromethylphenyl (**88**)
R_2 = 2,6-difluoro-4-cyanophenyl (**89**)
R_2 = 2-fluoro-4-cyanophenyl (**90**)
R_2 = 2,6-difluoro-4-chlorophenyl (**91**)
R_2 = 2,6-difluoro-4-nitrophenyl (**92**)

R_2 = phenyl (**93**)
R_2 = 4-fluorophenyl (**94**)
R_2 = 2-fluorophenyl (**95**)
R_2 = 2,4-difluorophenyl (**96**)
R_2 = 2,6-difluorophenyl (**97**)
R_2 = 3,5-difluorophenyl (**98**)
R_2 = 2,5-difluorophenyl (**99**)
R_2 = 3,4-difluorophenyl (**100**)
R_2 = 2,3,4-trifluorophenyl (**101**)
R_2 = 2,4,6-trifluorophenyl (**102**)
R_2 = 2,4,6-trifluorobenzyl (**103**)
R_2 = 2,6-difluoro-4-methylphenyl (**104**)
R_2 = 2,6-difluoro-4-trifluoromethylphenyl (**105**)
R_2 = 2,6-difluoro-4-cyanophenyl (**106**)
R_2 = 2-fluoro-4-cyanophenyl (**107**)
R_2 = 2,6-difluoro-4-chlorophenyl (**108**)
R_2 = 2,6-difluoro-4-nitrophenyl (**109**)

R_2 = 2,4,6-trifluorophenyl (**7**)
R_2 = phenyl (**8**)
R_2 = 4-fluorophenyl (**9**)
R_2 = 2-fluorophenyl (**10**)
R_2 = 2,4-difluorophenyl (**11**)
R_2 = 2,6-difluorophenyl (**12**)
R_2 = 3,5-difluorophenyl (**13**)
R_2 = 2,5-difluorophenyl (**14**)
R_2 = 3,4-difluorophenyl (**15**)
R_2 = 2,3,4-trifluorophenyl (**16**)
R_2 = 2,4,6-trifluorobenzyl (**17**)
R_2 = 2,6-difluoro-4-methylphenyl (**18**)
R_2 = 2,6-difluoro-4-trifluoromethylphenyl (**19**)
R_2 = 2,6-difluoro-4-cyanophenyl (**20**)
R_2 = 2,6-difluoro-4-chlorophenyl (**21**)
R_2 = 2,6-difluoro-4-nitrophenyl (**22**)
R_2 = 2,6-difluoro-4-aminophenyl (**23**)

[a]Reagents and reaction conditions: (a) For **76**−**85**, **87**−**89**, **91**: Ar-X, CuBr, NaH, 1,4-dioxane, 60−100 °C, 12 h, 19−74%; For **86**: Ar-CH_2Br, NaH, DMF, 0 °C, 1 h, 90%; For **90** and **92**: Ar-F, K_2CO_3, DMF, 60 °C, 4 h, 84−86%; (b) *N*-tributylamine, 170−180 °C, 2−6 h; (c) phosphorus oxychloride, 110−130 °C, 6−16 h, 46−58% over two steps; (d) appropriate amine, DMF, rt−90 °C, 1−18 h, 12−50%; (e) Fe, NH_4Cl, H_2O/MeOH (40/50), 80 °C, 2 h, 69%.

https://dx.doi.org/10.1021/acs.jmedchem.0c01605
J. Med. Chem. 2021, 64, 1073−1102

Scheme 2[a]

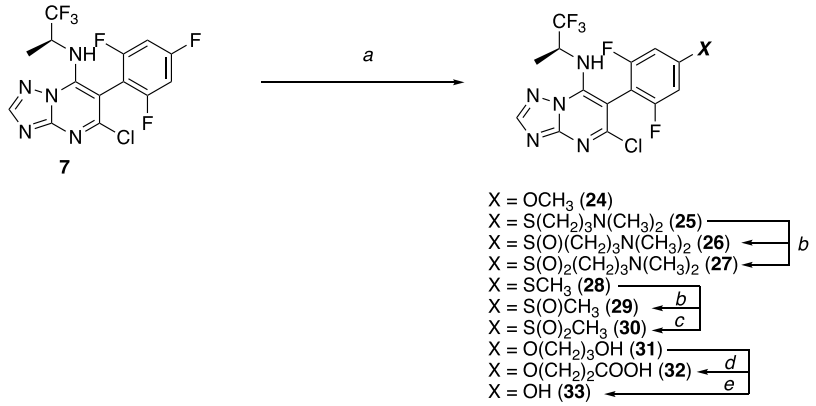

[a]Reagents and reaction conditions: (a) For **24**: NaOMe, THF, 0 to 60 °C, 14 h, 71%; For **25**, **31**: ROH or RSH, NaH, DMSO, 60 °C, 3 h, 81−95%; for **28**: CH_3SNa, DMSO, 60 °C, 3 h, quant; (b) *m*-CPBA (1 equiv), CH_2Cl_2, 20 °C, 2 h, 32% of **26**, 52% of **27**, 70% of **29**; (c) *m*-CPBA (3 equiv), CH_2Cl_2, 20 °C, 3 h, 71%; (d) TEMPO, BAIB, CH_2Cl_2/H_2O (90/70), 20 °C, 2 h, 59%; (e) LiOH, $MeOH/H_2O$ (1/1), 20 °C, 16 h, 39%.

CHEMISTRY

As part of these studies, a total of 68 compounds (**7**−**75**, Schemes 1-5) have been synthesized and tested, including eight previously described triazolopyrimidines (*i.e.*, **7**,[15] **11**,[15] **25**,[15] **31**−**33**,[20] **34**,[12] and **54**[13]); 23 compounds exemplified in the patent literature (*i.e.*, **10**, **12**, **14**, **16**, **18**, **24**, **28**−**30**, **35**, **41**, **45**−**48**, **50**, **51**, **52**, **57**, **60**, **61**, **64**, **65**); and 37 structurally novel congeners. In all cases, the triazolopyrimidine ring was accessed via cyclocondensation reaction between the appropriate diethylmalonate (**76**−**92**, Scheme 1) and 1*H*-1,2,4-triazol-5-amine. Next, treatment with phosphorous oxychloride provided the corresponding 5,7-dichloro triazolopyrimidines (**93**−**109**, Scheme 1). Chemoselective amination at C7 with (*S*)-1,1,1-trifluoropropan-2-amine furnished triazolopyrimidines **7**−**22** (Scheme 1). Reduction of the para nitro derivative **22** provided the corresponding aniline derivative **23** (Scheme 1).

Triazolopyrimidine **7** was then used to access additional derivatives bearing different substitutions at the para position of the fluorinated phenyl ring (**24**−**33**, Scheme 2). In these cases, the installation of the appropriate alcohol or thiol side-chain was conducted via S_NAr followed by HPLC purification of the final product. Sulfoxide (**26**, **29**) and sulfone (**27**, **30**) derivatives were obtained from the corresponding thioethers (*i.e.*, **25**, and **28**, respectively) upon treatment with *meta*-chloroperbenzoic acid (*m*-CPBA) (Scheme 2).

Triazolopyrimidine dichloride **102** was used to access a series of congeners modified at position C7 (*i.e.*, **34**−**61**, Scheme 3). In these cases, chemoselective displacement of the chloro substituent at C7 was accomplished in moderate to good yields by treating **102** with the appropriate amine. The synthesis of C7 alkyl derivative **62** (Scheme 4) was initially attempted adopting a known procedure[21] by reacting dichloride **102** with the methyl ester of 4,4,4-trifluoro-3-methylbutanoic acid in the presence of LiHMDS to obtain **110**, followed by a Krapcho decarboxylation.[22] The main product isolated from this synthesis was the tetracyclic compound **111** (Scheme 4) whose structure was confirmed

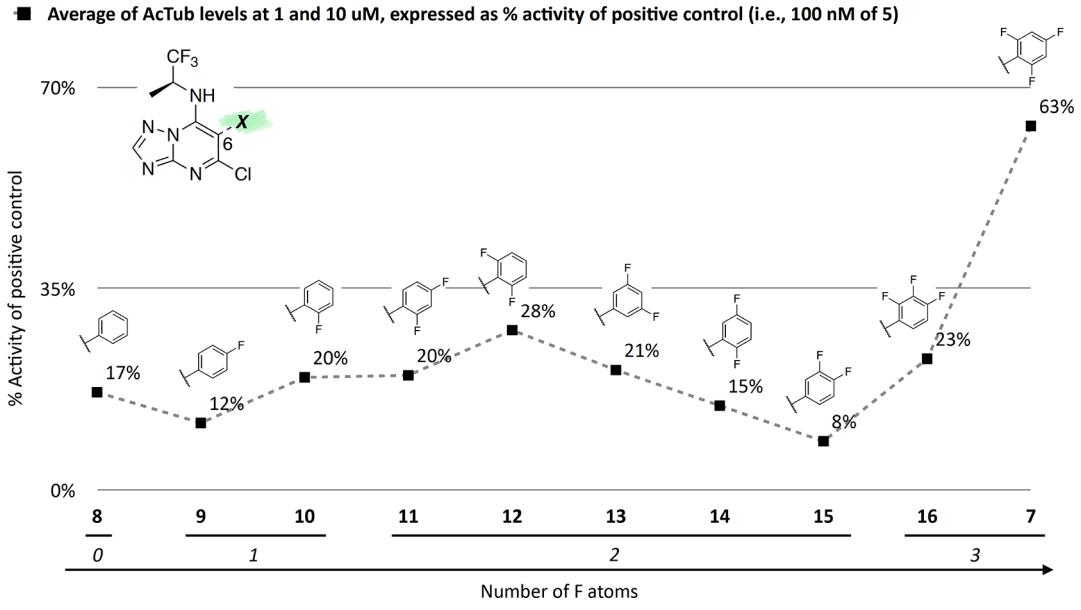

Figure 2. Effect of fluorination of the aryl group at C6 on MT-stabilizing activity of Class I triazolopyrimidines. Black squares indicate the average activity of test compounds at 1 and 10 μM, normalized to the activity of 100 nM of **5** (positive control).

https://dx.doi.org/10.1021/acs.jmedchem.0c01605
J. Med. Chem. 2021, 64, 1073−1102

Scheme 3[a]

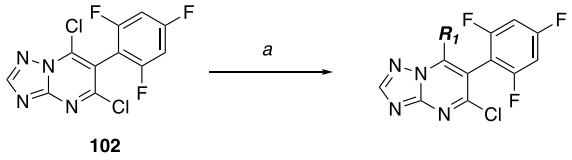

R_1 = NH_2 (**34**)
R_1 = NH*i*Pr (**35**)
R_1 = $NH(CH_2)_2CH_3$ (**36**)
R_1 = NH*i*Bu (**37**)
R_1 = OH (**38**)

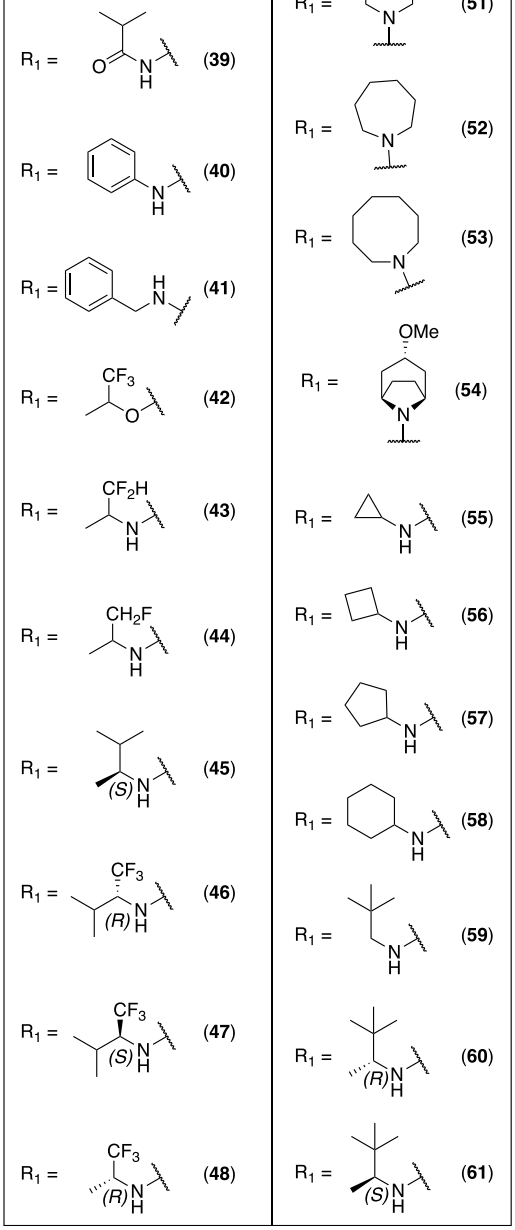

[a]Reagents and reaction conditions: (a) appropriate amine, base, DMF, 20−90 °C, 1−18 h, 12−50%.

by X-ray crystallography. The desired compound **62** was ultimately obtained employing a similar approach in which alkylation reaction at C7 was conducted using the *tert*-butyl ester of 4,4,4-trifluoro-3-methylbutanoic acid to obtain intermediate **112**, which was then subjected to TFA-mediated cleavage of the ester moiety and *in situ* decarboxylation (Scheme 4).

Finally, the synthesis of compounds **63**−**75** (Scheme 5) was conducted by reacting the appropriate triazolopyrimidine dichlorides (*i.e.*, **95**, **97**, **106**, or **107**) with amine fragments (Scheme 5). In selected cases (*i.e.*, **67** and **68**), purification via silica gel column chromatography afforded individual atropoisomers, the structures of which could be determined via single crystal X-ray structure determination of **68** (Scheme 5).

RESULTS

All test compounds were evaluated in a previously described[11] cell-based assay of MT-stabilization, in which compound-dependent changes in tubulin polymerization and total tubulin levels were determined after 4 h of incubation of QBI293 cells with 1 and 10 μM compound via quantification of acetylated α-tubulin (AcTub) and total α-tubulin (α-Tub) in cell lysates by ELISA. Although the changes in AcTub levels of compound-treated cells relative to DMSO-treated cells provide a valid assessment of the MT-stabilizing activity of test compounds, day-to-day differences in the responsiveness of cells to MT-stabilizing treatment can result in occasional variability in the fold-change in AcTub levels. Thus, to account for this variability and ultimately enable a ranking of different triazolopyrimidines based on MT-stabilizing activity, compound-dependent changes in AcTub levels relative to DMSO-treated cells (*i.e.*, negative control) were also normalized to the corresponding changes caused by 100 nM of cevipabulin (**5**), which was routinely used as positive control.[10]

Previous evaluations of the MT-stabilizing activity of selected examples of triazolopyrimidines in this assay suggested that the nature of the substituent in the para position of the fluorinated phenyl can elicit one of two distinct cellular responses: one characterized by a linear concentration-dependent increase of markers of stable MTs (*i.e.*, acetylated- and detyrosinated-α-tubulin) with no effect on total tubulin levels at tested concentrations, which is typically observed with triazolopyrimidines such as **3** and **7**, and a second response caused by compounds bearing the alkoxy side-chain (*e.g.*, **5** and **6**) that is characterized by a proteasome-dependent degradation of tubulin that is often associated with the appearance of a bell-shaped concentration−response relationship in the AcTub assay.[11] To facilitate the presentation and discussion of the SAR results, we will refer here to these two distinct cellular responses as "Class I" and "Class II", respectively, and triazolopyrimidines **7** and **6** are used as defining examples of these classes.

As the replacement of the alkoxy side-chain of **5** or **6** (Class II) with a fluorine atom (as in **7**, Class I) was found to produce a profound impact on the MT-stabilizing activity of the triazolopyrimidine compounds,[11] our investigations of SARs began by synthesizing and testing selected analogues (**18**−**33**, Table 1) that could help identify specific stereoelectronic characteristics of the substituent in the para position of the fluorinated phenyl ring that may be necessary/sufficient to impart Class I activity. Evaluation of these compounds in the QBI293 assay of MT-stabilization revealed a possible general trend, indicating that active congeners bearing electron-donating groups at the para position generally elicit a significant (*i.e.*, >15%) loss of α-Tub levels when tested at

https://dx.doi.org/10.1021/acs.jmedchem.0c01605
J. Med. Chem. 2021, 64, 1073−1102

Scheme 4[a]

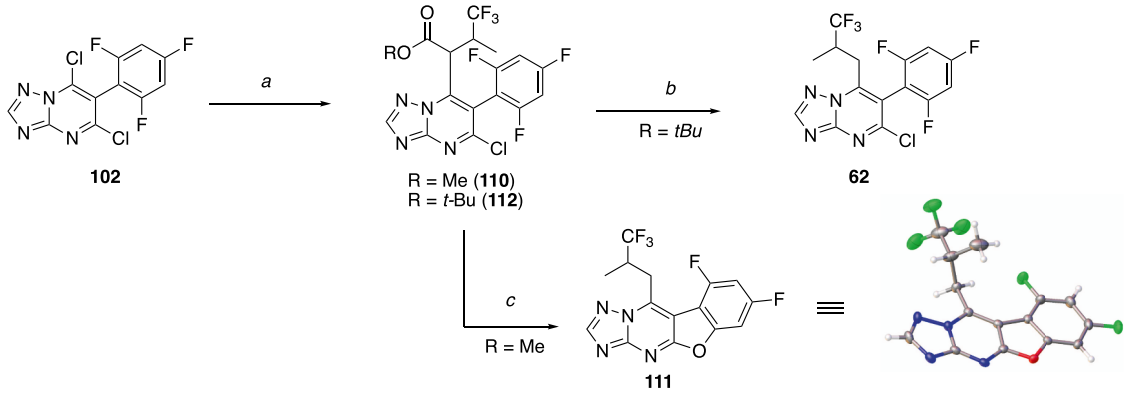

[a]Reagents and reaction conditions: (a) appropriate ester of 4,4,4-trifluoro-3-methylbutanoic acid, HMDS, *n*-BuLi, THF, −78 °C, 2.5 h, 70% for **110**, 25% for **112**; (b) TFA, CH_2Cl_2, 20 °C, 16 h, 68%; (c) LiCl, DMSO, 130 °C (microwave irradiation), 3 h, 76%.

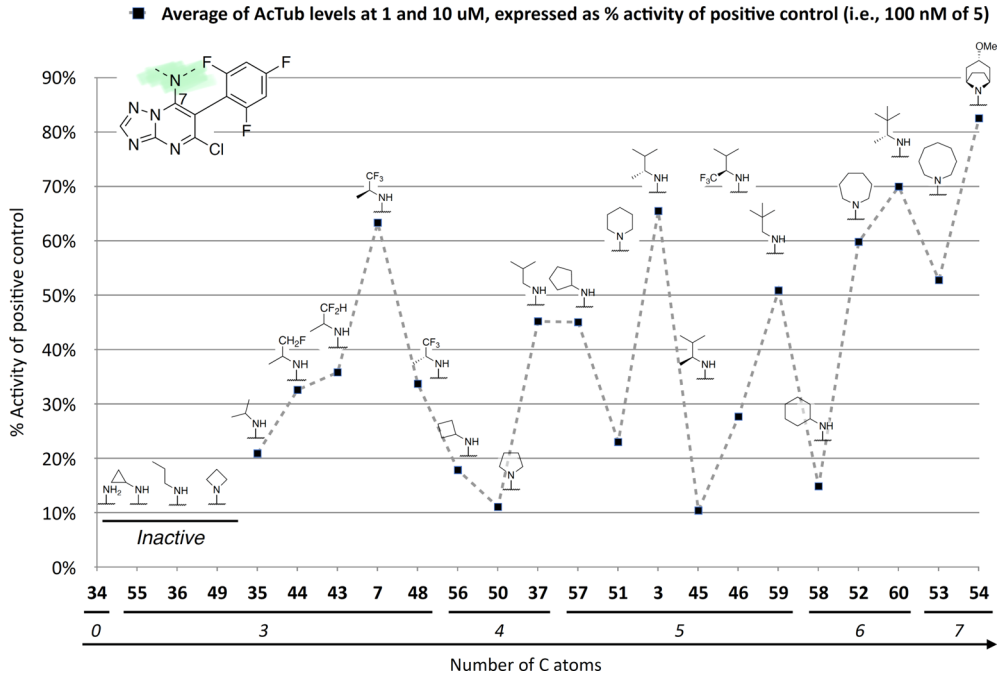

Figure 3. Effect of both branching of aliphatic acyclic amines and homologation of endo- and exo-cyclic amines on MT-stabilizing activity of Class I triazolopyrimidines. Test compounds are ordered along the X-axis based on the number of carbon atoms in the amine fragment. Black squares indicate the average activity of test compounds at 1 and 10 μM, normalized to the activity of 100 nM of **5** (positive control). Compounds that did not produce a statistically significant elevation in AcTub at either 1 or 10 μM are not plotted and marked as inactive.

either 1 and/or 10 μM concentration, which is characteristic of Class II compounds. For example, both *para* hydroxyl- (**33**) and methoxy- (**24**) derivatives as well as thioalkyl compounds, **25** and **28**, were all found to produce >20% reduction in cellular α-Tub. In contrast, active analogues bearing electron-withdrawing groups, such as cyano (**20**) and nitro (**22**), were found to increase AcTub levels without producing a significant reduction in α-Tub levels (*i.e.*, Class I phenotype). However, in cases such as **21**, where the chloro substituent produces opposite mesomeric (+M) and inductive (−I) effects, a comparatively more moderate but still significant loss of α-Tub (19%) was observed when the compound was tested at a 10 μM concentration. These results indicate that the electronic properties of the substituent in para may play an important role in determining the phenotypic response. However, differences in the shape/volume and/or the geometry of hydrogen bonding of the substituent can modulate significantly the MT-stabilizing activity, independent of the phenotype. This is best represented by comparing selected pairs of compounds, such as nitrile (**20**) and sulfone (**30**), or alkyl-sulfone (**27**) and the corresponding alkoxy compound (**6**). Docking studies (*vide infra*) indicate that the larger volume of the sulfone moiety is likely to affect negatively the interaction of the triazolopyrimidine with the binding site.

To investigate the effect of the degree and pattern of fluorination of the phenyl ring at C6, compounds **8**−**16** were evaluated in comparison with a Class I control compound, **7**. The results of these studies, summarized in Table 1 and Figure 2, show that all compounds within this series maintain MT-stabilizing activity that is qualitatively similar to **7** (*i.e.*, all compounds elicit Class I phenotype); however, depending on the number and position of the fluorine atoms, these

https://dx.doi.org/10.1021/acs.jmedchem.0c01605
J. Med. Chem. 2021, 64, 1073−1102

Scheme 5[a]

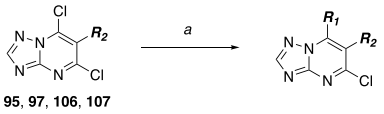

95, 97, 106, 107

Cpd #	R_1	R_2
63		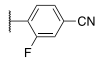
64		
65		
66		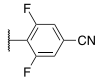
67		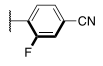
68		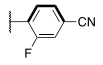
	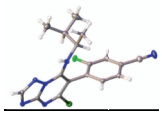	
69		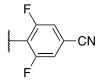
70		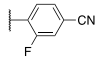
71		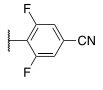
72		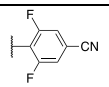
73		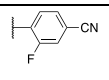
74		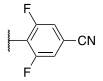
75		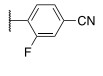

[a]Reagents and reaction conditions: (a) appropriate amine, DMF, rt, 1 h, 56−86%.

triazolopyrimidine congeners can differ significantly in terms of potency. In general, the Class I MT-stabilizing activity appears to increase with the number of fluorine atoms in the ring, with a preferred arrangement within the series being 2,4,6-trifluorophenyl (Figure 2). Among derivatives bearing a mono-fluorinated phenyl fragment at C6, the ortho fluoro derivative (**10**) appeared to be more active than the corresponding para substituted compound (**9**) at both 1 and 10 μM concentrations. Similarly, among triazolopyrimidines bearing a di-fluorinated phenyl at C6 (**11**−**15**), the 2,6-difluoro compound (**12**) was found to be the most active. Finally, homologation of the 2,4,6-trifluorophenyl of **7** to the corresponding 2,4,6-trifluorobenzyl congener (**17**) led to a drastic reduction of MT-stabilizing activity.

Comparative evaluation of Table 2 compounds (**3**, **34**−**62**) and **7** in the cell-based MT-stabilization assay helped define several SAR elements of the fragment linked at the C7 position of the triazolopyrimidine ring. Truncation of this fragment as in **34** and **38** led to a dramatic loss of MT-stabilizing activity. Replacement of the nitrogen atom at C7 of control compound, **7**, with an oxygen atom (**42**) revealed that the ether linkage is not permitted as it resulted in a drastic reduction of activity in the cellular assay. Conversely, replacement of the nitrogen atom at C7 with a methylene, as in **62**, showed that the alkyl linkage allows for retention of significant activity in the AcTub assay at both 1 and 10 μM. However, this compound was found to cause a significant reduction of α-Tub (*i.e.*, ∼22%) when tested at 10 μM. These observations demonstrate that the nature of the fragment linked at C7 can play an important role in determining both potency and cellular phenotype elicited by MT-active triazolopyrimidines and that the presence of a substituted nitrogen at this position may be a necessary condition for Class I activity.

Further investigation of the SAR of triazolopyrimidines featuring a substituted nitrogen at C7 included a comparison between selected aliphatic and aromatic amines as well as amides. Comparison of lead compound **3** with amide derivative, **39**, indicates that aliphatic amines may be preferred over amides. Similarly, comparison of aniline derivative, **40**, with the corresponding cyclohexyl amine congener, **58**, shows that whereas the former is essentially devoid of activity at both 1 and 10 μM, the aliphatic derivative, **58**, is significantly active at 10 μM without decreasing α-Tub levels. These results suggest that aliphatic amines at C7 may be generally preferred and, as a result, further exploration of the SAR focused on identifying the key requisites of the aliphatic amine fragment, which included an evaluation of linear, branched, and cyclic amines of different sizes. Comparison of the *in vitro* MT-stabilizing activity of lead compound, **3**, with congeners featuring amine substituents at C7 that are either substructures (*i.e.*, **35**−**37**) or that are incrementally larger fragments than the C7 substituent of **3** (*e.g.*, **60**) clearly suggests that the MT-stabilizing activity of triazolopyrimidines may increase with the size and branching of the aliphatic fragment. As highlighted in Figure 3, the extreme examples within this series are the linear amine derivative, **36**, which is devoid of MT-stabilizing activity in the QBI293 assay, and the *t*-butyl derivative, **60**, which exhibits relatively potent activity as revealed by the marked increases in AcTub levels at both 1 and 10 μM concentrations. A similar trend also emerges from the comparison of series of homologues featuring different endo- (*i.e.*, **49**−**54**) or exo-cyclic (*i.e.*, **55**−**58**) amines. Within each of these series, relatively bulky fragments led to marked elevations of AcTub

https://dx.doi.org/10.1021/acs.jmedchem.0c01605
J. Med. Chem. 2021, 64, 1073−1102

Table 1. MT-Stabilizing Activity of Triazolopyrimidines Modified at C6[a]

Cpd #	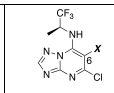	*AcTub*		*α-Tub*		*Class*[a]
		1 μM	*10 μM*	*1 μM*	*10 μM*	
6	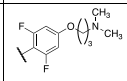	13.2 ± 1.8** (1.28)	1.92 ± 0.14 (0.19)	0.74 ± 0.05**	0.40 ± 0.01**	II
7		2.78 ± 0.17** (0.45)	5.04 ± 0.45** (0.82)	1.18 ± 0.09	1.22 ± 0.18	I
8		1.11 ± 0.04 (0.12)	2.07 ± 0.10** (0.30)	1.09 ± 0.03	1.03 ± 0.02	I
9		1.05 ± 0.05 (0.07)	2.41 ± 0.13** (0.16)	1.04 ± 0.06	1.13 ± 0.06	I
10		1.73 ± 0.02* (0.13)	3.56 ± 0.08** (0.26)	1.09 ± 0.01	1.05 ± 0.06	I
11		1.54 ± 0.05 (0.13)	3.19 ± 0.18** (0.27)	0.99 ± 0.02	0.86 ± 0.01	I
12		2.20 ± 0.13 (0.16)	5.28 ± 0.54** (0.39)	1.06 ± 0.14	1.02 ± 0.04	I
13		1.52 ± 0.074 (0.12)	3.97 ± 0.82* (0.30)	1.12 ± 0.13	1.12 ± 0.02	I
14		1.40 ± 0.38 (0.07)	4.10 ± 0.44* (0.22)	1.05 ± 0.11	0.90 ± 0.06	I
15		1.85 ± 0.09 (0.05)	4.76 ± 0.62** (0.12)	1.01 ± 0.08	1.13 ± 0.06	I
16		1.50 ± 0.03 (0.12)	4.28 ± 0.33** (0.34)	1.11 ± 0.05	0.88 ± 0.04	I
17		1.26 ± 0.06 (0.09)	1.43 ± 0.02 (0.10)	1.01 ± 0.07	1.05 ± 0.04	NA
18		1.62 ± 0.18** (0.28)	2.73 ± 0.18** (0.48)	0.99 ± 0.09	0.78 ± 0.07*	II
19		1.09 ± 0.04 (0.13)	1.39 ± 0.11* (0.16)	1.06 ± 0.02	1.02 ± 0.03	I
20		1.90 ± 0.06* (0.27)	3.56 ± 0.31** (0.51)	0.94 ± 0.02	0.95 ± 0.05	I
21		1.88 ± 0.03** (0.31)	4.28 ± 0.17** (0.70)	0.93 ± 0.02	0.81 ± 0.06**	II
22		3.24 ± 0.36** (0.60)	6.65 ± 0.45** (1.23)	0.96 ± 0.01	0.94 ± 0.05	I
23		0.94 ± 0.27 (0.17)	0.69 ± 0.37 (0.13)	0.97 ± 0.03	0.96 ± 0.02	NA
24		3.16 ± 0.29** (0.64)	2.07 ± 0.07** (0.42)	0.72 ± 0.09**	0.51 ± 0.05**	II
25	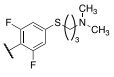	3.90 ± 0.66** (0.90)	1.49 ± 0.48 (0.34)	0.83 ± 0.05*	1.07 ± 0.02	II

https://dx.doi.org/10.1021/acs.jmedchem.0c01605
J. Med. Chem. 2021, 64, 1073−1102

Table 1. continued

Cpd #		AcTub		α-Tub		Class[a]
		1 μM	10 μM	1 μM	10 μM	
26	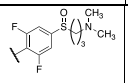	1.49 ± 0.48 (0.34)	1.39 ± 0.11 (0.32)	1.22 ± 0.06	0.98 ± 0.24	NA
27	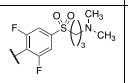	1.13 ± 0.10 (0.24)	1.08 ± 0.11 (0.23)	0.70 ± 0.58	1.07 ± 0.07	NA
28		1.75 ± 0.37* (0.27)	2.23 ± 0.15** (0.35)	0.88 ± 0.05*	0.56 ± 0.06**	II
29		0.84 ± 0.21 (0.21)	0.87 ± 0.21 (0.21)	0.96 ± 0.02	0.93 ± 0.03	NA
30		1.21 ± 0.38 (0.19)	1.23 ± 0.37 (0.19)	1.03 ± 0.02	1.02 ± 0.04	NA
31		7.25 ± 0.23** (1.34)	1.33 ± 0.15 (0.25)	0.73 ± 0.06**	0.37 ± 0.02**	II
33		1.22 ± 0.73 (0.23)	4.11 ± 0.76** (0.77)	0.84 ± 0.07	0.57 ± 0.02**	II

[a]Fold-changes in AcTub and total α-Tub levels in QBI293 cells after 4 h of incubation with test compounds at either 1 or 10 μM. Reported values for AcTub and α-Tub represent the fold-change over control (DMSO)-treated cells (*$p < 0.05$ and **$p < 0.01$ by one-way ANOVA); numbers in parentheses represent the fold-change of AcTub over positive control-treated cells (*i.e.*, 100 nM of **5**). [b]Class I compounds are those producing a concentration-dependent increase in AcTub levels and that do not cause >15% reduction in α-Tub at either concentration; Class II compounds are those that cause >15% decrease in α-Tub at either 1 or 10 μM compound concentration. NA = not applicable as the test compound does not cause significant changes in AcTub or total α-Tub when tested at a 1 or a 10 μM concentration.

levels. However, comparison of the average MT-stabilizing activity at 1 and 10 μM, relative to the positive control, suggested that the optimal ring size in the endo- and exo-cyclic amine series may be different. Whereas in the exocyclic amine series, the five-membered ring (**57**) seemed optimal, in the case of endocyclic amines, the presence of a seven-membered ring system (**52**) or a fused bicyclic system (**54**) produced the highest activity (Figure 3). Finally, an evaluation of the effect of fluorination and chiral configuration of the branched amine fragment at C7 was also conducted. Comparison of **7**, which features a fluorinated isopropyl amine at C7, with corresponding analogues **43**, **44**, and **35** that exhibit either 2, 1, or no fluorine substituents in the amine fragment indicates the general trend linking the degree of fluorination of the amine fragment with potency. Similarly, fluorination of **45** resulted in a comparatively more potent congener (**46**). With respect to the chiral configuration, in the majority of cases examined, the chirality of the amine was found to influence the potency of the compound with one enantiomer being typically more active than the other (*cf.*, **3** and **45**; **7** and **48**; **60** and **61**). In one case, however, the chiral configuration of the amine substituent of **46** (*R*) and **47** (*S*) was also found to impact significantly the cellular phenotype. Whereas the *R*-enantiomer was found to be relatively potent in the AcTub QBI293 assay without evidence of a reduction in α-Tub levels, the opposite enantiomer (*S*) produced a marked reduction in cellular α-Tub of approximately ∼39% when tested at 10 μM, suggesting that **47** is likely to negatively impact MT integrity. Notwithstanding this notable exception, all other MT-active triazolopyrimidines shown in Table 2 that feature an amine fragment at C7 were found to be MT-stabilizing without producing losses in α-Tub.

Having identified the main characteristics of both the C6 and C7 fragments that may be required to obtain Class I MT-stabilizing triazolopyrimidines, a focused series of derivatives was designed by combining the most promising C6 and C7 fragments. In particular, as the C6 fragment SAR studies highlighted the importance of a fluorine atom in the ortho position of the phenyl ring, whereas the para position may be left unsubstituted or occupied by an electron-withdrawing group, such as a fluorine, a nitro, or a nitrile, we chose, in addition to the 2,4,6-trifluorophenyl fragment, the corresponding 2-fluoro-, 2,6-difluoro-, 2-fluoro-4-cyano-, and 2,6-difluoro-4-cyano-phenyl C6 fragments. Similarly, among the amine fragments at C7, all instances matched by molecular pair analysis that were found to produce comparable or better activity than **3** (*i.e.*, **7**, **52**−**54** and **60**) were selected. By systematically combining the preferred set of C6 and C7 fragments, a panel of 25 compounds could be designed that based on SAR findings would be expected to exhibit relatively potent Class I MT-stabilizing activity. As summarized in Table 3, several examples (13) from this set were synthesized and tested. In all cases, these compounds were confirmed to be active Class I triazolopyrimidines. Nine analogues exhibited comparable (*i.e.*, **66**, **67**, **73**, and **74**) or improved (*i.e.*, **64**, **69** and **70**−**72**) *in vitro* potency compared to lead compound **3**, with **72** being particularly effective in the AcTub assay when tested at either 10 or 1 μM. Evaluation of individual atropoisomers, **67** and **68**, indicated that the former may be more potent than the latter. Among derivatives bearing

https://dx.doi.org/10.1021/acs.jmedchem.0c01605
J. Med. Chem. 2021, 64, 1073−1102

Table 2. MT-Stabilizing Activity of Triazolopyrimidines Modified at C7[a]

Cpd #		*AcTub*		*α-Tub*		*Class*[b]
		1 μM	*10 μM*	*1 μM*	*10 μM*	
3		2.14 ± 0.15* (0.59)	2.57 ± 0.15* (0.71)	1.10 ± 0.17	0.90 ± 0.16	I
34		1.18 ± 0.01 (0.09)	1.12 ± 0.08 (0.08)	1.08 ± 0.07	1.05 ± 0.02	NA
35		1.15 ± 0.15 (0.15)	2.01 ± 0.17** (0.27)	0.92 ± 0.10	0.98 ± 0.03	I
36		1.15 ± 0.07 (0.27)	1.14 ± 0.14 (0.26)	1.14 ± 0.23	0.86 ± 0.24	NA
37		1.63 ± 0.14** (0.38)	2.28 ± 0.17** (0.53)	1.30 ± 0.04	0.99 ± 0.25	I
38		1.04 ± 0.04 (0.17)	1.03 ± 0.08 (0.17)	1.06 ± 0.03	1.02 ± 0.05	NA
39		1.09 ± 0.01 (0.07)	1.31 ± 0.47 (0.09)	1.00 ± 0.03	0.97 ± 0.07	NA
40		1.14 ± 0.26 (0.09)	1.05 ± 0.06 (0.08)	1.10 ± 0.17	0.96 ± 0.01	NA
41		1.05 ± 0.16 (0.16)	1.49 ± 0.04* (0.22)	1.00 ± 0.12	1.06 ± 0.06	I
42		0.91 ± 0.04 (0.19)	1.01 ± 0.07 (0.21)	1.03 ± 0.04	1.04 ± 0.05	NA
43		1.28 ± 0.09 (0.30)	1.82 ± 0.10** (0.35)	1.19 ± 0.13	1.17 ± 0.01	I
44		1.32 ± 0.26 (0.30)	1.50 ± 0.09* (0.35)	0.92 ± 0.12	1.09 ± 0.03	I
45		1.32 ± 0.14 (0.06)	3.49 ± 0.07** (0.15)	0.95 ± 0.01	0.89 ± 0.01*	I
46		3.12 ± 0.25** (0.17)	6.78 ± 0.18** (0.38)	1.04 ± 0.01	1.06 ± 0.01	I
47		2.79 ± 0.04** (0.16)	13.0 ± 0.54** (0.73)	1.10 ± 0.09	0.61 ± 0.02**	II
48		1.39 ± 0.11 (0.24)	2.47 ± 0.10* (0.43)	1.23 ± 0.21	1.47 ± 0.06*	I
49		0.98 ± 0.07 (0.26)	1.22 ± 0.02* (0.32)	0.96 ± 0.07	1.17 ± 0.05	I
50		1.14 ± 0.37 (0.07)	2.74 ± 0.23* (0.16)	1.12 ± 0.31	1.18 ± 0.10	I
51		2.21 ± 0.36 (0.13)	5.84 ± 1.38** (0.33)	1.23 ± 0.05	1.20 ± 0.22	I
52		4.16 ± 0.97** (0.45)	6.87 ± 0.04** (0.74)	0.99 ± 0.03	0.99 ± 0.04	I
53		3.70 ± 0.32** (0.36)	7.16 ± 0.11** (0.70)	1.01 ± 0.14	1.28 ± 0.03**	I
54		3.65 ± 0.15** (0.54)	7.43 ± 0.93** (1.11)	1.12 ± 0.08	1.38 ± 0.19**	I
55		1.17 ± 0.15 (0.07)	1.27 ± 0.06 (0.07)	1.20 ± 0.03	1.26 ± 0.03	NA
56		0.97 ± 0.15 (0.13)	1.75 ± 0.03** (0.23)	0.94 ± 0.01	0.95 ± 0.02	I
57		2.03 ± 0.04* (0.27)	4.83 ± 0.04** (0.45)	1.03 ± 0.02	0.98 ± 0.02	I
58		1.13 ± 0.11 (0.07)	3.51 ± 0.19** (0.23)	1.07 ± 0.05	0.99 ± 0.05	I
59		2.04 ± 0.11* (0.30)	4.79 ± 0.74** (0.71)	1.03 ± 0.07	1.06 ± 0.08	I
60		5.70 ± 0.27** (0.56)	8.42 ± 0.20** (0.83)	0.97 ± 0.02	1.08 ± 0.03	I
61[c]		3.36 ± 0.13** (10 μM) (0.43)	4.29 ± 0.04** (30 μM) (0.55)	1.08 ± 0.05 (10 μM)	1.22 ± 0.03 (30 μM)	I
62		2.30 ± 0.59* (0.53)	2.29 ± 0.38* (0.53)	1.03 ± 0.07	0.78 ± 0.05	II

[a]Fold-changes in AcTub and α-Tub levels in QBI293 cells after 4 h of incubation with test compounds at either 1 or 10 μM. Reported values for AcTub and α-Tub represent the fold-change over control (DMSO)-treated cells (*p < 0.05 and **p < 0.01 by one-way ANOVA); numbers in parentheses represent the fold-change of AcTub over positive control-treated cells (*i.e.*, 100 nM of **5**). [b]Class I compounds are those producing a concentration-dependent increase in AcTub levels and that do not cause >15% reduction in α-Tub at either concentration; class II compounds are those that cause >15% decrease in α-Tub at either 1 or 10 μM compound concentration. NA = not applicable as the test compound does not cause significant changes in AcTub or total α-Tub when tested at a 1 or a 10 μM concentration. [c]Test compound was tested at 10 and 30 μM.

https://dx.doi.org/10.1021/acs.jmedchem.0c01605
J. Med. Chem. 2021, 64, 1073−1102

Table 3. MT-Stabilizing Activity of Triazolopyrimidines Modified at C7 and/or C6[a]

Cpd #	Structure	AcTub		α-Tub	
		1 μM	10 μM	1 μM	10 μM
63	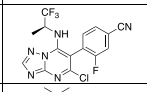	2.01 ± 0.38* (0.37)	3.64 ± 0.26** (0.67)	1.00 ± 0.01	1.00 ± 0.01
64	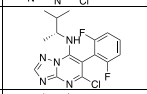	4.36 ± 0.72** (0.96)	4.88 ± 0.72** (1.07)	1.00 ± 0.02	0.96 ± 0.01
65	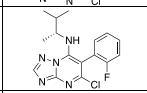	0.95 ± 0.26 (0.20)	2.10 ± 0.31** (0.43)	1.00 ± 0.04	1.04 ± 0.07
66	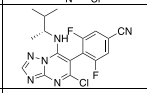	3.80 ± 0.15* (0.62)	4.28 ± 0.14** (0.69)	0.93 ± 0.02	0.94 ± 0.02
67	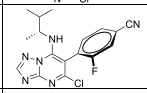	2.79 ± 1.11 (0.61)	3.42 ± 0.55* (0.75)	0.99 ± 0.02	0.93 ± 0.02
68	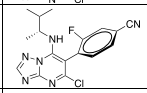	2.15 ± 0.36* (0.47)	2.29 ± 0.30* (0.50)	0.95 ± 0.02	0.92 ± 0.01
69	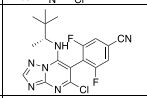	2.83 ± 0.33** (0.68)	4.60 ± 0.35** (1.10)	0.98 ± 0.03	1.03 ± 0.03
70	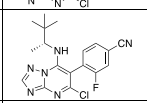	4.41 ± 0.27** (0.71)	7.67 ± 0.70** (1.24)	0.86 ± 0.03	0.93 ± 0.08
71	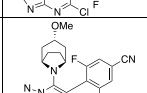	2.61 ± 0.26** (0.64)	4.32 ± 0.29** (1.06)	0.99 ± 0.01	1.00 ± 0.03
72	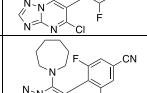	6.40 ± 0.61** (1.04)	11.2 ± 0.77** (1.82)	0.98 ± 0.03	0.99 ± 0.02
73	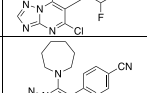	7.17 ± 1.09** (0.55)	12.6 ± 2.8** (0.97)	1.04 ± 0.05	0.99 ± 0.03
74	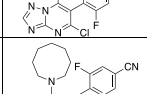	3.24 ± 0.80** (0.58)	4.40 ± 0.34** (0.79)	1.01 ± 0.02	0.99 ± 0.02
75	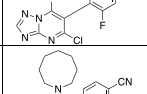	1.09 ± 0.22 (0.22)	2.89 ± 0.56** (0.59)	0.97 ± 0.02	0.95 ± 0.07

[a]Fold-changes in AcTub and α-Tub levels in QBI293 cells after 4 h of incubation with test compounds at either 1 or 10 μM. Reported values for AcTub and α-Tub represent the fold-change over control (DMSO)-treated cells (*p < 0.05 and **p < 0.01 by one-way ANOVA); numbers in parentheses represent the fold-change of AcTub over positive control-treated cells (*i.e.*, 100 nM of **5**).

fluorinated cyanobenzene fragments at C6, evaluation of a representative example (**69**) in primary neurons confirmed that compounds of this type increase AcTub levels and prevent the characteristic loss of neuronal MTs that is observed after incubation with the phosphatase inhibitor, okadaic acid (OA) (Figure 4). Although the cellular data do not allow for resolution of a detailed MT structure, the AcTub staining clearly shows that incubation with **69** protects the MT network from OA-induced collapse (Figure 4).

Interestingly, an assessment of lipophilicity of several compounds (Figure 5), as determined by experimental determinations of the distribution coefficient between *n*-octanol and water at pH 7.4 (*i.e.*, log $D_{7.4}$ values), revealed that the presence of a nitrile moiety in the para position of the phenyl ring at C6 produces a significant lowering of log $D_{7.4}$ values that becomes more pronounced in 2,6-difluorophenyl congeners, such as **66**, **69**, and **72**.

Importantly, an evaluation of brain-to-plasma (B/P) ratios of selected examples 1 h after administration to mice confirmed that the nitrile derivatives **66**, **69**, and **72** are readily brain-penetrant with B/P values >0.6 (Table 4). This result was confirmed by a 16 h brain and plasma PK study with **69** (Figure 6A). Moreover, a comparison of plasma PK of lead compound **3** and **69** indicates a greater metabolic stability of the nitrile-containing congener (Figure 6B).

Computational Studies. To investigate the nature of the interaction of Class I triazolopyrimidines with tubulin and to develop an *in silico* model that may ultimately be predictive of MT-stabilizing activity, we conducted docking studies with both active and inactive triazolopyrimidine congeners using the X-ray cocrystal structure of a tubulin preparation in complex

https://dx.doi.org/10.1021/acs.jmedchem.0c01605
J. Med. Chem. 2021, 64, 1073−1102

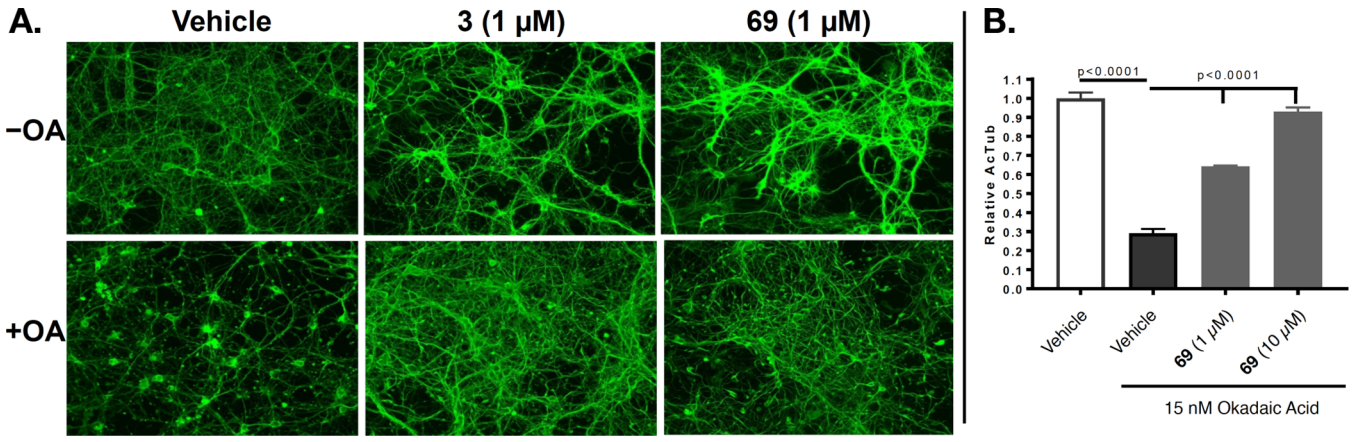

Figure 4. To confirm that the nitrile-containing triazolopyrimidine derivatives identified in these studies can stabilize neuronal MTs under conditions of tau loss-of-function, we examined the ability of representative compound, **69**, to prevent the MT collapse that occurs from reduced binding of hyperphosphorylated tau to axonal MTs after treatment of neuron cultures with the phosphatase inhibitor, OA. (A) Primary rat cortical neurons treated with 1 μM reference compound **3** or **69** in the absence of OA (−OA) show increased axonal acetyl-tubulin staining relative to those receiving vehicle only. Upon treatment with OA (+OA) in the absence of a compound (Vehicle), there is a dramatic reduction in axonal AcTub staining with fragmentation of MTs and neuronal processes (also see ref 11). Co-addition of **3** or **69** (1 μM) with OA results in normalization of AcTub staining and axonal processes. (B) ELISA determination of AcTub levels in homogenates from primary mouse cortical neurons treated with 1 or 10 μM of **69**, or vehicle, in the presence of OA. The higher concentration of **69** resulted in AcTub levels comparable to those in neurons without OA treatment.

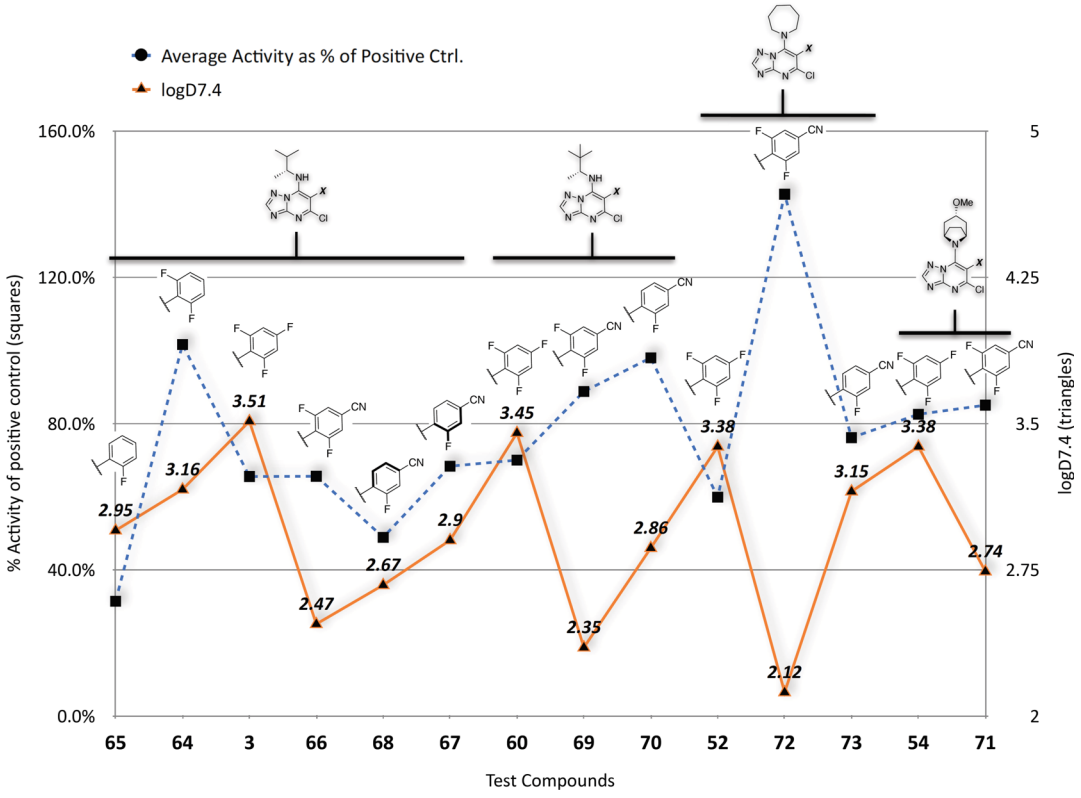

Figure 5. Comparison of selected compounds based on experimental log $D_{7.4}$ values (triangles) and MT-stabilizing activity (squares) expressed as the average activity in the AcTub assay at 1 and 10 μM normalized to positive control (*i.e.*, 100 nM **5**). log $D_{7.4}$ values were determined via the shake flask method (experiments run by Analiza, Inc.).

with Class I triazolopyrimidine **54**[13,23] (PDB: 5NJH; Figure 7A). The X-ray studies highlighted two key $\pi-\pi$ interactions between **54** and tubulin: one involving the pyrimidine core and Tyr224 of α-Tub and a second between the trifluorophenyl group and Tyr210 (α-Tub).[13] Both of these interactions are likely essential for a correct orientation of the triazolopyrimidine derivative within the binding pocket and substituents that interfere with these critical interactions are likely to result in reduced binding and biological activity. Indeed, docking of inactive derivative, **30**, within the triazolopyrimidine binding site suggests that the relatively large volume of the sulfone moiety disrupts the critical $\pi-\pi$ stacking interaction with the two tyrosine residues, leading to a different binding pose (Figure 7B) and, ultimately, a dramatic loss in MT-stabilizing

https://dx.doi.org/10.1021/acs.jmedchem.0c01605
J. Med. Chem. 2021, 64, 1073−1102

Table 4. Ratio between Brain and Plasma Compound Concentration 1 h after Administration (i.p. Injection) of the Test Compound

cpd #	i.p. dose (mg/kg)	B/P
3	5	2.7
66[a]	2.5	0.7
60	5	2.1
69[a]	2.5	0.7
52	5	1.4
72[a]	2.5	0.7

[a]Cassette dosing of three compounds (**66**, **69**, and **72**).

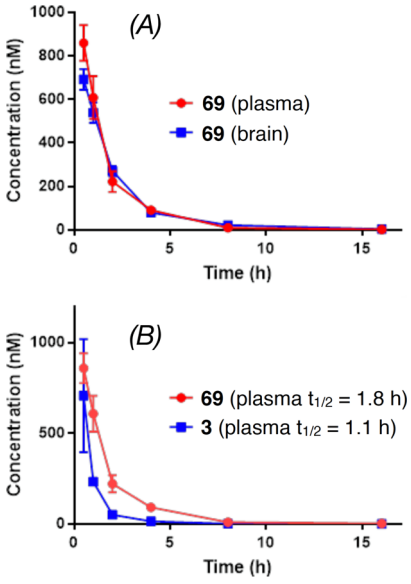

Figure 6. Brain and plasma pharmacokinetics of **69** after 5 mg/kg i.p. dosing to CD1 mice (A) and comparison of plasma pharmacokinetics of **69** and **3**.[12]

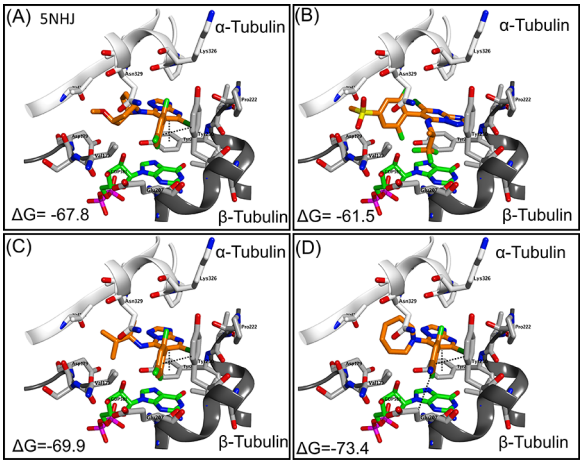

Figure 7. Different views of the cocrystal structure (PBD: 5NJH) of **54** bound within a tubulin preparation (A) and the docked structures of **30** (B), **3** (C), and **72** (D) within the triazolopyrimidine binding site.

activity. In the case of active Class I compounds, including lead compound **3** (Figure 7C), docking studies generally identify very similar binding poses and sets of interactions as seen in the cocrystal structure of **54**. However, for derivatives bearing a nitro or a nitrile at the para position of the fluorinated ring at C6, an additional H-bond interaction with the backbone of Glu207 (α-Tub) is also observed, which, in some cases (*e.g.*, **72**), may contribute to better ΔG of binding (Figure 7D) and MT-stabilizing activity (see Figure 5).

The binding modes of the different compounds were further evaluated by calculating the free energy of binding via a Molecular Mechanics Generalized Born Surface Area (MMGBSA) approach.[24] Interestingly, by plotting the computed MMGBSA free energetics of the Class I ligands in complex with tubulin against the MT-stabilizing activity (expressed as the average of the activity at 1 and 10 μM compound concentrations in the QBI293 AcTub assay, relative to the positive control), a moderately high Pearson correlation was found [$r = -0.70$, P-value (two-tailed) < 0.0001, Figure 8].

A 3D-QSAR study was also performed through a "field points" template, obtained from the cocrystallized compound. These field points define the shape and electrostatic and hydrophobic properties of the molecules and their spatial distribution.[25] For this study, 52 active and inactive Class I compounds were randomly partitioned to a training set (47) and a test set (5), while the experimental *in vitro* activity was computed using the normalized activity, expressed as the log of the average of the activity at 1 and 10 μM in the AcTub assay relative to the positive control (**5**) and defined as a dependent variable. In this case, the model shows a comparatively better correlation with a Pearson $r = 0.90$ (Figure 9A), which was cross-validated by leave-one-out (LOO) technique, $q^2 = 0.62$. Interestingly, the 3D-QSAR model highlighted the following steric and electrostatic contributions to the predicted activity (Figure 9B): a favorable electrostatic contribution (green) near the para position of the phenyl ring at C6 and strong steric contributions of the amine fragment at C7, as indicated by the large size of the dark teal field point (Figure 9B). Importantly, the combination of the binding free energies and the QSAR models (Figure 10) appeared to accurately place all of the most active MT-stabilizing compounds identified in this study within a well-defined area of lower ΔG of binding and higher QSAR predicted activity. Thus, the combinations of these models may provide a valuable tool to guide future design of novel potent MT-stabilizing triazolopyrimidines.

DISCUSSION

CNS-active MT-stabilizing compounds have been proposed as promising therapeutic candidates to treat AD and related neurodegenerative tauopathies.[26] In this context, the essential prerequisites for compound selection and advancement are the ability to both cross the blood–brain barrier and normalize the dynamics of MTs in the axons of neurons, such that efficient axonal transport can be maintained or restored. MT-stabilizing triazolopyrimidines have a number of potentially attractive features as MT-stabilizing compounds for CNS indications,[9] including synthetic tractability, a generally good brain penetration, and oral bioavailability. Selected members from this class of compounds have already been the focus of mechanism-of-action[13] and SAR studies that were based largely on cell-free experiments and cytotoxicity studies in cancer cell-lines.[15,16,27] Although clearly informative, such studies did not provide particular insight into the effects that triazolopyrimidines can have on cellular MTs. Studies from our laboratories in which the activity of MT-active triazolopyrimidines was evaluated by monitoring compound-dependent changes in cellular levels of tubulin as well as changes in levels of known markers of MT-stabilization, such as acetylated- and

https://dx.doi.org/10.1021/acs.jmedchem.0c01605
J. Med. Chem. 2021, 64, 1073−1102

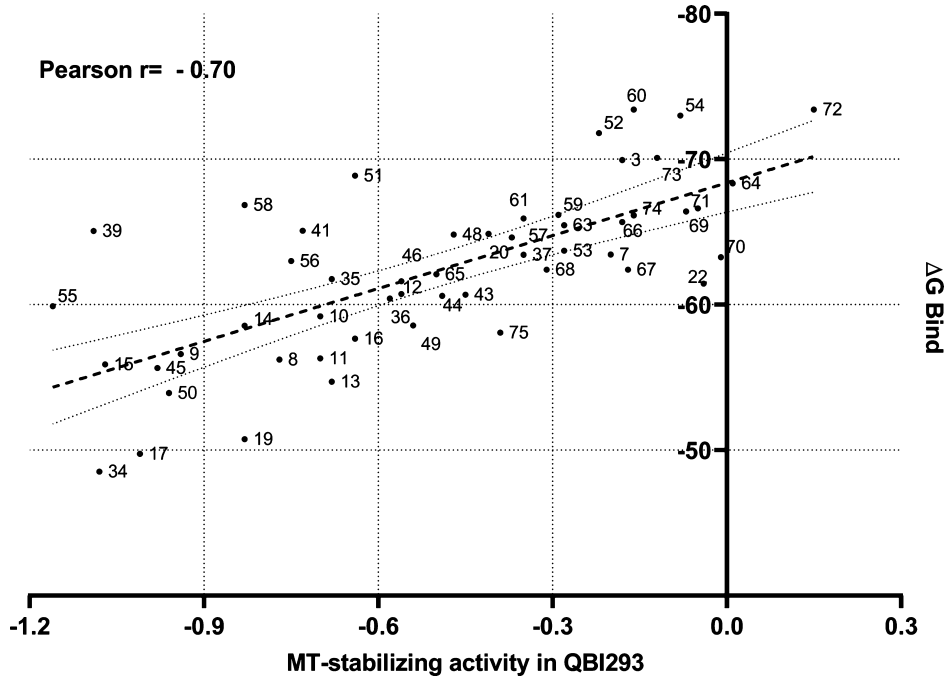

Figure 8. MMGBSA scores for the Class I compounds *vs* MT-stabilizing activity in QBI293 cells expressed as the log of the average of the activity at 1 and 10 μM in the AcTub assay, relative to the positive control, $\log\left(\frac{\text{avg AcTub}_{1\&10\,\mu M}}{\text{AcTub}_{0.1\,\mu M\text{ of }5}}\right)$.

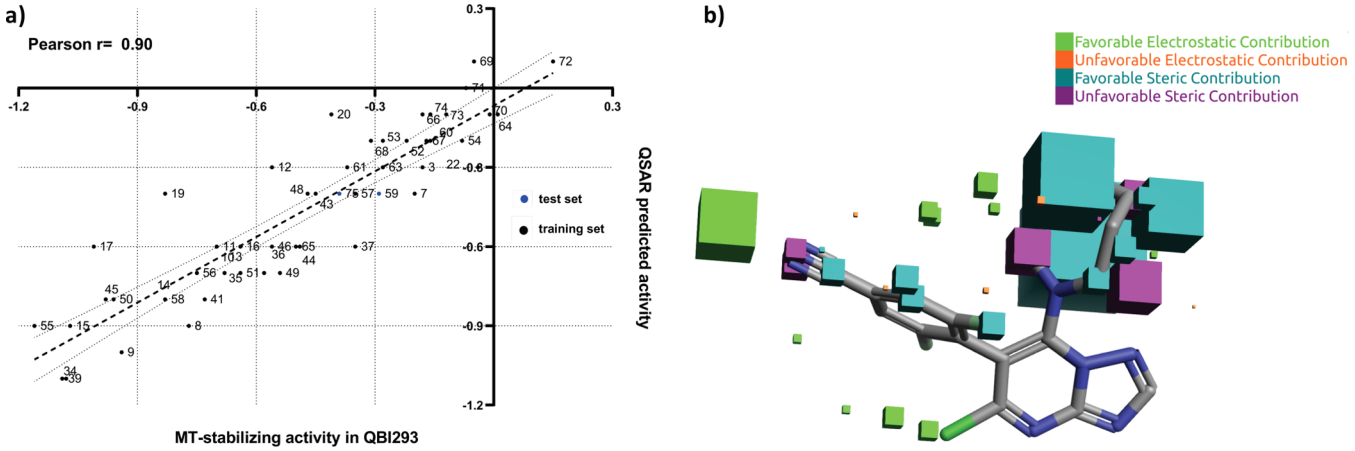

Figure 9. (A) QSAR predicted *vs* experimental MT-stabilizing activity in QBI293 cells for training and test sets. In both cases, MT-stabilizing activity is expressed as the log of the average of the activity at 1 and 10 μM in the AcTub assay, relative to the positive control, $\log\left(\frac{\text{avg AcTub}_{1\&10\mu M}}{\text{AcTub}_{0.1\mu M\text{ of }5}}\right)$. (B) Visual representation of the field and steric contributions to predicted activity for compound **72**.

detyrosinated-α-tubulin, showed that different congeners can generally elicit one of two cellular responses discriminated by whether (Class II) or not (Class I) these compounds reduce tubulin levels.[11] Furthermore, although one selected prototype from Class I triazolopyrimidines, **3**, has proven useful in obtaining validation of this class in mouse models of AD, further characterization of the structural determinants that may be most important to impart the desired MT-stabilizing effect in cells is a necessary step that could facilitate the identification of candidates for clinical development.

Given that our previous studies showed that the substituent in the para position of the phenyl ring (C6 fragment) of triazolopyrimidines can play an important role in determining the particular cellular response (*i.e.*, Class I or II) elicited by these compounds, whereas the C7 fragment may be especially important for potency as well as ADME-PK properties,[11,12] our exploration of the SAR of triazolopyrimidines focused primarily on identifying specific features (*e.g.*, electrostatic, hydrophobic, shape) of the C6 and C7 fragments that may be preferred for Class I MT-stabilizing triazolopyrimidines. Data from the cell-based MT-stabilization assays revealed different structural and property features that appear to have a relatively high impact on the biological activity. In particular, a comparison of active congeners of either class suggests that the electrostatic characteristics of the substituent in the para position of the phenyl ring at C6 play an important role in determining the cellular phenotype, while the degree and pattern of fluorination can modulate potency (Figure 2). Indeed, an analysis of *in vitro* biological activity *versus* the Hammett σ values of the different substituents in para suggests

https://dx.doi.org/10.1021/acs.jmedchem.0c01605
J. Med. Chem. 2021, 64, 1073−1102

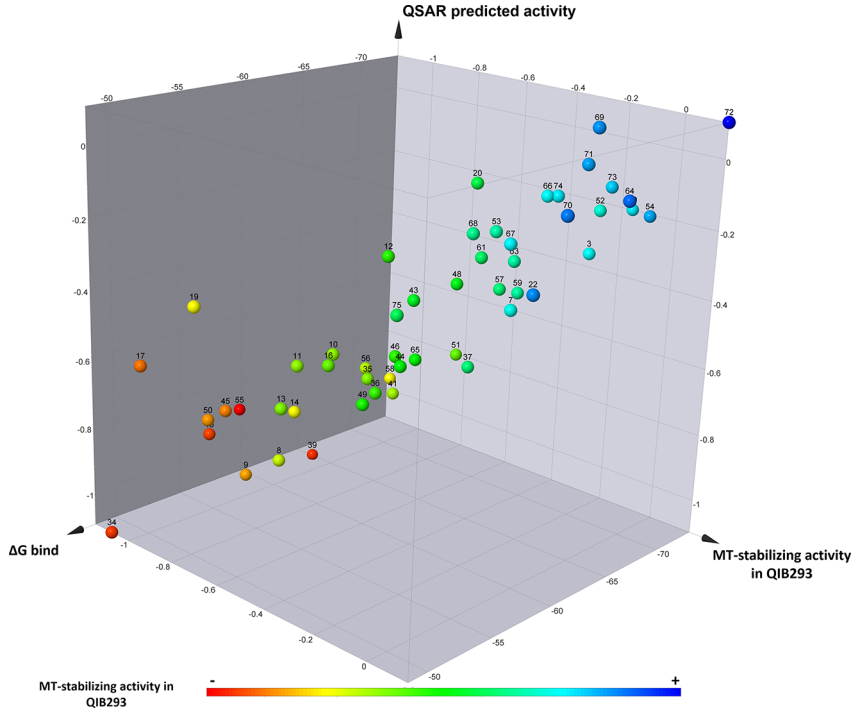

Figure 10. 3D summary plot of Class I triazolopyrimidines showing the experimental MT-stabilizing activity in the QBI293 assay, the MMGBSA score value (Δ*G* bind), and the QSAR predicted activity. The experimental MT-stabilizing activity of test compounds is plotted both via color coding and as the log of the average of the activity at 1 and 10 μM in the AcTub assay, relative to the positive control, $\log\left(\frac{\text{avg AcTub}_{1\&10\mu M}}{\text{AcTub}_{0.1\mu M}\text{ of 5}}\right)$, see the Experimental Section for further details.

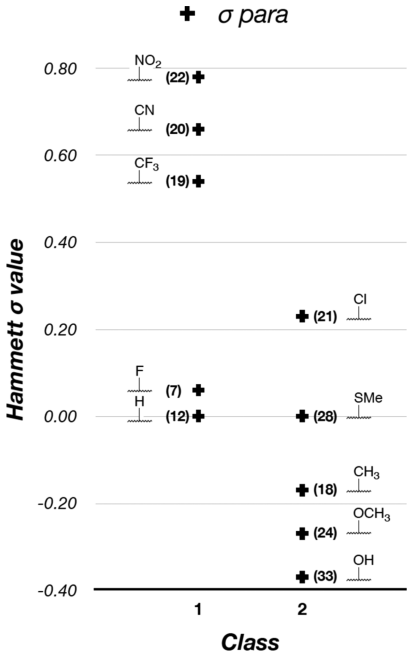

Figure 11. Effect of the stereoelectronic properties of the substituent in para. Active Class I and II compounds are ranked based on the Hammett σ_p values.[28]

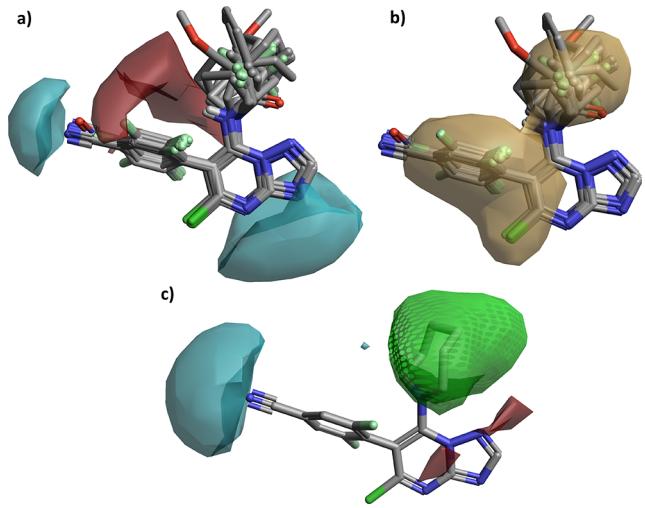

Figure 12. Activity atlas analysis revealing key features of Class I triazolopyrimidines that are necessary for MT-stabilizing activity: (a) red and cyan colors show positive and negative field regions, respectively; (b) brown beige regions show hydrophobic interaction sites required for activity; (c) activity cliffs analysis revealing a favorable hydrophobic region (green) and a favorable negative electrostatic region (cyan).

a general trend, whereby with the sole exception of the *para*-chloro derivative, **21**, positive σ values (*e.g.*, fluorine, nitro, or nitrile) are typically conducive to Class I activity, whereas σ values < 0 (*e.g.*, hydroxyl or methoxy groups) appear to be associated with the Class II phenotype (Figure 11). Thus, the SAR data of the C6 fragment of triazolopyrimidines indicate that the desired Class I MT-stabilizing activity generally requires the presence of an electron-poor phenyl ring. Different fluorinated phenyl fragments can be tolerated, especially those bearing either one or two fluorine atoms in the ortho positions, and a para position that is either unsubstituted or substituted with an additional fluorine or other electron-withdrawing groups, such as nitro and nitrile.

https://dx.doi.org/10.1021/acs.jmedchem.0c01605
J. Med. Chem. 2021, 64, 1073−1102

With respect to the SAR of the fragment linked at C7, the data presented in Table 2 revealed a number of structural and property requirements for optimal MT-stabilizing activity. In particular, in addition to aliphatic amines being typically preferred (*e.g.*, over ethers or aromatic amines), a general trend emerged linking MT-stabilizing activity in cells with the lipophilic character and size of the C7 fragment (Figure 3). An interesting observation made during these studies was the fact that in specific instances, the chirality of the aliphatic amine fragment can play a role in determining the cellular phenotype elicited by the triazolopyrimidine. Although the configuration of the chiral center of the amine fragment of **3** or **7** appears to impact the potency of these compounds in the AcTub assay without affecting α-Tub levels (*cf.*, **7** with **48**, and **3** with **45**), in selected cases, such as compounds **46** and **47**, the inversion of chiral configuration was found to cause a shift in the cellular phenotype, with **46** being a Class I compound while its enantiomer, **47**, clearly produced a marked reduction (~40%) in α-Tub (Class II). Interestingly, docking studies with **46** and **47** did not reveal significant differences in binding modes that could help explain the different cellular phenotypes elicited by the two enantiomers. In addition, a side-by-side comparison of the cytotoxicity of enantiomers **46** (Class I) and **47** (Class II) in rapidly dividing QBI293 or HeLa cells did not reveal significant differences in IC_{50} values (Supporting Information), suggesting that both Class I and II triazolopyrimidines exhibit comparable antimitotic effects. These observations indicate that neither docking nor IC_{50} values in cell cytotoxicity assays should be used to predict whether a triazolopyrimidine would stabilize or disrupt the MT network. Given that such a distinction is an essential aspect driving the prioritization of candidates for neurodegenerative tauopathies, an evaluation of compounds in a cellular assay that assesses compound effect on α/β-tubulin levels as well as increases in markers of MT stabilization is ultimately a necessary step. Although such assays have some limitations, such as a relatively low-throughput and possible day-to-day variability that can be minimized by normalizing the activity of test compounds to a positive control, the SAR data generated in this study led to the identification of several characteristics that are important for Class I MT-stabilizing triazolopyrimidines. Indeed, a qualitative assessment of the combined C6 and C7 SAR data of all Class I triazolopyrimidines tested in this study, which was conducted using Activity atlas analysis,[29] identified distinct regions/characteristics that are shared by the vast majority of Class I congeners (Figure 12A,B); these include a positive electrostatic region in the proximity of the amine fragment at C7 (indicated in red, Figure 12A), a negative electrostatic region in the proximity of the para position of the aryl group at C6 (cyan, Figure 12A), and two hydrophobic interaction regions near the fluorinated phenyl at C6 and the aliphatic amine fragment at C7 (yellow, Figure 12B). Furthermore, an activity cliff analysis (Figure 12C), which highlights structural differences of similar compounds that produce a disproportionally high impact on the biological activity (*i.e.*, activity cliff regions),[30] revealed that an increase of negative electrostatic field at the para position of the phenyl ring (cyan), as associated with substituents such as nitro and nitrile, as well as the presence of a favorable hydrophobic region in C7 (green), produce a drastic increase in MT-stabilizing activity. Collectively, these findings, combined with the development of relatively predictive models that are based on calculated binding free energies and QSAR, provide valuable insights that could facilitate the design of Class I triazolopyrimidines.

Importantly, by combining the preferred C6 and C7 fragments found in the course of these SAR studies, several new Class I triazolopyrimidine analogues have been identified (Table 3), including multiple examples (**64**, **69**, and **70**−**72**) that exhibit both improved *in vitro* activity as well as reduced lipophilic character compared to lead compound **3**. In primary cortical neurons, **69** was found to protect the MT-network against OA-induced collapse in a manner comparable to **3** (Figure 4), suggesting that these new congeners, like **3**, may be beneficial in normalizing MT-deficits in tauopathy neurons. Interestingly, although the effect of the nitrile moiety in lowering lipophilicity is well documented,[31] a direct comparison of experimentally determined log $D_{7.4}$ values of matched paired compounds bearing a nitrile moiety in the para position of the ring at C6 (*cf.*, **66** with **67**/**68**; **69** with **70**; and **72** with **73**) demonstrates that the fluorination state of the aromatic ring plays an equally important role as evidenced by the significantly lower log $D_{7.4}$ values observed when both ortho positions are fluorinated (Figure 5). Of notice, in spite of the reduced lipophilic character of **66**, **69**, and **72** compared to the corresponding 2,4,6-trifluorophenyl congeners (**3**, **60**, and **52**), these compounds retained excellent brain penetration (Table 4). Furthermore, evaluation of brain/plasma PK of **69** after i.p. injection revealed that this compound exhibits greater metabolic stability (*i.e.*, reduced clearance and increased plasma half-life) compared to existing lead (**3**). Thus, taken together, our results show that an appropriate combination of relatively bulky/lipophilic aliphatic amines at C7 with polar fluorinated cyanobenzene fragments at C6 results in Class I congeners that exhibit both improved MT-stabilizing activity in cells as well as improved lipophilic efficiency and metabolic stability.

CONCLUSIONS

Brain-penetrant, MT-stabilizing triazolopyrimidines have produced promising results in different mouse models of AD, suggesting that compounds from this class may be considered as candidate therapeutics for neurodegenerative tauopathies. However, depending on the substitution pattern, this type of compounds can elicit very different cellular responses by either promoting MT stabilization or, conversely, disrupting MT integrity in cells. The studies presented here define the most important stereoelectronic characteristics of the C6 and C7 fragments of MT-active triazolopyrimidines that can lead to relatively potent MT-stabilizing activity in cells without reduction in cellular tubulin levels. These results, which provide additional insight into the SAR of MT-stabilizing triazolopyrimidines, enabled both the development of predictive models as well as the design of congeners exhibiting improved properties and *in vitro* biological activity. Compounds of this type hold promise as candidate treatments for neurodegenerative tauopathies.

EXPERIMENTAL SECTION

Materials and Methods. All solvents were of reagent grade. All reagents were purchased from Aldrich or Acros and used as received. Thin-layer chromatography (TLC) was performed with 0.25 mm E. Merck precoated silica gel plates. Silica gel column chromatography was performed with silica gel 60 (particle size 0.040−0.062 mm) supplied by Silicycle and Sorbent Technologies. TLC spots were detected by viewing under a UV light. Melting points (mp) were

https://dx.doi.org/10.1021/acs.jmedchem.0c01605
J. Med. Chem. 2021, 64, 1073−1102

acquired on a Mel-Temp II (model: 1001) and are uncorrected. Infrared (IR) spectra were recorded on a Bruker, model Alpha spectrometer (part number 1003271/03). Proton (^{1}H) and carbon (^{13}C) NMR spectra were recorded on a 500 MHz Bruker AMX-500 spectrometer or 600 MHz Bruker AVANCE III spectrometer. Fluorine (^{19}F) NMR spectra were recorded on a 500 MHz Bruker AVANCE II spectrometer. Chemical shifts were reported relative to solvents. Data for ^{1}H NMR spectra are reported as follows: chemical shift [ppm, referenced to protium; s = singlet, d = doublet, t = triplet, q = quartet, quint = quintet, dd = doublet of doublets, td = triplet of doublets, ddd = doublet of doublet of doublets, bs = broad singlet, m = multiplet, coupling constant (Hz), and integration]. High-resolution mass spectra were measured using an Agilent 6230 time-of-flight mass spectrometer with a Jet stream electrospray ionization source. Single-crystal X-ray structure determinations were performed using a Bruker MicroStar with an APEX II detector, double-bounce micro-focus optics, and a Cu rotating anode source. Analytical reverse-phase (Sunfire C18; 4.6 mm × 50 mm, 5 mL) HPLC was performed with a Gilson HPLC equipped with UV and a mass detector. All samples were analyzed employing a linear gradient from 10 to 90% of ACN in H_2O over 8 min and flow rate of 1 mL/min. Preparative reverse-phase HPLC purifications were performed on a Gilson instrument employing Waters SunFire preparative C_{18} OBD columns (5 μm 19 mm × 50 mm or 19 mm × 100 mm). Purifications were carried out employing a linear gradient from 10 to 90% of ACN in H_2O for 15 min with a flow rate of 20 mL/min. All final compounds were found to be >95% pure by HPLC.

General Procedure A (Synthesis of Diethylmalonate Derivatives). To a suspension of NaH (60 wt % in mineral oil) (1.00 equiv) in anhydrous 1,4-dioxane (previously degassed with N_2) at 60 °C under N_2 was slowly added diethyl malonate (3.00 equiv) and the resulting mixture was stirred for 10 min. CuBr (1.20 equiv) and aryl bromide derivate were then added and the reaction mixture (1.75 mol/L of aryl bromide derivate) was heated to reflux overnight. The reaction mixture was then cooled to rt, quenched with HCl 12 N (1.40 equiv), filtered, and washed with H_2O. The filtrate was extracted with EtOAc (×3). The combined organic extracts were washed with brine, dried over $MgSO_4$, filtered, and concentrated under reduced pressure. Purification via silica gel column chromatography or preparative reverse-phase HPLC provided the desired diethylmalonate derivatives.

General Procedure B (Synthesis of Dichloro-triazolopyrimidine Derivatives). A mixture of the appropriate diethylmalonate derivate (1.00 equiv), 3-amino-1,2,4-triazole (1.05 equiv), and tributylamine (1.05 equiv) in a sealed tube was stirred at 170 °C for 2 h. After cooling to 130 °C, the reaction mixture was diluted with toluene to reach approximately a concentration of 1.00 M of the diethylmalonate derivative. The reaction was then cooled to 50 °C and an aqueous solution of NaOH (50 wt %) (0.160 mL/mmol of diethylmalonate derivate) was added. The resulting mixture was stirred at 0 °C for 10 min and then filtered to obtain the triazolopyrimidine disodic salt intermediate as a solid, which was washed with cold toluene, dried, and used directly without further purification. This disodic derivate (1.00 equiv) and $POCl_3$ (17.80 equiv) were mixed in a sealed tube and heated to 130 °C for 6 h. The reaction was then quenched with H_2O and extracted with EtOAc (×2). The combined organic extracts were washed with H_2O (×5), then brine, dried over $MgSO_4$, filtered, and concentrated under reduced pressure. The resulting dichloro-triazolopyrimidine was used directly without further purification.

General Procedure C (Addition of the Amine). According to a reported procedure,[15] to a solution of 5,7-dichloro-6-(2,4,6-trifluorophenyl)-[1,2,4]triazolo[1,5-*a*]pyrimidine (1.0 equiv) in *N*,*N*-dimethylformamide (DMF) (0.1 M) at rt was added the appropriate amine (1.5−3.0 equiv either as HCl salt or free base) followed by *i*-Pr_2NEt (3.0 equiv) or Et_3N (3.0 equiv), if necessary. The reaction mixture was stirred for 0.5−16 h and then diluted with H_2O. The organic layer was washed with a 1 N HCl (×2), the aqueous phase was extracted with EtOAc (×3), and the combined organic layers were washed with brine (×2), dried over $MgSO_4$, filtered, and concentrated. Finally, purification via silica gel flash chromatography or by reverse-phase HPLC yielded the desired product.

General Procedure D (Addition of the Side Chain). According to reported procedures,[15,16] to a suspension of NaH (4.0 equiv) in a 2:1 mixture of DMSO and tetrahydrofuran (THF) (0.35 M) was added the appropriate aminoalcohol (4.0 equiv), and the mixture was heated to 60 °C for 1 h. The resulting solution was treated with a solution of trifluoroarene (1.0 equiv) in a 1:1 mixture DMSO and THF (0.5 M). The reaction mixture was stirred at 60 °C for 3 h and monitored by LCMS. If the starting material remained after 3 h, additional aminoalcohol (4.0 equiv) and NaH (4.0 equiv) were added, sequentially, and the reaction mixture was heated for 16 h. Following complete consumption of the starting material, the reaction mixture was cooled to rt and diluted with H_2O and EtOAc. The organic layer was washed with H_2O and brine, and the combined aqueous layers were extracted with EtOAc (×3). The combined organic layers were dried over $MgSO_4$, filtered, and concentrated. Purification by reverse-phase HPLC provided the desired product.

(*S*)-5-Chloro-6-phenyl-*N*-(1,1,1-trifluoropropan-2-yl)-[1,2,4]-triazolo[1,5-*a*]pyrimidin-7-amine (8). General procedure C was followed using 5,7-dichloro-6-phenyl-[1,2,4]triazolo[1,5-*a*]pyrimidine (0.500 g, 1.88 mmol) (**93**) and (*S*)-2-amino-1,1,1-trifluoropropane hydrochloride (0.840 g, 5.64 mmol). Purification via preparative reverse-phase chromatography provided the title compound as a white powder (0.066 g, 0.19 mmol, 10%).^{1}H NMR (500 MHz, $CDCl_3$): δ 8.40 (s, 1H), 7.62−7.52 (m, 3H), 7.42−7.36 (m, 1H), 7.35−7.28 (m, 1H), 5.68 (s, 1H), 4.63 (s, 1H), 1.29 (d, J = 6.8 Hz, 3H) ppm; ^{13}C NMR (126 MHz, $CDCl_3$): δ 157.17, 155.44, 145.72, 131.67, 131.51, 130.54, 130.09, 129.96, 129.82, 124.90 (q, J = 282.4 Hz), 105.26, 50.67 (q, J = 31.5 Hz), 15.02 (q, J = 1.7 Hz) ppm; IR (film) ν: 3435, 1619, 1577, 1491, 1460, 1384, 1366, 1338, 1264, 1248, 1179, 1145, 1085, 1024, 955, 906, 767, 742, 702, 652, 615 cm^{-1}; HRMS (ES$^+$): calcd for $C_{14}H_{12}ClF_3N_5$ [M + H]$^+$, 342.0728; found, 342.0726.

(*S*)-5-Chloro-6-(4-fluorophenyl)-*N*-(1,1,1-trifluoropropan-2-yl)-[1,2,4]triazolo[1,5-*a*]pyrimidin-7-amine (9). General procedure C was followed using 5,7-dichloro-4-fluorophenyl-[1,2,4]-triazolo[1,5-*a*]pyrimidine (0.300 g, 1.04 mmol) (**94**) and (*S*)-2-amino-1,1,1-trifluoropropane hydrochloride (0.465 g, 3.11 mmol). Purification via preparative reverse-phase chromatography provided the title compound as a white powder (0.126 g, 0.35 mmol, 34%). ^{1}H NMR (500 MHz, $CDCl_3$): δ 8.39 (s, 1H), 7.42−7.35 (m, 1H), 7.36−7.24 (m, 3H), 5.65 (s, 1H), 4.77 (s, 1H), 1.34 (d, J = 6.8 Hz, 3H) ppm; ^{13}C NMR (126 MHz, $CDCl_3$): δ 163.57 (d, J = 251.3 Hz), 157.29, 155.56, 153.93, 145.86, 133.63 (d, J = 8.4 Hz), 132.61 (d, J = 8.4 Hz), 127.57 (d, J = 3.7 Hz), 124.94 (q, J = 282.4 Hz), 117.34 (d, J = 22.0 Hz), 117.16 (d, J = 22.0 Hz), 104.31, 50.83 (q, J = 31.6 Hz), 15.04 (d, J = 2.1 Hz) ppm; IR (film) ν: 3421, 1619, 1574, 1504, 1461, 1366, 1337, 1247, 1180, 1146, 1096, 1024, 957, 841, 766, 738, 610 cm^{-1}; HRMS (ES$^+$): calcd for $C_{14}H_{10}ClF_4N_5Na$ [M + Na]$^+$, 382.0459; found, 382.0464.

5-Chloro-6-(2-fluorophenyl)-*N*-(-1,1,1-trifluoropropan-2-yl)-[1,2,4]triazolo[1,5-*a*]pyrimidin-7-amine (10). General procedure C was followed using 5,7-dichloro-6-(2-fluorophenyl)-[1,2,4]triazolo-[1,5-*a*]pyrimidine (0.300 g, 1.04 mmol) (**95**) and (*S*)-2-amino-1,1,1-trifluoropropane hydrochloride (0.465 g, 3.11 mmol). Purification via silica gel column chromatography (0−30% EtOAc in hexanes) provided the title compound as a white powder (0.060 g, 0.17 mmol, 16%). ^{1}H NMR (500 MHz, $CDCl_3$): mixture of diastereomers δ 8.39 (s, 1H), 7.61−7.52 (m, 1H), 7.40−7.27 (m, 3H), 6.08−5.49 (m, 1H), 4.95−4.22 (m, 1H), 1.34 (d, J = 6.8 Hz, 3H) ppm; ^{13}C NMR (126 MHz, $CDCl_3$): δ 161.79, 161.59, 159.80, 159.61, 157.71, 157.50, 155.50, 155.43, 154.20, 153.83, 145.83, 145.41, 133.41, 133.39, 132.79, 132.72, 132.66, 132.35, 132.34, 128.18, 128.00, 125.93, 125.76, 125.50, 125.47, 125.44, 125.41, 123.69, 123.51, 121.45, 121.27, 119.42, 119.30, 119.18, 117.21, 117.04, 116.70, 116.53, 99.20, 98.22, 51.26, 51.00, 50.75, 50.49, 50.24, 15.18, 15.16, 15.07, 15.05 ppm; IR (film) ν: 3435, 1618, 1554, 1491, 1460, 1368, 1248, 1179, 1144, 1094, 1025, 960, 759, 651, 616 cm^{-1}; HRMS (ES$^+$): calcd for $C_{14}H_{10}ClF_4N_5Na$ [M + Na]$^+$, 382.0459; found, 382.0441.

https://dx.doi.org/10.1021/acs.jmedchem.0c01605
J. Med. Chem. 2021, 64, 1073−1102

(*S*)-5-Chloro-6-(2,6-difluorophenyl)-*N*-(1,1,1-trifluoropropan-2-yl)-[1,2,4]triazolo[1,5-*a*]pyrimidin-7-amine (12). General procedure C was followed using 5,7-dichloro-6-(2,6-difluorophenyl)-[1,2,4]triazolo[1,5-*a*]pyrimidine (0.280 g, 0.93 mmol) (**97**) and (*S*)-2-amino-1,1,1-trifluoropropane hydrochloride (0.417 g, 2.79 mmol). Purification via preparative reverse-phase chromatography provided the title compound as a white powder (0.024 g, 0.06 mmol, 7%). ^{1}H NMR (500 MHz, $CDCl_3$): δ 8.33 (s, 1H), 7.54−7.45 (m, 1H), 7.10−7.00 (m, 2H), 6.19−6.10 (m, 1H), 4.76 (s, 1H), 1.39 (d, J = 6.9 Hz, 3H) ppm; ^{13}C NMR (126 MHz, $CDCl_3$): δ 161.12 (dd, J = 252.3, 5.5 Hz), 160.82 (dd, J = 250.9, 5.3 Hz), 157.72, 155.26, 154.16, 145.89, 133.01 (t, J = 10.0 Hz), 124.59 (dd, J = 564.1, 282.1 Hz), 112.43 (dd, J = 21.5, 3.4 Hz), 112.07 (dd, J = 21.5, 3.6 Hz), 108.90 (t, J = 20.2 Hz), 92.39, 50.86 (q, J = 32.3 Hz), 14.98 ppm. IR (film) ν: 3227, 1630, 1602, 1460, 1383, 1266, 1239, 1195, 1126, 1003, 900, 809, 765, 652, 622 cm^{-1}; HRMS (ES$^+$): calcd for $C_{14}H_{10}ClF_5N_5$ [M + H]$^+$, 378.0539; found, 378.0556.

(*S*)-5-Chloro-6-(3,5-difluorophenyl)-*N*-(1,1,1-trifluoropropan-2-yl)-[1,2,4]triazolo[1,5-*a*]pyrimidin-7-amine (13). General procedure C was followed using 5,7-dichloro-6-(3,5-difluorophenyl)-[1,2,4]triazolo[1,5-*a*]pyrimidine (0.350 g, 1.16 mmol) (**98**) and (*S*)-2-amino-1,1,1-trifluoropropane hydrochloride (0.521 g, 3.49 mmol). Purification via silica gel column chromatography (0−30% EtOAc in hexanes) provided the title compound as a white powder (0.148 g, 0.39 mmol, 34%). ^{1}H NMR (500 MHz, $CDCl_3$): δ 8.40 (s, 1H), 7.03 (dt, J = 8.6, 2.3 Hz, 1H), 6.96 (d, J = 8.3 Hz, 1H), 6.90 (d, J = 7.5 Hz, 1H), 5.64 (s, 1H), 4.82 (s, 1H), 1.38 (d, J = 6.8 Hz, 3H) ppm; ^{13}C NMR (126 MHz, $CDCl_3$): δ 163.72 (dd, J = 253.2, 13.0 Hz), 163.66 (dd, J = 251.7, 11.7 Hz), 156.45, 155.71, 153.96, 145.57, 134.65 (t, J = 10.0 Hz), 124.85 (q, J = 282.4 Hz), 115.03 (dd, J = 21.9, 3.7 Hz), 114.04 (dd, J = 21.9, 3.7 Hz), 105.99 (t, J = 24.8 Hz), 103.18, 51.07 (q, J = 31.6 Hz), 15.02 (d, J = 1.9 Hz) ppm; IR (film) ν: 3435, 1620, 1590, 1521, 1493, 1460, 1434, 1384, 1362, 1333, 1264, 1192, 1159, 1125, 1081, 1028, 987, 956, 906, 855, 763, 670, 653, 628 cm^{-1}; HRMS (ES$^-$): calcd for $C_{14}H_8ClF_5N_5$ [M − H]$^-$, 376.0394; found, 376.0376.

(*S*)-5-Chloro-6-(2,5-difluorophenyl)-*N*-(-1,1,1-trifluoropropan-2-yl)-[1,2,4]triazolo[1,5-*a*]pyrimidin-7-amine (14). General procedure C was followed using 5,7-dichloro-6-(2,5-difluorophenyl)-[1,2,4]triazolo[1,5-*a*]pyrimidine (0.400 g, 1.33 mmol) (**99**) and (*S*)-2-amino-1,1,1-trifluoropropane hydrochloride (0.596 g, 3.99 mmol). Purification via silica gel column chromatography (0−30% EtOAc in hexanes) provided the title compound as a white powder (0.020 g, 0.05 mmol, 4%). ^{1}H NMR (500 MHz, $CDCl_3$): mixture of diastereomers δ 8.40 (s, 1H), 7.32−7.24 (m, 2H), 7.15−7.02 (m, 1H), 6.07−5.46 (m, 1H), 4.71 (d, J = 156.9 Hz, 1H), 1.39 (d, J = 6.8 Hz, 3H) ppm; ^{13}C NMR (126 MHz, $CDCl_3$): mixture of diastereomers δ 159.86, 159.84, 157.90, 157.88, 157.71, 157.68, 157.28, 157.15, 155.95, 155.93, 155.76, 155.73, 155.64, 155.58, 154.21, 153.94, 145.78, 145.47, 128.12, 127.98, 125.88, 125.74, 123.64, 123.49, 121.39, 121.25, 120.68, 120.62, 120.56, 120.54, 120.50, 120.47, 120.41, 120.35, 119.99, 119.97, 119.80, 119.78, 119.54, 119.51, 119.47, 119.44, 119.35, 119.32, 119.28, 119.25, 118.91, 118.89, 118.72, 118.70, 118.52, 118.45, 118.33, 118.26, 118.00, 117.93, 117.81, 117.74, 98.19, 97.30, 51.46, 51.25, 51.21, 50.99, 50.95, 50.74, 50.70, 50.49, 15.19, 15.18, 15.09, 15.08 ppm; IR (film) ν: 3441, 1622, 1494, 1461, 1424, 1383, 1251, 1182, 1145, 1092, 1025, 979, 877, 821, 775 cm^{-1}; HRMS (ES$^+$): calcd for $C_{14}H_{10}ClF_5N_5$ [M + H]$^+$, 378.0539; found, 378.0509.

(*S*)-5-Chloro-6-(3,4-difluorophenyl)-*N*-(1,1,1-trifluoropropan-2-yl)-[1,2,4]triazolo[1,5-*a*]pyrimidin-7-amine (15). General procedure C was followed using 5,7-dichloro-6-(3,4-difluorophenyl)-[1,2,4]triazolo[1,5-*a*]pyrimidine (0.150 g, 0.50 mmol) (**100**) and (*S*)-2-amino-1,1,1-trifluoropropane hydrochloride (0.223 g, 1.49 mmol). Purification via preparative reverse-phase chromatography provided the title compound as a white powder (0.007 g, 0.02 mmol, 4%).^{1}H NMR (500 MHz, $CDCl_3$): mixture of diastereomers δ 8.42 (s, 1H), 7.45−7.34 (m, 1H), 7.22−7.05 (m, 2H), 5.71−5.47 (m, 1H), 5.02−4.63 (m, 1H), 1.37 (d, J = 6.9 Hz, 3H) ppm; ^{13}C NMR (126 MHz, $CDCl_3$): mixture of diastereomers δ 157.04, 157.01, 156.89, 156.88, 155.78, 155.73, 155.72, 155.66, 152.56, 152.50, 152.43, 152.38, 152.33, 152.20, 152.09, 151.96, 150.51, 150.46, 150.38, 150.35, 150.17, 150.06, 149.94, 145.95, 145.91, 145.82, 145.78, 145.74, 128.38, 128.34, 128.30, 127.36, 127.31, 127.28, 126.04, 125.99, 123.80, 123.75, 121.58, 121.55, 121.18, 121.05, 120.19, 120.17, 120.06, 120.05, 119.34, 119.29, 119.24, 119.19, 119.16, 119.02, 103.47, 103.35, 51.42, 51.35, 51.16, 51.10, 50.91, 50.84, 50.65, 50.59, 15.08 ppm; IR (film) ν: 3436, 2923, 2853, 1632, 1463, 1383, 1270, 1147 cm^{-1}; HRMS (ES$^+$): calcd for $C_{14}H_{10}ClF_5N_5$ [M + H]$^+$, 378.0539; found, 378.0550.

(*S*)-5-Chloro-6-(2,3,4-trifluorophenyl)-*N*-(-1,1,1-trifluoropropan-2-yl)-[1,2,4]triazolo[1,5-*a*]pyrimidin-7-amine (16). General procedure C was followed using 5,7-dichloro-6-(2,3,4-trifluorophenyl)-[1,2,4]triazolo[1,5-*a*]pyrimidine (0.300 g, 0.94 mmol) (**101**) and (*S*)-2-amino-1,1,1-trifluoropropane hydrochloride (0.422 g, 2.82 mmol). Purification via preparative reverse-phase chromatography provided the title compound as a white powder (0.050 g, 0.13 mmol, 13%). ^{1}H NMR (500 MHz, $CDCl_3$): mixture of diastereomers δ 8.37 (s, 1H), 7.24−7.05 (m, 2H), 6.05−5.61 (m, 1H), 5.20−4.47 (m, 1H), 1.42 (d, J = 6.3 Hz, 3H) ppm; ^{13}C NMR (126 MHz, $CDCl_3$): mixture of diastereomers δ 157.56, 157.24, 155.75, 155.67, 154.40, 153.95, 153.77, 153.74, 153.69, 153.67, 153.62, 153.59, 151.74, 151.71, 151.66, 151.63, 151.58, 151.56, 151.39, 151.36, 151.31, 151.28, 151.06, 151.03, 150.98, 150.95, 149.37, 149.34, 149.29, 149.26, 149.05, 149.02, 148.97, 148.94, 146.17, 145.67, 142.19, 142.07, 141.95, 141.86, 141.74, 141.62, 140.16, 140.04, 139.91, 139.83, 139.70, 139.58, 128.20, 127.95, 127.23, 127.20, 127.18, 127.17, 127.14, 126.15, 126.14, 126.11, 126.10, 126.09, 126.08, 126.05, 125.95, 125.70, 123.71, 123.46, 121.47, 121.22, 117.07, 117.04, 116.96, 116.93, 116.91, 116.84, 116.80, 113.96, 113.92, 113.91, 113.88, 113.81, 113.78, 113.77, 113.74, 97.55, 96.47, 51.59, 51.34, 51.31, 51.08, 51.05, 50.83, 50.80, 50.55, 15.21, 15.19, 15.07, 15.06 ppm. IR (film) ν: 3388, 3338, 1619, 1553, 1509, 1486, 1463, 1367, 1352, 1251, 1181, 1143, 1090, 1041, 1025, 987, 957, 906, 878, 808, 766, 738, 698, 680, 653, 619 cm^{-1}; HRMS (ES$^+$): calcd for $C_{14}H_9ClF_6N_5$ [M + H]$^+$, 396.0445; found, 396.0464.

(*S*)-5-Chloro-6-(2,4,6-trifluorobenzyl)-*N*-(1,1,1-trifluoropropan-2-yl)-[1,2,4]triazolo[1,5-*a*]pyrimidin-7-amine (17). General procedure C was followed using 5,7-dichloro-6-(2,4,6-trifluorobenzyl)-[1,2,4]triazolo[1,5-*a*]pyrimidine (0.300 g, 0.90 mmol) (**103**) and (*S*)-2-amino-1,1,1-trifluoropropane hydrochloride (0.404 g, 2.70 mmol). Purification via silica gel column chromatography (0−25% EtOAc in hexanes) provided the title compound as a white powder (0.085 g, 0.21 mmol, 23%). ^{1}H NMR (500 MHz, $CDCl_3$): δ 8.32 (s, 1H), 6.73 (t, J = 8.3 Hz, 2H), 6.32−6.12 (m, 1H), 5.23 (d, J = 10.2 Hz, 1H), 4.27−4.08 (m, 2H), 1.50 (d, J = 6.9 Hz, 3H) ppm; ^{13}C NMR (126 MHz, $CDCl_3$): δ 162.21 (dt, J = 251.1, 16.0 Hz), 161.52 (dd, J = 247.9, 10.9 Hz), 161.41 (dd, J = 248.0, 10.8 Hz), 157.36, 155.42, 154.39, 146.49, 125.14 (q, J = 282.1 Hz), 108.38 (td, J = 19.0, 4.8 Hz), 101.31−100.77 (m), 100.73, 51.82 (q, J = 31.5 Hz), 21.06, 15.30 (d, J = 2.2 Hz) ppm; IR (film) ν: 3427, 3276, 3143, 3001, 2926, 2855, 1621, 1552, 1496, 1464, 1443, 1378, 1337, 1274, 1244, 1182, 1145, 1118, 1091, 1035, 999, 959, 910, 842, 804, 762, 734, 680, 648, 613 cm^{-1}; HRMS (ES$^+$): calcd for $C_{15}H_{11}ClF_6N_5$ [M + H]$^+$, 410.0602; found, 410.0608.

(*S*)-5-Chloro-6-(2,6-difluoro-4-methylphenyl)-*N*-(1,1,1-trifluoropropan-2-yl)-[1,2,4]triazolo[1,5-*a*]pyrimidin-7-amine (18). General procedure C was followed using 5,7-dichloro-6-(2,6-difluoro-4-methylphenyl)-[1,2,4]triazolo[1,5-*a*]pyrimidine (0.050 g, 0.16 mmol) (**104**) and (*S*)-1,1,1-trifluoropropan-2-amine (0.038 g, 0.33 mmol). Purification via silica gel column chromatography (0−25% EtOAc in hexanes) provided the title compound as a white powder (0.028 g, 0.071 mmol, 65%). ^{1}H NMR (600 MHz, $CDCl_3$): δ 8.36 (s, 1H), 6.91 (d, J = 9.0 Hz, 2H), 6.00−5.94 (m, 1H), 4.73 (s, 1H), 2.45 (s, 3H), 1.39 (d, J = 7.0 Hz, 3H) ppm; ^{13}C NMR (150 MHz, $CDCl_3$): δ 160.75 (dd, J = 251.4, 7.0 Hz), 160.50 (dd, J = 249.9, 7.3 Hz), 158.07, 155.34, 154.11, 145.83, 144.86 (t, J = 10.2 Hz), 124.59 (q, J = 282.1 Hz), 112.93 (ddd, J = 65.8, 21.3, 4.0 Hz), 105.67 (t, J = 20.9 Hz), 92.50, 22.72−20.28 (m), 15.19 ppm; IR

https://dx.doi.org/10.1021/acs.jmedchem.0c01605
J. Med. Chem. 2021, 64, 1073−1102

(film) ν: 1618, 1559, 1143, 840 cm^{-1}; HRMS (ES^+): calcd for $C_{15}H_{12}N_5ClF_5$ $[M + H]^+$, 392.0696; found, 392.0693.

(*S*)-5-Chloro-6-(2,6-difluoro-4-(trifluoromethyl)phenyl)-*N*-(1,1,1-trifluoropropan-2-yl)-[1,2,4]triazolo[1,5-*a*]pyrimidin-7-amine (19). General procedure C was followed using 5,7-dichloro-6-(2,6-difluoro-4-(trifluoromethyl)phenyl)-[1,2,4]triazolo[1,5-*a*]-pyrimidine (0.350 g, 1.16 mmol) (**105**) and (*S*)-2-amino-1,1,1-trifluoropropane hydrochloride (0.389 g, 2.60 mmol). Purification via silica gel column chromatography (0−30% EtOAc in hexanes) provided the title compound as a white powder (0.240 g, 0.54 mmol, 62%). ^1H NMR (500 MHz, $CDCl_3$): δ 8.42 (s, 1H), 7.42 (d, J = 7.3 Hz, 2H), 5.87 (d, J = 10.5 Hz, 1H), 4.74 (s, 1H), 1.44 (d, J = 6.9 Hz, 3H) ppm; ^{13}C NMR (126 MHz, $CDCl_3$): δ 161.32 (dd, J = 255.5, 5.5 Hz), 160.96 (dd, J = 253.8, 5.6 Hz), 157.25, 155.74, 154.36, 145.83, 135.62 (qt, J = 35.0, 9.8 Hz), 124.53 (q, J = 280.6 Hz), 122.33 (qt, J = 273.4, 2.9 Hz), 112.99 (t, J = 20.1 Hz), 110.42 (dp, J = 24.9, 3.7 Hz), 109.93 (dp, J = 25.0, 3.8 Hz), 91.17, 51.21 (q, J = 32.2 Hz), 15.31 (d, J = 1.9 Hz) ppm; IR (film) ν: 3208, 2925, 2855, 1620, 1555, 1461, 1436, 1369, 1249, 1179, 1143, 1111, 1090, 1037, 963, 909, 896, 868, 819, 767, 734, 680, 652, 612 cm^{-1}; HRMS (ES^+): calcd for $C_{15}H_9ClF_8N_5$ $[M + H]^+$, 446.0413; found, 446.0438.

(*S*)-4-(5-Chloro-7-((1,1,1-trifluoropropan-2-yl)amino)-[1,2,4]triazolo[1,5-*a*]pyrimidin-6-yl)-3,5-difluorobenzonitrile (20). General procedure C was followed using 4-(5,7-dichloro-[1,2,4]triazolo[1,5-*a*]pyrimidin-6-yl)-3,5-difluorobenzonitrile (0.030 g, 0.09 mmol) (**106**) and (*S*)-1,1,1-trifluoropropan-2-amine (0.022 g, 0.19 mmol). Purification via silica gel column chromatography (0−40% EtOAc in hexanes) provided the title compound as a white powder (0.020 g, 0.05 mmol, 54%). ^1H NMR (600 MHz, $CDCl_3$): δ 8.41 (s, 1H), 7.44 (t, J = 7.1 Hz, 2H), 6.00 (d, J = 10.7 Hz, 1H), 4.77 (s, 1H), 1.45 (d, J = 6.9 Hz, 3H) ppm; ^{13}C NMR (150 MHz, $CDCl_3$): δ 161.28 (dd, J = 256.4, 5.9 Hz), 160.87 (dd, J = 254.7, 6.0 Hz), 156.84, 155.68, 154.32, 124.46 (q, J = 282.1 Hz), 116.58 (t, J = 11.8 Hz), 116.47 (ddd, J = 67.6, 25.4, 4.1 Hz), 115.79 (d, J = 3.5 Hz), 114.93 (t, J = 20.0 Hz), 90.61, 51.27 (q, J = 32.2 Hz), 29.83, 15.14 ppm; ^{19}F NMR (469 MHz): δ −78.31, −102.98, −105.00 ppm; IR (KBr): 2923, 2239, 1617, 1556, 1141 cm^{-1}; HRMS (ES^+): calcd for $C_{15}H_9N_6ClF_5$ $[M + H]^+$, 403.0492; found, 403.0486.

(*S*)-5-Chloro-6-(4-chloro-2,6-difluorophenyl)-*N*-(1,1,1-trifluoropropan-2-yl)-[1,2,4]triazolo[1,5-*a*]pyrimidin-7-amine (21). General procedure C was followed using 5,7-dichloro-6-(4-chloro-2,6-difluorophenyl)-[1,2,4]triazolo[1,5-*a*]pyrimidine (0.050 g, 0.15 mmol) (**108**) and (*S*)-1,1,1-trifluoropropan-2-amine (0.035 g, 0.31 mmol). Purification via silica gel column chromatography (0−40% EtOAc in hexanes) provided the title compound as a white powder (0.035 g, 0.085 mmol, 57%). ^1H NMR (600 MHz, $CDCl_3$): δ 8.40 (s, 1H), 7.18−7.16 (m, 2H), 5.93−5.88 (m, 1H), 4.75 (s, 1H), 1.43 (d, J = 6.9 Hz, 3H) ppm; ^{13}C NMR (150 MHz, $CDCl_3$): δ 160.84 (ddd, J = 253.4, 48.9, 9.1 Hz), 157.67, 155.57, 154.21, 145.82, 138.62 (t, J = 14.0 Hz), 124.53 (q, J = 280.5 Hz), 114.47−113.17 (m), 51.00 (q, J = 32.9 Hz), 15.27 ppm. IR (film) ν: 3000, 1571, 1517, 1142 cm^{-1}; HRMS (ES^+): calcd for $C_{14}H_9Cl_2F_5N_5$ $[M + H]^+$, 412.0150; found, 412.0146.

(*S*)-5-Chloro-6-(2,6-difluoro-4-nitrophenyl)-*N*-(1,1,1-trifluoropropan-2-yl)-[1,2,4]triazolo[1,5-*a*]pyrimidin-7-amine (22). General procedure C was followed using 5,7-dichloro-6-(2,6-difluoro-4-nitrophenyl)-[1,2,4]triazolo[1,5-*a*]pyrimidine (0.070 g, 0.21 mmol) (**109**) and (*S*)-1,1,1-trifluoropropan-2-amine (0.048 g, 0.42 mmol). Purification via silica gel column chromatography (0−40% EtOAc in hexanes) provided the title compound as a white powder (0.075 g, 0.18 mmol, 88%). ^1H NMR (600 MHz, $CDCl_3$): δ 8.41 (s, 1H), 8.00−7.98 (m, 2H), 5.99 (d, J = 10.6 Hz, 1H), 4.78 (s, 1H), 1.46 (d, J = 6.8 Hz, 3H) ppm; ^{13}C NMR (150 MHz, $CDCl_3$): δ 161.15 (dd, J = 257.2, 5.8 Hz), 160.73 (dd, J = 255.3, 6.1 Hz), 156.78, 155.75, 154.37, 150.43 (t, J = 10.5 Hz), 145.80, 124.47 (q, J = 282.2 Hz), 116.00 (t, J = 20.5 Hz), 108.53 (ddd, J = 61.2, 27.3, 4.0 Hz), 90.62, 51.38 (q, J = 32.1 Hz), 15.20 (d, J = 1.5 Hz) ppm; IR (film) ν: 1618, 1530, 1489, 1143, 1043 cm^{-1}; HRMS (ES^+): calcd for $C_{14}H_9ClF_5N_6O_2$ $[M + H]^+$, 423.0390; found, 423.0384.

(*S*)-6-(4-Amino-2,6-difluorophenyl)-5-chloro-*N*-(1,1,1-trifluoropropan-2-yl)-[1,2,4]triazolo[1,5-*a*]pyrimidin-7-amine (23). To a solution of (*S*)-5-chloro-6-(2,6-difluoro-4-nitrophenyl)-*N*-(1,1,1-trifluoropropan-2-yl)-[1,2,4]triazolo[1,5-*a*]pyrimidin-7-amine (0.025 g, 0.059 mmol) (**22**) in 0.100 mL of H_2O/MeOH (1:1) were added iron powder (0.017 g, 0.30 mmol) and ammonium chloride (0.013 g, 0.24 mmol). The mixture was stirred at 80 °C for 2 h and then filtered and rinsed with hot methanol. The filtrate was evaporated under reduced pressure, and the resulting mixture was purified by HPLC to afford the product as a white solid (0.016 g, 0.04 mmol, 69%). ^1H NMR (600 MHz, $CDCl_3$): δ 8.37 (s, 1H), 6.37 (t, J = 9.8 Hz, 2H), 5.93 (s, 1H), 4.86 (s, 1H), 4.28 (s, 2H), 2.17 (s, 1H), 1.41−1.39 (m, 3H) ppm; ^{13}C NMR (150 MHz, $CDCl_3$): δ 161.86 (ddd, J = 246.8, 32.1, 8.7 Hz), 158.99, 155.32, 154.09, 151.02 (t, J = 13.9 Hz), 146.15, 130.31, 128.98, 124.72 (q, J = 281.8 Hz), 98.19 (ddd, J = 63.6, 25.1, 3.2 Hz), 97.13 (t, J = 21.1 Hz), 92.99, 50.71 (q, J = 32.4 Hz), 31.08, 15.35 ppm; IR (film) ν: 3341, 1651, 1614, 1587, 1346 cm^{-1}; HRMS (ES^+): calcd for $C_{14}H_{11}ClF_5N_6$ $[M + H]^+$, 393.0648; found, 393.0646.

(*S*)-5-Chloro-6-(2,6-difluoro-4-methoxyphenyl)-*N*-(1,1,1-trifluoropropan-2-yl)-[1,2,4]triazolo[1,5-*a*]pyrimidin-7-amine (24). To a solution of (*S*)-5-chloro-6-(2,4,6-trifluorophenyl)-*N*-(1,1,1-trifluoropropan-2-yl)-[1,2,4]triazolo[1,5-*a*]pyrimidin-7-amine (0.020 g, 0.05 mmol) (**7**) in 0.3 mL of THF was added 0.04 mL of a 30% sodium methoxide solution in methanol at 0 °C. The reaction mixture was heated for 2 h at 60 °C in a microwave reactor and then cooled to rt and diluted with aqueous ammonium chloride solution. The aqueous phase was extracted with EtOAc (×3). The combined organic layers were washed with brine (×2), dried ($MgSO_4$), filtered, and concentrated. Purification by reverse-phase HPLC provided the title compound as a white solid (0.015 g, 0.036 mmol, 71% yield). ^1H NMR (500 MHz; $CDCl_3$): δ 8.45 (s, 1H), 6.67−6.65 (m, 2H), 5.94−5.93 (m, 1H), 4.77−4.74 (m, 1H), 3.90 (s, 3H), 1.41 (d, J = 6.8 Hz, 3H) ppm; ^{13}C NMR (126 MHz; $CDCl_3$): δ 163.48 (t, J = 13.9 Hz), 161.80 (dd, J = 249.9, 9.0 Hz), 161.54 (dd, J = 248.4, 8.9 Hz), 159.55 (q, J = 40.7 Hz), 158.79, 155.09, 146.15, 124.63 (q, J = 282.0 Hz), 100.62 (t, J = 21.1 Hz), 98.93 (td, J = 26.8, 3.0 Hz), 92.71, 56.30, 50.87 (q, J = 32.1 Hz), 15.32 ppm; IR (film) ν: 3340, 2953, 2924, 2848, 1642, 1618, 1579, 1553, 1147 cm^{-1}; HRMS (ES^+): calcd for $C_{15}H_{12}ClF_5N_5O$ $[M + H]^+$, 408.0651; found, 408.0652.

(*S*)-5-Chloro-6-(4-((3-(dimethylamino)propyl)sulfinyl)-2,6-difluorophenyl)-*N*-((*S*)-1,1,1-trifluoropropan-2-yl)-[1,2,4]-triazolo[1,5-*a*]pyrimidin-7-amine (26) and (*S*)-5-Chloro-6-(4-((3-(dimethylamino)propyl)sulfonyl)-2,6-difluorophenyl)-*N*-(1,1,1-trifluoropropan-2-yl)-[1,2,4]triazolo[1,5-*a*]pyrimidin-7-amine (27). To a solution of (*S*)-5-chloro-6-(4-((3-(dimethylamino)propyl)thio)-2,6-difluorophenyl)-*N*-(1,1,1-trifluoropropan-2-yl)-[1,2,4]triazolo[1,5-*a*]pyrimidin-7-amine (0.050 g, 0.100 mmol) (**25**) in CH_2Cl_2 (1.00 mL) was added *m*-CPBA (70%, 0.025 g, 0.100 mmol). After 2 h, the reaction mixture was concentrated under reduced pressure and purified by reverse-phase HPLC to obtain **26** (0.017 g, 0.03 mmol, 32%) and **27** (0.027 g, 0.05 mmol, 52%). (**26**): ^1H NMR (600 MHz, $CDCl_3$): δ 8.37 (s, 1H), 8.19 (s, 1H), 7.02 (d, J = 8.0 Hz, 2H), 6.69 (s, 1H), 5.41 (s, 1H), 3.76−3.67 (m, 2H), 3.40 (d, J = 10.2 Hz, 7H), 3.22−3.15 (m, 2H), 2.44−2.37 (m, 2H), 1.43 (d, J = 6.9 Hz, 3H) ppm; ^{13}C NMR (150 MHz, $CDCl_3$): δ 166.95, 161.56 (dd, J = 253.3, 6.8 Hz), 160.98 (dd, J = 252.6, 6.6 Hz), 157.65, 155.36, 154.85, 146.84, 125.91 (q), 112.00−110.04 (m), 107.56−105.57 (m), 92.69, 68.14, 57.73 (d, J = 11.8 Hz), 51.16 (q, J = 31.8 Hz), 29.62 (d, J = 2.0 Hz), 22.63 (d, J = 1.7 Hz), 14.82 ppm; IR (film) ν: 3053, 1589, 1535, 1178 cm^{-1}; HRMS (ES^+): calcd for $C_{19}H_{21}ClF_5N_6OS$ $[M + H]^+$, 511.1101; found, 511.1100. (**27**): ^1H NMR (600 MHz, $CDCl_3$): mixture of diastereomers δ 8.38 (s, 1H), 8.11 (s, 1H), 7.50 (dd, J = 16.6, 7.4 Hz, 1H), 7.17 (d, J = 7.0 Hz, 0.5H), 5.88 (s, 0.5H), 5.59 (s, 0.5H), 3.86−3.78 (m, 1H), 3.77−3.70 (m, 0.5H), 3.69−3.62 (m, 1H), 3.36 (dd, J = 25.9, 3.6 Hz, 6H), 3.40−3.27 (m, 0.5H), 2.99−2.90 (m, 1H), 2.51−2.40 (m, 1H), 2.36−2.26 (m, 1H), 1.42 (dd, J = 6.9, 2.9 Hz, 3H) ppm; ^{13}C NMR (150 MHz, $CDCl_3$): δ 167.52, 163.09−161.10 (m), 161.44 (ddd, J = 256.9, 21.4, 4.9 Hz), 157.00, 156.86, 155.45−155.33 (m), 155.12, 129.28−119.96 (m), 112.17 (td, J = 20.5, 4.6 Hz), 109.28−107.40 (m), 92.88, 92.30, 67.84, 67.54, 58.59, 58.51, 57.34, 56.93, 52.19, 51.77, 51.29 (td, J =

https://dx.doi.org/10.1021/acs.jmedchem.0c01605
J. Med. Chem. 2021, 64, 1073−1102

31.8, 17.1 Hz), 15.61, 15.10, 14.68, 14.46 (d, J = 1.7 Hz) ppm; IR (film) ν: 3285, 1589, 1535, 1142 cm^{-1}; HRMS (ES^+): calcd for $C_{19}H_{21}ClF_5N_6O_2S$ $[M + H]^+$, 527.1050; found, 527.1045.

(*S*)-5-Chloro-6-(2,6-difluoro-4-(methylthio)phenyl)-*N*-(1,1,1-trifluoropropan-2-yl)-[1,2,4]triazolo[1,5-*a*]pyrimidin-7-amine (28). To a suspension of sodium methanethiolate (0.331 mL, 0.71 mmol, 4 equiv) in DMSO (2 mL) at rt was added (*S*)-5-chloro-6-(2,4,6-trifluorophenyl)-*N*-(1,1,1-trifluoropropan-2-yl)-[1,2,4]triazolo-[1,5-*a*]pyrimidin-7-amine (0.070 g, 0.18 mmol, 1 equiv) (**7**) and the mixture was heated for 3 h at 60 °C before it was quenched at rt with a saturated NH_4Cl solution. The mixture was extracted with EtOAc and the combined organic layers were washed 5 times with H_2O, dried, and concentrated under reduced pressure to furnish the title compound as a white solid (0.070 g, 0.17 mmol, 93%). ^1H NMR (600 MHz, $CDCl_3$): δ 8.38 (s, 1H), 6.94−6.92 (m, 2H), 5.92 (br s, 1H), 4.79 (br s, 1H), 2.56 (s, 3H), 1.41 (d, J = 6.0 Hz, 3H) ppm; ^{13}C NMR (150 MHz, $CDCl_3$): δ 161.79 (dd, J = 40.77, 6.0 Hz), 160.11 (dd, J = 39.3, 7.6 Hz), 158.15, 155.51, 154.22, 146.81 (t, J = 10.6 Hz), 145.95, 124.63 (q, J = 282.4 Hz), 109.06 (dd, J = 24.2, 3.0 Hz), 108.69 (dd, J = 24.9, 3.0 Hz), 104.03 (t, J = 9.0 Hz), 92.28, 50.81 (q, J = 18.1 Hz), 15.31, 15.10 ppm; HRMS (ES^+): calcd for $C_{14}H_8N_4ClF_6O$ $[M + H]^+$, 397.0285; found, 397.0279.

5-Chloro-6-(2,6-difluoro-4-(methylsulfinyl)phenyl)-*N*-((*S*)-1,1,1-trifluoropropan-2-yl)-[1,2,4]triazolo[1,5-*a*]pyrimidin-7-amine (29). To a solution of (*S*)-5-chloro-6-(2,6-difluoro-4-(methylthio)phenyl)-*N*-(1,1,1-trifluoropropan-2-yl)-[1,2,4]triazolo-[1,5-*a*]pyrimidin-7-amine (0.029 g, 0.07 mmol, 1 equiv) (**28**) in CH_2Cl_2 (0.7 mL) at rt was added *m*-CPBA (0.012 g, 0.07 mmol, 1 equiv). After 1 h, the reaction was quenched with H_2O and extracted twice with EtOAc. The combined organic fractions were washed with a sat. aq. $Na_2S_2O_3$ solution, dried, and concentrated under vacuum. The crude yellow material was purified by reverse-phase HPLC (C18 column, H_2O/ACN 90/10 to 10/90, 15 min ramp) and lyophilized to furnish the title compound (0.021 g, 0.05 mmol, 70%) as a white solid. ^1H NMR (600 MHz, $CDCl_3$): mixture of diastereomers δ 8.43 (s, 1H), 8.08 (s, 1H), 7.98 (d, J = 6.0 Hz, 1H), 7.58 (d, J = 6.0 Hz, 1.6H), 7.51 (d, J = 6.0 Hz, 0.4H), 7.42 (d, J = 9.0 Hz, 1H), 7.38 (d, J = 6.0 Hz, 0.4H), 7.33 (d, J = 6.0 Hz, 0.6H), 5.93 (br s, 0.5H), 5.87 (br s, 0.3H), 4.75 (br s, 0.4H), 4.62 (br s, 0.5H), 2.88 (s, 3H), 1.44−1.42 (m, 3H) ppm; HRMS (ES^+): calcd for $C_{14}H_8N_4ClF_6O$ $[M + H]^+$, 440.0366; found, 440.0365.

(*S*)-5-Chloro-6-(2,6-difluoro-4-(methylsulfonyl)phenyl)-*N*-(1,1,1-trifluoropropan-2-yl)-[1,2,4]triazolo[1,5-*a*]pyrimidin-7-amine (30). To a solution of (*S*)-5-chloro-6-(2,6-difluoro-4-(methylthio)phenyl)-*N*-(1,1,1-trifluoropropan-2-yl)-[1,2,4]triazolo-[1,5-*a*]pyrimidin-7-amine (0.017 g, 0.04 mmol, 1 equiv) (**28**) in CH2Cl2 (0.7 mL) at rt was added 3-chlorobenzoperoxoic acid (0.021 g, 0.12 mmol, 3 equiv). After 1 h, the reaction was quenched with H_2O and extracted twice with EtOAc. The combined organic fractions were washed with a sat. aq $Na_2S_2O_3$ solution, dried, and concentrated under vacuum. Purification by reverse-phase HPLC (C18 column, H_2O/ACN 90/10 to 10/90, 15 min ramp) provided the title compound (0.013 g, 0.03 mmol, 71%) as a white solid. ^1H NMR (600 MHz, $CDCl_3$): δ 8.43 (s, 1H), 7.73 (d, J = 6.0 Hz, 2H), 5.82 (d, J = 6.0 Hz, 1H), 4.78 (br s, 1H), 3.21 (s, 3H), 1.45 (d, J = 6.0 Hz, 3H) ppm; HRMS (ES^+): calcd for $C_{14}5H_{12}N_45ClF_5O_2S$ $[M + H]^+$, 456.0315; found, 456.0311.

5-Chloro-*N*-isopropyl-6-(2,4,6-trifluorophenyl)-[1,2,4]-triazolo[1,5-*a*]pyrimidin-7-amine (35). Following general procedure C using 5,7-dichloro-6-(2,4,6-trifluorophenyl)-[1,2,4]triazolo-[1,5-*a*]pyrimidine (0.064 g, 0.20 mmol) (**102**), propan-2-amine (0.036 g, 0.60 mmol), *i*-Pr_2NEt (0.078 g, 0.60 mmol), and reverse-phase HPLC purification afforded the title compound as a white solid (0.030 g, 0.09 mmol, 44% yield). ^1H NMR (500 MHz; $CDCl_3$): δ 8.46 (s, 1H), 6.90−6.85 (m, 2H), 6.32 (d, J = 8.7 Hz, 1H), 3.62−3.60 (m, 1H), 1.19 (d, J = 6.4 Hz, 6H) ppm; ^{13}C NMR (126 MHz; $CDCl_3$): δ 164.27 (dt, J = 254.4, 15.2 Hz), 161.64 (dd, J = 251.0, 8.4 Hz), 161.53 (dd, J = 251.0, 8.4 Hz), 159.04, 153.77, 145.89, 106.92 (td, J = 20.7, 4.9 Hz), 101.46−101.02 (m), 90.00, 46.34, 23.82 ppm; IR (film) ν: 3344, 2982, 2936, 2873, 1615, 1579, 1264, 1208, 1171, 1124 cm^{-1}; HRMS (ES^+): calcd for $C_{14}H_{12}ClF_3N_5$ $[M + H]^+$, 342.0733; found, 342.0733.

5-Chloro-*N*-propyl-6-(2,4,6-trifluorophenyl)-[1,2,4]triazolo-[1,5-*a*]pyrimidin-7-amine (36). General procedure C was followed using 5,7-dichloro-6-(2,4,6-trifluorophenyl)-[1,2,4]triazolo[1,5-*a*]-pyrimidine (0.030 g, 0.09 mmol) (**102**) and propan-1-amine (0.012 g, 0.20 mmol). Purification via silica gel column chromatography (0−40% EtOAc in hexanes) provided the title compound as a white powder (0.020 g, 0.06 mmol, 62%). ^1H NMR (600 MHz, $CDCl_3$): δ 8.33 (s, 1H), 6.84−6.82 (m, 2H), 6.48 (t, J = 5.9 Hz, 1H), 2.98 (q, J = 6.7 Hz, 2H), 1.57 (h, J = 7.3 Hz, 2H), 0.85 (t, J = 7.4 Hz, 4H) ppm; ^{13}C NMR (150 MHz, $CDCl_3$): δ 163.93 (dt, J = 253.7, 15.4 Hz), 161.77 (ddd, J = 250.6, 14.9, 8.5 Hz), 158.16, 155.07, 153.65, 146.36, 107.18 (td, J = 20.8, 4.9 Hz), 101.12−100.62 (m), 88.91, 45.31, 29.83, 23.33, 11.04 ppm; IR (film) ν: 2923, 1573, 1439, 1122 cm^{-1}; HRMS (ES^+): calcd for $C_{14}H_{12}N_5ClF_3$ $[M + H]^+$, 342.0728; found, 342.0725.

5-Chloro-*N*-*iso*-butyl-6-(2,4,6-trifluorophenyl)-[1,2,4]-triazolo[1,5-*a*]pyrimidin-7-amine (37). General procedure C was followed using 5,7-dichloro-6-(2,4,6-trifluorophenyl)-[1,2,4]triazolo-[1,5-*a*]pyrimidine (0.030 g, 0.09 mmol) (**102**) and 2-methylpropan-1-amine (0.014 g, 0.20 mmol). Purification via silica gel column chromatography (0−40% EtOAc in hexanes) provided the title compound as a white powder (0.027 g, 0.08 mmol, 81%). ^1H NMR (600 MHz, $CDCl_3$): δ 8.33 (s, 1H), 6.88−6.81 (m, 2H), 6.56 (t, J = 6.1 Hz, 1H), 2.84 (t, J = 6.5 Hz, 2H), 1.77−1.70 (m, 1H), 0.84 (d, J = 6.7 Hz, 8H) ppm; ^{13}C NMR (150 MHz, $CDCl_3$): δ 164.05 (dt, J = 253.8, 15.1 Hz), 161.72 (ddd, J = 250.4, 14.9, 8.4 Hz), 158.13, 155.05, 153.63, 146.42, 107.31 (td, J = 20.8, 4.8 Hz), 102.26−98.14 (m), 88.95, 50.83, 29.05, 19.79 ppm; IR (film) ν: 2961, 2924, 1637, 1577, 1434 cm^{-1}; HRMS (ES^+): calcd for $C_{15}H_{14}N_5ClF_3$ $[M + H]^+$, 356.0884; found, 356.0887.

5-Chloro-6-(2,4,6-trifluorophenyl)-[1,2,4]triazolo[1,5-*a*]-pyrimidin-7-ol (38). This compound has been obtained as a side product from the attempt at synthetizing 5-chloro-*N*-isobutyl-*N*-(2,2,2-trifluoroethyl)-6-(2,4,6-trifluorophenyl)-[1,2,4]triazolo[1,5-*a*]-pyrimidin-7-amine. General procedure C was followed using 5,7-dichloro-6-(2,4,6-trifluorophenyl)-[1,2,4]triazolo[1,5-*a*]pyrimidine (0.064 g, 0.20 mmol) (**102**), 2-methyl-*N*-(2,2,2-trifluoroethyl)-propan-1-amine hydrochloride (0.115 g, 0.60 mmol), and *i*-Pr_2NEt (0.139 mL, 0.80 mmol). Purification via preparative reverse-phase HPLC provided the title compound (0.023 g, 0.08 mmol, 38%). ^1H NMR (500 MHz; MeOD): δ 8.74 (s, 1H), 6.97 (dd, J = 8.7, 7.8 Hz, 2H) ppm; ^{13}C NMR (126 MHz; MeOD): δ 164.78 (dt, J = 250.7, 16.4 Hz), 162.77 (ddd, J = 248.8, 15.2, 9.5 Hz), 159.40, 156.62, 108.75 (td, J = 21.2, 4.8 Hz), 102.66, 101.52−101.06 (m) ppm; IR (film) ν: 3446, 2789, 2684, 2549, 1683, 1667, 1655, 1635, 1616, 1600, 1558, 1532 cm^{-1}.

***N*-(5-Chloro-6-(2,4,6-trifluorophenyl)-[1,2,4]triazolo[1,5-*a*]-pyrimidin-7-yl)isobutyramide (39).** To a solution of 5-chloro-6-(2,4,6-trifluorophenyl)-[1,2,4]triazolo[1,5-*a*]pyrimidin-7-amine (0.035 g, 0.12 mmol, 1.00 equiv) (**102**) in anhydrous CH_2Cl_2 (0.450 mL) was added Et_3N (0.022 mL, 0.15 mmol, 1.30 equiv) and DMAP (0.001 g, 0.01 mmol, 0.10 equiv) under N_2 and the resulting solution was stirred at 0 °C. *iso*-Butyryl chloride (0.015 mL, 0.14 mmol, 1.20 equiv) was slowly added and the reaction was stirred at 0 °C for 30 min and rt for 18 h. Then, Et_3N (0.022 mL, 0.15 mmol, 1.30 equiv) and *iso*-butyryl chloride (0.015 mL, 0.14 mmol, 1.20 equiv) were added and the reaction was stirred at rt for 2 h. The reaction mixture was then concentrated under reduced pressure. Purification via preparative reverse-phase HPLC provided the title compound (0.023 g, 0.06 mmol, 53%). ^1H NMR (500 MHz, $CDCl_3$): δ 8.72 (s, 1H), 8.47 (s, 1H), 6.81 (t, J = 8.1 Hz, 2H), 2.66 (hept, J = 6.9 Hz, 1H), 1.12 (d, J = 6.9 Hz, 6H) ppm; ^{13}C NMR (126 MHz, $CDCl_3$): δ 173.47, 163.85 (dt, J = 252.8, 15.4 Hz), 160.51 (dd, J = 251.6, 9.0 Hz), 160.39 (dd, J = 251.7, 8.9 Hz), 158.48, 156.09, 153.73, 141.44, 107.40 (td, J = 19.8, 4.9 Hz), 104.48, 100.85 (td, J = 26.1, 3.4 Hz), 36.73, 19.10 ppm; IR (film) ν: 3415, 2974, 1732, 1618, 1515, 1487, 1440, 1384, 1263, 1230, 1153, 1126, 1040, 997, 842, 738, 669 cm^{-1};

https://dx.doi.org/10.1021/acs.jmedchem.0c01605
J. Med. Chem. 2021, 64, 1073−1102

HRMS (ES^+): calcd for $C_{15}H_{11}ClF_3N_5NaO$ $[M + Na]^+$, 392.0502; found, 392.0488.

5-Chloro-*N*-phenyl-6-(2,4,6-trifluorophenyl)-[1,2,4]triazolo-[1,5-*a*]pyrimidin-7-amine (40). To a solution of 5,7-dichloro-6-(2,4,6-trifluorophenyl)-[1,2,4]triazolo[1,5-*a*]pyrimidine (0.053 g, 0.17 mmol) (**102**) and aniline (0.015 mL, 0.17 mmol) in DMF (1.67 mL) was added K_2CO_3 (0.046 g, 0.33 mmol) and the resulting mixture was stirred for 24 h at 30 °C. The reaction mixture was then diluted with H_2O. The organic layer was washed with a 1 N HCl (×2), the aqueous phase was extracted with EtOAc (×3), and the combined organic layers were washed with brine (×2), dried over $MgSO_4$, filtered, and concentrated. Purification via silica gel column chromatography (0−40% EtOAc in hexanes) provided the title compound as a white powder (0.049 g, 0.13 mmol, 78%). ^1H NMR (500 MHz, $CDCl_3$): δ 8.43 (s, 1H), 8.24 (s, 1H), 7.16−7.11 (m, 3H), 7.10−7.00 (m, 2H), 6.36 (t, J = 8.2 Hz, 2H) ppm; ^{13}C NMR (126 MHz, $CDCl_3$): δ 164.69 (dt, J = 255.2, 15.1 Hz), 161.57 (ddd, J = 253.8, 15.0, 8.2 Hz), 161.32 (ddd, J = 251.3, 14.9, 8.2 Hz), 158.29, 155.56, 153.98, 146.56, 124.53 (q, J = 283.5 Hz), 101.86 (td, J = 25.8, 4.1 Hz), 101.36 (td, J = 25.2, 2.4 Hz), 90.99, 58.99 (q, J = 29.4 Hz), 28.34, 19.81, 16.74 ppm; IR (film) ν: 3423, 1638, 1613, 1563, 1491, 1440, 1335, 1261, 1197, 1122, 1036, 998, 940, 840, 766, 694, 668 cm^{-1}; HRMS (ES^+): calcd for $C_{17}H_{10}ClF_3N_5$ $[M + H]^+$, 376.0571; found, 376.0571.

***N*-Benzyl-5-chloro-6-(2,4,6-trifluorophenyl)-[1,2,4]triazolo-[1,5-*a*]pyrimidin-7-amine (41).** Following general procedure C using 5,7-dichloro-6-(2,4,6-trifluorophenyl)-[1,2,4]triazolo[1,5-*a*]-pyrimidine (0.064 g, 0.20 mmol) (**102**) and benzylamine (0.064 g, 0.60 mmol), reverse-phase HPLC purification afforded the title compound as a yellow solid (0.024 g, 0.06 mmol, 31% yield). ^1H NMR (500 MHz; $CDCl_3$): δ 8.45 (s, 1H), 7.33−7.31 (m, 3H), 7.08−7.06 (m, J = 6.5, 2.7 Hz, 2H), 6.89−6.88 (m, 1H), 6.89−6.86 (m, 1H), 6.72 (dd, J = 8.5, 6.8 Hz, 2H), 4.33 (d, J = 5.9 Hz, 2H) ppm; ^{13}C NMR (126 MHz; $CDCl_3$): δ 164.32 (dt, J = 254.1, 15.1 Hz), 164.01, 161.77 (ddd, J = 250.8, 14.9, 8.2 Hz), 159.63 (q, J = 40.8 Hz), 159.26, 154.03, 146.40, 135.30, 129.28, 128.75, 126.77, 106.56 (td, J = 20.7, 4.8 Hz), 101.15−100.70 (m), 90.43, 47.76 ppm; IR (film) ν: 3352, 3268, 3113, 3067, 3033, 2928, 1642, 1617, 1595, 1575, 1495, 1441, 1124, 1036 cm^{-1}; HRMS (ES^+): calcd for $C_{18}H_{12}ClF_3N_5$ $[M + H]^+$, 390.0733; found, 390.0730.

5-Chloro-6-(2,4,6-trifluorophenyl)-7-((1,1,1-trifluoropropan-2-yl)oxy)-[1,2,4]triazolo[1,5-*a*]pyrimidine (42). To sodium hydride (60%, 0.015 g, 0.38 mmol) suspended in THF (3 mL) was added 1,1,1-trifluoropropan-2-ol (0.034 mL, 0.38 mmol) and the resulting mixture was stirred for 2 h while heating to reflux. 5,7-Dichloro-6-(2,4,6-trifluorophenyl)-[1,2,4]triazolo[1,5-*a*]pyrimidine (0.100 g, 0.31 mmol) (**102**) was then added at rt. The reaction mixture was stirred for 20 min before the reaction was quenched with H_2O (5 mL) and extracted with EtOAc (×3). The combined organic layers were dried over $MgSO_4$, filtered, and concentrated under reduced pressure. Purification via silica gel column chromatography (0−40% EtOAc in hexanes) provided the title compound (0.046 g, 0.11 mmol, 37%). ^1H NMR (600 MHz, $CDCl_3$): δ 8.51 (s, 1H), 6.89−6.77 (m, 2H), 6.21−6.12 (m, 1H), 1.63 (d, J = 6.6 Hz, 4H) ppm; ^{13}C NMR (150 MHz, $CDCl_3$): δ 164.14 (dt, J = 253.1, 15.2 Hz), 161.12 (ddd, J = 252.7, 15.1, 8.7 Hz), 160.86 (ddd, J = 251.3, 15.0, 8.6 Hz), 158.43, 156.71, 155.59 (d, J = 43.8 Hz), 151.92, 123.23 (q, J = 281.1 Hz), 104.10 (td, J = 20.5, 4.9 Hz), 102.40−98.42 (m), 76.02 (q, J = 32.7, 31.8 Hz), 14.07, 12.80 ppm; IR (film) ν: 2925, 2854, 1606, 1517, 1493 cm^{-1}; HRMS (ES^+): calcd for $C_{14}H_8N_4ClF_6O$ $[M + H]^+$, 397.0285; found, 397.0279.

5-Chloro-*N*-(1,1-difluoropropan-2-yl)-6-(2,4,6-trifluorophenyl)-[1,2,4]triazolo[1,5-*a*]pyrimidin-7-amine (43). General procedure C was followed using 5,7-dichloro-6-(2,5-difluorophenyl)-[1,2,4]triazolo[1,5-*a*]pyrimidine (0.053 g, 0.17 mmol) (**102**), 1,1-difluoropropan-2-amine hydrochloride (0.045 g, 0.34 mmol), and Et_3N (0.093 mL, 0.67 mmol). Purification via silica gel column chromatography (0−30% EtOAc in hexanes) provided the title compound as a white powder (0.035 g, 0.09 mmol, 56%). ^1H NMR (500 MHz, $CDCl_3$): δ 8.37 (s, 1H), 6.89 (t, J = 7.9 Hz, 2H), 6.00 (d, J = 8.2 Hz, 1H), 5.75 (td, J = 55.4, 1.6 Hz, 1H), 4.32 (br s, 1H), 1.31 (d, J = 6.8 Hz, 3H) ppm; ^{13}C NMR (151 MHz, $CDCl_3$): δ 164.46 (dt, J = 254.9, 15.1 Hz), 161.5 (ddd, J = 250.66, 8.4, 5.4 Hz), 161.41 (ddd, J = 252.17, 8.3, 5.3 Hz), 157.94, 155.46, 154.22, 114.59 (t, J = 246.2 Hz), 105.90 (td, J = 20.5, 4.8 Hz), 101.54 (dtd, J = 29.9, 25.9, 4.1 Hz), 90.88, 51.09 (t, J = 24.16 Hz), 42.38 (t, J = 552.1 Hz), 29.82, 14.61 (t, J = 3.8 Hz) ppm; IR (film) ν: 1613, 1578, 1552, 1527, 1492, 1461, 1440, 1360, 1263, 1124, 1208, 1171, 1134, 1122, 1100, 1083 cm^{-1}; HRMS (ES^+): calcd for $C_{15}H_{10}ClF_5N_4$ $[M + H]^+$, 378.0539; found, 378.0537.

5-Chloro-*N*-(1-fluoropropan-2-yl)-6-(2,4,6-trifluorophenyl)-[1,2,4]triazolo[1,5-*a*]pyrimidin-7-amine (44). General procedure C was followed using 5,7-dichloro-6-(2,5-difluorophenyl)-[1,2,4]-triazolo[1,5-*a*]pyrimidine (0.073 g, 0.23 mmol) (**102**), 1-fluoropropan-2-amine hydrochloride (0.053 g, 0.47 mmol), and Et_3N (0.130 mL, 0.91 mmol). Purification via silica gel column chromatography (0−30% EtOAc in hexanes) provided the title compound as a white powder (0.059 g, 0.16 mmol, 72%). ^1H NMR (600 MHz, $CDCl_3$): δ 8.35 (s, 1H), 6.93−6.83 (m, 2H), 6.26 (d, J = 8.1 Hz, 1H), 4.37 (ddd, J = 66, 9.6, 3.5 Hz, 1H), 4.29 (ddd, J = 66, 9.6, 4.3 Hz, 1H), 4.01 (br s, 1H), 1.26 (d, J = 6.8 Hz, 3H) ppm; ^{13}C NMR (151 MHz, $CDCl_3$): δ 164.29 (dt, J = 254.6, 15.2 Hz), 161.53 (ddd, J = 250.7, 14.9, 8.3, Hz), 161.52 (ddd, J = 249.9, 14.9, 8.3, Hz), 157.98, 155.28, 154.08, 146.19, 106.53 (td, J = 20.7, 4.7 Hz), 101.39 (tdd, J = 25.9, 9.1, 4.1 Hz), 90.03, 85.42 (d, J = 175.2 Hz), 49.79 (d, J = 19.6 Hz), 17.59 (d, J = 5.3 Hz), 14.32 ppm; IR (film) ν: 1639, 1611, 1594, 1580, 1492, 1468, 1440, 1358, 1239, 1207, 1171 cm^{-1}; HRMS (ES^+): calcd for $C_{15}H_{11}ClF_4N_4$ $[M + H]^+$, 360.0634; found, 360.0636.

(*S*)-5-Chloro-*N*-(3-methylbutan-2-yl)-6-(2,4,6-trifluorophenyl)-[1,2,4]triazolo[1,5-*a*]pyrimidin-7-amine (45). General procedure C was followed using 5,7-dichloro-6-(2,4,6-trifluorophenyl)-[1,2,4]triazolo[1,5-*a*]pyrimidine (0.119 g, 0.37 mmol) (**102**) and (*S*)-3-methylbutan-2-amine (0.090 mL, 0.78 mmol). Purification via silica gel column chromatography (0−15% EtOAc in hexanes) provided the title compound as a white powder (0.099 g, 0.27 mmol, 72%). The spectroscopic properties of the compound were identical to those reported for its enantiomer, **3**.[11]

(*R*)-5-Chloro-*N*-(1,1,1-trifluoro-3-methylbutan-2-yl)-6-(2,4,6-trifluorophenyl)-[1,2,4]triazolo[1,5-*a*]pyrimidin-7-amine (46). General procedure C was followed using 5,7-dichloro-6-(2,4,6-trifluorophenyl)-[1,2,4]triazolo[1,5-*a*]pyrimidine (0.123 g, 0.38 mmol) (**102**) and (*R*)-1,1,1-trifluoro-3-methyl-2-butylamine (0.152 mL, 1.15 mmol). Purification via silica gel column chromatography (0−15% EtOAc in hexanes) provided the title compound as a white powder (0.056 g, 0.13 mmol, 35%). ^1H NMR (500 MHz, $CDCl_3$): δ 8.41 (s, 1H), 7.01−6.77 (m, 2H), 6.28 (s, 1H), 3.96 (s, 1H), 2.26−2.09 (m, 1H), 1.03 (d, J = 6.9 Hz, 3H), 0.97 (d, J = 6.8 Hz, 3H) ppm; ^{13}C NMR (126 MHz, $CDCl_3$): δ 164.69 (dt, J = 255.2, 15.1 Hz), 161.57 (ddd, J = 253.8, 15.0, 8.2 Hz), 161.32 (ddd, J = 251.3, 14.9, 8.2 Hz), 158.29, 155.56, 153.98, 146.56, 124.53 (q, J = 283.5 Hz), 101.86 (td, J = 25.8, 4.1 Hz), 101.36 (td, J = 25.2, 2.4 Hz), 90.99, 58.99 (q, J = 29.4 Hz), 28.34, 19.81, 16.74 ppm; IR (film) ν: 3339, 2972, 2928, 1618, 1562, 1493, 1442, 1364, 1264, 1170, 1126, 1090, 1039, 999, 937, 911, 846, 768, 734, 705, 653 cm^{-1}; HRMS (ES^+): calcd for $C_{16}H_{12}ClF_6N_5Na$ $[M + Na]^+$, 446.0583; found, 446.0598.

(*S*)-5-Chloro-*N*-(1,1,1-trifluoro-3-methylbutan-2-yl)-6-(2,4,6-trifluorophenyl)-[1,2,4]triazolo[1,5-*a*]pyrimidin-7-amine (47). General procedure C was followed using 5,7-dichloro-6-(2,4,6-trifluorophenyl)-[1,2,4]triazolo[1,5-*a*]pyrimidine (0.123 g, 0.38 mmol) (**102**) and (*S*)-1,1,1-trifluoro-3-methyl-2-butylamine (0.152 mL, 1.15 mmol). Purification via silica gel column chromatography (0−15% EtOAc in hexanes) provided the title compound as a white powder (0.039 g, 0.09 mmol, 24%). ^1H NMR (500 MHz, $CDCl_3$): δ 8.41 (s, 1H), 6.99−6.84 (m, 2H), 6.29 (s, 1H), 3.98 (s, 1H), 2.24−2.10 (m, J = 6.7 Hz, 1H), 1.03 (d, J = 6.8 Hz, 3H), 0.97 (d, J = 6.8 Hz, 3H) ppm; ^{13}C NMR (126 MHz, $CDCl_3$): δ 164.63 (dt, J = 255.2, 15.0 Hz), 161.50 (ddd, J = 253.8, 14.9, 8.2 Hz), 161.25 (ddd, J = 251.3, 14.9, 8.2 Hz), 158.23, 155.49, 153.90, 146.50, 124.47 (q, J = 283.5 Hz), 101.80 (td, J = 25.8, 4.2 Hz), 101.30 (td, J = 27.1, 26.1, 3.7 Hz), 90.92, 58.93 (q, J = 29.4 Hz), 28.28, 19.75, 16.68 ppm; IR (film)

https://dx.doi.org/10.1021/acs.jmedchem.0c01605
J. Med. Chem. 2021, 64, 1073−1102

ν: 3339, 2972, 2930, 1618, 1562, 1493, 1459, 1442, 1364, 1264, 1170, 1126, 1090, 1066, 1038, 999, 938, 846, 768, 738, 704, 628 cm^{-1}; HRMS (ES^+): calcd for $C_{16}H_{13}ClF_6N_5$ $[M + H]^+$, 424.0758; found, 424.0762.

(*R*)-5-Chloro-6-(2,4,6-trifluorophenyl)-*N*-(1,1,1-trifluoropropan-2-yl)-[1,2,4]triazolo[1,5-*a*]pyrimidin-7-amine (48). General procedure A was followed using (*R*)-1,1,1-trifluoropropan-2-amine hydrochloride (0.090 g, 0.60 mmol), *i*-Pr_2NEt (0.078 g, 0.60 mmol), and 5,7-dichloro-6-(2,4,6-trifluorophenyl)-[1,2,4]triazolo[1,5-*a*]-pyrimidine (0.064 g, 0.20 mmol) (**102**). Purification via reverse-phase HPLC afforded the title compound as a white solid (0.017 g, 0.04 mmol, 21% yield). ^1H NMR (500 MHz; $CDCl_3$): δ 8.39 (s, 1H), 6.91 (dd, J = 8.4, 7.1 Hz, 2H), 5.92 (d, J = 10.3 Hz, 1H), 4.73 (s, 1H), 1.43 (d, J = 6.9 Hz, 3H) ppm; ^{13}C NMR (126 MHz; $CDCl_3$): δ 164.64 (dt, J = 255.3, 15.1 Hz), 161.65 (ddd, J = 253.4, 15.1, 8.2 Hz), 161.32 (ddd, J = 251.7, 14.9, 8.2 Hz), 157.97, 155.60, 154.26, 145.97, 124.57 (q, J = 282.0 Hz), 105.51 (td, J = 20.7, 4.8 Hz), 101.61 (dtd, J = 52.6, 26.1, 4.0 Hz), 91.50, 51.02 (q, J = 32.2 Hz), 15.30 ppm; IR (film) ν: 3335, 3205, 2924, 2852, 1621, 1558, 1272, 1251, 1175, 1145, 1120 cm^{-1}; HRMS (ES^+): calcd for $C_{14}H_9ClF_6N_5$ $[M + H]^+$, 396.0451; found, 396.0451.

7-(Azetidin-1-yl)-5-chloro-6-(2,4,6-trifluorophenyl)-[1,2,4]-triazolo[1,5-*a*]pyrimidine (49). General procedure C was followed using 5,7-dichloro-6-(2,4,6-trifluorophenyl)-[1,2,4]triazolo[1,5-*a*]-pyrimidine (0.064 g, 0.20 mmol) (**102**) and azetidine (0.034 g, 0.60 mmol). Purification via reverse-phase HPLC afforded the title compound as a white solid (0.005 g, 0.02 mmol, 8% yield). ^1H NMR (500 MHz; $CDCl_3$): δ 8.34 (s, 1H), 6.84−6.79 (m, 2H), 4.49−4.45 (m, 4H), 2.37 (quintet, J = 7.9 Hz, 2H) ppm; ^{13}C NMR (126 MHz; $CDCl_3$): δ 164.10 (dt, J = 253.9, 15.2 Hz), 162.35 (dd, J = 249.8, 8.2 Hz), 162.23 (dd, J = 249.7, 8.4 Hz), 158.12, 155.06, 155.04, 154.45, 146.35, 106.96 (td, J = 21.0, 4.6 Hz), 100.80−100.36 (m), 89.00, 56.73, 29.86, 17.36 ppm; IR (film) ν: 2957, 2924, 2852, 1594, 1558, 1455, 1255, 1167, 1120, 1041 cm^{-1}; HRMS (ES^+): calcd for $C_{14}H_9ClF_3N_5$ $[M + H]^+$, 340.0577; found, 340.0573.

5-Chloro-7-(pyrrolidin-1-yl)-6-(2,4,6-trifluorophenyl)-[1,2,4]triazolo[1,5-*a*]pyrimidine (50). General procedure C was followed using 5,7-dichloro-6-(2,4,6-trifluorophenyl)-[1,2,4]triazolo-[1,5-*a*]pyrimidine (0.064 g, 0.20 mmol) (**102**) and pyrrolidine (0.043 g, 0.60 mmol). Purification by reverse-phase HPLC afforded the title compound as a yellow solid (0.009 g, 0.03 mmol, 14% yield). ^1H NMR (500 MHz; $CDCl_3$): δ 8.37 (s, 1H), 6.81 (dd, J = 8.4, 6.9 Hz, 2H), 3.71 (t, J = 6.5 Hz, 4H), 1.91 (dt, J = 6.2, 3.3 Hz, 4H) ppm; ^{13}C NMR (126 MHz; $CDCl_3$): δ 163.80 (dt, J = 252.3, 14.5 Hz), 161.66 (dd, J = 248.1, 7.1 Hz), 161.55 (dd, J = 249.6, 8.3 Hz), 158.54, 155.74, 154.26, 148.57, 109.66 (td, J = 20.7, 4.9 Hz), 100.94−100.50 (m), 92.85, 53.27, 25.94 ppm; IR (film) ν: 3444, 1636, 1594, 1537, 1455, 1333, 1253, 1123 cm^{-1}. HRMS (ES^+): calcd for $C_{15}H_{12}ClF_3N_5$ $[M + H]^+$: 354.0733; found, 354.0723.

5-Chloro-7-(piperidin-1-yl)-6-(2,4,6-trifluorophenyl)-[1,2,4]-triazolo[1,5-*a*]pyrimidine (51). General procedure C was followed using 5,7-dichloro-6-(2,4,6-trifluorophenyl)-[1,2,4]triazolo[1,5-*a*]-pyrimidine (0.064 g, 0.20 mmol) (**102**) and piperidine (0.051 g, 0.60 mmol). Purification via reverse-phase HPLC afforded the title compound as a yellow solid (0.012 g, 0.03 mmol, 17% yield). ^1H NMR (500 MHz; $CDCl_3$): δ 8.40 (s, 1H), 6.86 (dd, J = 8.4, 7.3 Hz, 2H), 3.27 (br s, 4H), 1.64 (br s, 6H) ppm; ^{13}C NMR (126 MHz; $CDCl_3$): δ 163.71 (dt, J = 252.8, 15.4 Hz), 161.19 (dd, J = 250.3, 8.7 Hz), 161.08 (dd, J = 250.1, 8.8 Hz), 158.24, 155.29, 151.15, 108.64 (td, J = 20.2, 4.8 Hz), 101.30−100.86 (m), 98.10, 51.13, 25.98, 23.71 ppm; IR (film) ν: 2945, 2929, 2857, 1595, 1558, 1538, 1506, 1446, 1361, 1121, 1035 cm^{-1}; HRMS (ES^+): calcd for $C_{16}H_{14}ClF_3N_5$ $[M + H]^+$, 368.0890; found, 368.0877.

7-(Azepan-1-yl)-5-chloro-6-(2,4,6-trifluorophenyl)-[1,2,4]-triazolo[1,5-*a*]pyrimidine (52). General procedure C was followed using 5,7-dichloro-6-(2,4,6-trifluorophenyl)-[1,2,4]triazolo[1,5-*a*]-pyrimidine (0.197 g, 0.62 mmol) (**102**) and azepane (0.184 g, 1.85 mmol). Purification via silica gel column chromatography (0−15% EtOAc in hexanes) provided the title compound as a white powder (0.057 g, 0.15 mmol, 24%). ^1H NMR (500 MHz, $CDCl_3$): δ 8.36 (s, 1H), 6.85 (t, J = 8.1 Hz, 2H), 3.45−3.39 (m, 4H), 1.76−1.67 (m, 4H), 1.65−1.58 (m, 4H) ppm; ^{13}C NMR (126 MHz, $CDCl_3$): δ 163.64 (dt, J = 253.0, 15.4 Hz), 161.10 (dd, J = 250.2, 8.8 Hz), 160.98 (dd, J = 250.3, 8.8 Hz), 158.21, 155.45, 155.08, 152.31, 109.08 (td, J = 20.4, 5.0 Hz), 102.17−100.48 (m), 98.50, 53.70, 28.28, 28.23 ppm; IR (film) ν: 3436, 2932, 2858, 1637, 1593, 1525, 1492, 1443, 1357, 1284, 1259, 1231, 1200, 1171, 1152, 1125, 1100, 1035, 998, 968, 931, 842, 776, 760, 732, 656, 636, 614 cm^{-1}; HRMS (ES^+): calcd for $C_{17}H_{16}ClF_3N_5$ $[M + H]^+$, 382.1041; found, 382.1031.

7-(Azocan-1-yl)-5-chloro-6-(2,4,6-trifluorophenyl)-[1,2,4]-triazolo[1,5-*a*]pyrimidine (53). General procedure C was followed using 5,7-dichloro-6-(2,4,6-trifluorophenyl)-[1,2,4]triazolo[1,5-*a*]-pyrimidine (0.191 g, 0.60 mmol) (**102**) and azocane (0.142 g, 1.26 mmol). Purification via silica gel column chromatography (0−20% EtOAc in hexanes) provided the title compound as a white powder (0.177 g, 0.45 mmol, 75%).

^1H NMR (500 MHz, $CDCl_3$): δ 8.32 (s, 1H), 6.81 (t, J = 7.9 Hz, 2H), 3.49−3.38 (m, 4H), 1.78−1.15 (m, 10H) ppm; ^{13}C NMR (126 MHz, $CDCl_3$): δ 163.63 (dt, J = 253.5, 15.2 Hz), 160.93 (dd, J = 250.6, 8.9 Hz), 160.81 (dd, J = 250.5, 8.7 Hz), 158.19, 155.50, 154.73, 151.18, 108.91 (td, J = 20.2, 4.8 Hz), 102.27−100.10 (m), 98.25, 51.91, 27.67, 26.77, 24.36 ppm; IR (film) ν: 3450, 2927, 2860, 1637, 1593, 1529, 1494, 1440, 1375, 1356, 1266, 1230, 1212, 1171, 1151, 1124, 1091, 1035, 998, 967, 914, 846, 761, 735, 656, 636, 612 cm^{-1}; HRMS (ES^+): calcd for $C_{18}H_{18}ClF_3N_5$ $[M + H]^+$, 396.1197; found, 396.1201.

5-Chloro-*N*-cyclopropyl-6-(2,4,6-trifluorophenyl)-[1,2,4]-triazolo[1,5-*a*]pyrimidin-7-amine (55). General procedure C was followed using 5,7-dichloro-6-(2,4,6-trifluorophenyl)-[1,2,4]triazolo-[1,5-*a*]pyrimidine (0.064 g, 0.20 mmol) (**102**), cyclopropanamine (0.057 g, 0.60 mmol), and *i*-Pr_2NEt (0.078 g, 0.60 mmol). Purification via reverse-phase HPLC afforded the title compound as a beige solid (0.021 g, 0.06 mmol, 30% yield). ^1H NMR (500 MHz; $CDCl_3$): δ 8.34 (s, 1H), 6.84−6.80 (m, 3H), 2.36−2.33 (m, 1H), 0.68−0.65 (m, 2H), 0.48−0.44 (m, 2H) ppm; ^{13}C NMR (126 MHz; $CDCl_3$): δ 163.93 (dt, J = 252.6, 13.5 Hz), 162.00 (dd, J = 249.8, 8.5 Hz), 161.88 (dd, J = 250.1, 9.0 Hz), 158.41, 155.18, 153.53, 147.23, 147.17, 108.06 (td, J = 20.8, 5.0 Hz), 100.71−100.27 (m), 89.74, 89.70, 25.70, 25.56, 9.00, 8.96 ppm; IR (film) ν: 3361, 3260, 3104, 2919, 1597, 1576, 1494, 1441, 1264, 1123, 1032 cm^{-1}; HRMS (ES^+): calcd for $C_{14}H_{19}ClF_3N_5$ $[M + H]^+$, 340.0577; found, 340.0574.

5-Chloro-*N*-cyclobutyl-6-(2,4,6-trifluorophenyl)-[1,2,4]-triazolo[1,5-*a*]pyrimidin-7-amine (56). General procedure C was followed using 5,7-dichloro-6-(2,4,6-trifluorophenyl)-[1,2,4]triazolo-[1,5-*a*]pyrimidine (0.030 g, 0.09 mmol) (**102**) and cyclobutanamine (0.014 g, 0.20 mmol). Purification via silica gel column chromatography (0−40% EtOAc in hexanes) provided the title compound as a white powder (0.025 g, 0.07 mmol, 75%). ^1H NMR (600 MHz, $CDCl_3$): δ 8.35 (s, 1H), 6.85−6.81 (m, 2H), 6.61 (d, J = 7.5 Hz, 1H), 3.71 (q, J = 7.7 Hz, 1H), 2.08−1.94 (m, 4H), 1.80−1.73 (m, 1H), 1.60−1.51 (m, 1H), 1.24 (s, 1H) ppm; ^{13}C NMR (150 MHz, $CDCl_3$): δ 164.03 (dt, J = 253.8, 15.4 Hz), 161.71 (ddd, J = 250.5, 15.1, 8.4 Hz), 158.22, 155.04, 145.33, 120.10, 102.32−99.71 (m), 89.07, 48.80, 31.96, 14.62 ppm; IR (film) 3285, 2838, 2178, 1571 cm^{-1}; HRMS (ES^+): calcd for $C_{15}H_{12}ClF_3N_5$ $[M + H]^+$, 354.0728; found, 354.0726.

5-Chloro-*N*-cyclopentyl-6-(2,4,6-trifluorophenyl)-[1,2,4]-triazolo[1,5-*a*]pyrimidin-7-amine (57). General procedure C was followed using 5,7-dichloro-6-(2,4,6-trifluorophenyl)-[1,2,4]triazolo-[1,5-*a*]pyrimidine (0.030 g, 0.09 mmol) (**102**) and cyclopentanamine (0.017 g, 0.20 mmol). Purification via silica gel column chromatography (0−40% EtOAc in hexanes) provided the title compound as a white powder (0.027 g, 0.07 mmol, 78%). ^1H NMR (600 MHz, $CDCl_3$): δ 8.31 (s, 1H), 6.84−6.81 (m, 2H), 6.42 (d, J = 8.3 Hz, 1H), 3.63 (s, 1H), 1.82−1.59 (m, 4H), 1.62−1.38 (m, 4H) ppm. ^{13}C NMR (150 MHz, $CDCl_3$): δ 163.99 (dt, J = 253.7, 15.2 Hz), 161.66 (ddd, J = 250.5, 15.0, 8.4 Hz), 158.19, 154.93, 145.81, 101.30−100.53 (m), 88.98, 55.11, 34.64, 23.92 ppm; IR (film) ν: 3195, 2838, 1678, 1553 cm^{-1}; HRMS (ES^+): calcd for $C_{16}H_{14}N_5ClF_3$ $[M + H]^+$, 368.0884; found, 368.0881.

https://dx.doi.org/10.1021/acs.jmedchem.0c01605
J. Med. Chem. 2021, 64, 1073−1102

5-Chloro-*N*-cyclohexyl-6-(2,4,6-trifluorophenyl)-[1,2,4]-triazolo[1,5-*a*]pyrimidin-7-amine (58). General procedure C was followed using 5,7-dichloro-6-(2,4,6-trifluorophenyl)-[1,2,4]triazolo-[1,5-*a*]pyrimidine (0.100 g, 0.31 mmol) (**102**) and cyclohexanamine (0.094 g, 0.94 mmol). Purification via silica gel column chromatography (0−40% EtOAc in hexanes) provided the title compound as a white powder (0.119 g, 0.31 mmol, 99%). ^{1}H NMR (500 MHz, $CDCl_3$): δ 8.33 (s, 1H), 6.92−6.81 (m, 2H), 6.37 (d, J = 8.7 Hz, 1H), 3.14−2.98 (m, 1H), 1.86−1.77 (m, 2H), 1.74−1.64 (m, 2H), 1.53 (dt, J = 13.2, 3.8 Hz, 1H), 1.30−1.18 (m, 2H), 1.12 (tdd, J = 12.9, 9.8, 6.1 Hz, 1H), 1.01−0.85 (m, 2H) ppm; ^{13}C NMR (126 MHz, $CDCl_3$): δ 164.08 (dt, J = 253.8, 15.1 Hz), 161.76 (dd, J = 250.7, 8.5 Hz), 161.65 (dd, J = 250.7, 8.4 Hz), 158.12, 155.00, 153.74, 145.59, 107.50 (td, J = 20.7, 4.8 Hz), 102.70−97.55 (m), 88.82, 52.94, 34.06, 24.92, 24.75 ppm; IR (film) ν: 3341, 3103, 2934, 2856, 2239, 1636, 1610, 1578, 1492, 1439, 1367, 1341, 1313, 1263, 1207, 1159, 1125, 1036, 998, 976, 957, 930, 844, 766, 733, 655, 627 cm^{-1}; HRMS (ES$^+$): calcd for $C_{17}H_{16}ClF_3N_5$ [M + H]$^+$, 382.1041; found, 382.1054.

5-Chloro-*N*-neopentyl-6-(2,4,6-trifluorophenyl)-[1,2,4]-triazolo[1,5-*a*]pyrimidin-7-amine (59). General procedure C was followed using 5,7-dichloro-6-(2,4,6-trifluorophenyl)-[1,2,4]triazolo-[1,5-*a*]pyrimidine (0.050 g, 0.16 mmol) (**102**) and 2,2-dimethylpropan-1-amine (0.039 mL, 0.33 mmol). Purification via silica gel column chromatography (0−30% EtOAc in hexanes) provided the title compound as a white powder (0.033 g, 0.09 mmol, 57%). ^{1}H NMR (500 MHz, $CDCl_3$): δ 8.33 (s, 1H), 6.85 (dd, J = 8.0, 7.2 Hz, 2H), 6.45 (s, 1H), 2.80 (d, J = 5.7 Hz, 2H), 0.88 (s, 9H) ppm; ^{13}C NMR (126 MHz, $CDCl_3$): δ 164.63 (dt, J = 255.2, 15.0 Hz), 161.50 (ddd, J = 253.8, 14.9, 8.2 Hz), 161.25 (ddd, J = 251.3, 14.9, 8.2 Hz), 158.23, 155.49, 153.90, 146.50, 124.47 (q, J = 283.5 Hz), 101.80 (td, J = 25.8, 4.2 Hz), 101.30 (td, J = 27.1, 26.1, 3.7 Hz), 90.92, 58.93 (q, J = 29.4 Hz), 28.28, 19.75, 16.68 ppm; IR (film) ν: 2959, 1636, 1611, 1573, 1495, 1438, 1358, 1263, 1250, 1124, 1036, 998, 843, 766, 533 cm^{-1}; HRMS (ES$^+$): calcd for $C_{16}H_{15}ClF_3N_5$ [M + H]$^+$, 370.1041; found, 370.1039.

(*R*)-5-Chloro-*N*-(3,3-dimethylbutan-2-yl)-6-(2,4,6-trifluorophenyl)-[1,2,4]triazolo[1,5-*a*]pyrimidin-7-amine (60). General procedure C was followed using 5,7-dichloro-6-(2,4,6-trifluorophenyl)-[1,2,4]triazolo[1,5-*a*]pyrimidine (0.150 g, 0.47 mmol) (**102**) and (*R*)-3,3-dimethylbutan-2-amine (0.132 mL, 0.99 mmol). Purification via silica gel column chromatography (0−30% EtOAc in hexanes) provided the title compound as a white powder (0.157 g, 0.86 mmol, 87%). The spectroscopic properties of the compound were identical to those reported for **61**.

(*S*)-5-Chloro-*N*-(3,3-dimethylbutan-2-yl)-6-(2,4,6-trifluorophenyl)-[1,2,4]triazolo[1,5-*a*]pyrimidin-7-amine (61). General procedure C was followed using 5,7-dichloro-6-(2,4,6-trifluorophenyl)-[1,2,4]triazolo[1,5-*a*]pyrimidine (0.100 g, 0.31 mmol) (**102**) and (*S*)-3,3-dimethylbutan-2-amine (0.088 mL, 0.66 mmol). Purification via silica gel column chromatography (0−30% EtOAc in hexanes) provided the title compound as a white powder (0.094 g, 0.24 mmol, 78%). ^{1}H NMR (500 MHz, $CDCl_3$): δ 8.31 (s, 1H), 6.92−6.74 (m, 2H), 6.44 (s, 1H), 3.08 (s, 1H), 1.00 (d, J = 6.7 Hz, 4H), 0.82 (s, 11H) ppm; ^{13}C NMR (126 MHz, $CDCl_3$): δ 164.07 (dt, J = 254.0, 15.2 Hz), 161.52 (ddd, J = 250.8, 14.8, 8.4 Hz), 161.27 (ddd, J = 250.6, 14.9, 8.4 Hz), 158.13, 154.94, 153.61, 146.25, 107.54 (td, J = 20.6, 5.1 Hz), 101.51−100.58 (m), 88.60, 58.07, 34.72, 25.78, 16.58 ppm; IR (film) ν: 1608, 1578, 1490, 1438, 1354, 1264, 1252, 1124, 999, 767, 623, 540 cm^{-1}; HRMS (ES$^+$): calcd for $C_{17}H_{17}ClF_3N_5$ [M + H]$^+$, 384.1197; found, 384.1198.

5-Chloro-7-(3,3,3-trifluoro-2-methylpropyl)-6-(2,4,6-trifluorophenyl)-[1,2,4]triazolo[1,5-*a*]pyrimidine (62). To a solution of *tert*-butyl 2-(5-chloro-6-(2,4,6-trifluorophenyl)-[1,2,4]-triazolo[1,5-*a*]pyrimidin-7-yl)-4,4,4-trifluoro-3-methylbutanoate (0.026 g, 0.05 mmol, 1 equiv) (**112**) in CH_2Cl_2 (2 mL) at rt was added 2,2,2-trifluoroacetic acid (0.125 mL, 1.60 mmol, 30 equiv). The mixture was stirred for 16 h at rt and then diluted with CH_2Cl_2 and quenched with a saturated $NaHCO_3$ solution. The aqueous layer was then extracted with CH_2Cl_2 and the combined organic layers were dried over $MgSO_4$, filtered, and concentrated under reduced pressure. Purification via preparative reverse-phase HPLC (C18 column, 20 mL/min, 10 min ramp, 10 to 90% ACN/H_2O + 0.1% formic acid, tr = 8.5 min) provided the title compound (0.014 g, 0.04 mmol, 68%) as a tan solid. ^{1}H NMR (600 MHz, $CDCl_3$): δ 8.56 (s, 1H), 6.92−6.88 (m, 2H), 3.34 (dd, J = 13.9, 6.2 Hz, 1H), 3.22 (m, 1H), 3.05 (dd, J = 13.9, 8.4 Hz, 1H), 1.03 (d, J = 7.0 Hz, 4H) ppm; ^{13}C NMR (151 MHz, $CDCl_3$): δ 164.45 (dt, 256.7, 18.1 Hz), 160.86 (ddd, 252.2, 15.1, 9.1 Hz), 160.61 (ddd, 250.7, 15.1, 9.06 Hz), 157.19, 157.02, 154.03, 148.77, 127.25 (q, 280.11 Hz) 112.29, 106.39 (td, 21.14, 4.9 Hz), 101.48 (dtd, J = 30.1, 25.9, 4.1 Hz), 35.37 (q, J = 27.6 Hz), 30.65, 12.88 ppm; IR (film) ν: 1639, 1609, 1599, 1516, 1495, 1442, 1278, 1265, 1207, 1186, 1172, 1146, 1122, 1039, 999 cm^{-1}; HRMS (ES$^+$): calcd for $C_{15}H_9ClF_6N_4$ [M + H]$^+$, 395.0493; found, 395.0486.

(*S*)-4-(5-Chloro-7-((1,1,1-trifluoropropan-2-yl)amino)-[1,2,4]triazolo[1,5-*a*]pyrimidin-6-yl)-3-fluorobenzonitrile (63). General procedure C was followed using 4-(5,7-dichloro-[1,2,4]-triazolo[1,5-*a*]pyrimidin-6-yl)-3-fluorobenzonitrile (0.040 g, 0.13 mmol) (**107**) and (*S*)-1,1,1-trifluoropropan-2-amine (0.031 g, 0.27 mmol). Purification by reverse-phase HPLC provided the title compound as a white powder (0.031 g, 0.07 mmol, 54%). ^{1}H NMR (600 MHz, $CDCl_3$): mixture of diastereomers δ 8.41 (s, 1H), 7.68 (ddd, J = 7.8, 3.8, 1.5 Hz, 1H), 7.61 (ddd, J = 8.4, 3.8, 1.5 Hz, 1H), 7.57 (t, J = 7.4 Hz, 1H), 7.50 (t, J = 7.3 Hz, 1H), 5.94 (d, J = 11.0 Hz, 1H), 5.57 (d, J = 10.8 Hz, 1H), 4.97 (s, 1H), 4.50 (s, 1H), 1.40 (d, J = 6.9 Hz, 3H) ppm; ^{13}C NMR (150 MHz, $CDCl_3$): δ 161.29 (d, J = 52.0 Hz), 159.61 (d, J = 50.4 Hz), 156.65 (d, J = 24.9 Hz), 155.72 (d, J = 11.0 Hz), 154.20 (d, J = 57.5 Hz), 145.65 (d, J = 62.8 Hz), 135.00 (d, J = 2.0 Hz), 133.84 (d, J = 2.2 Hz), 129.21 (d, J = 4.2 Hz), 124.97 (dd, J = 16.2, 13.1 Hz), 124.67 (qd, J = 282.3, 34.7 Hz), 120.62 (dd, J = 74.3, 25.2 Hz), 116.67 (d, J = 2.8 Hz), 116.33 (dd, J = 9.3, 5.2 Hz), 97.66, 96.61, 51.26 (dq, J = 37.9, 31.8 Hz), 15.13, 14.99 ppm; HRMS (ES$^+$): calcd for $C_{15}H_{10}ClF_4N_6$ [M + H]$^+$, 385.0586; found, 385.0589.

(*R*)-5-Chloro-6-(2,6-difluorophenyl)-*N*-(3-methylbutan-2-yl)-[1,2,4]triazolo[1,5-*a*]pyrimidin-7-amine (64). General procedure C was followed using 5,7-dichloro-6-(3,5-difluorophenyl)-[1,2,4]triazolo[1,5-*a*]pyrimidine (0.048 g, 0.16 mmol) (**97**) and (*R*)-3-methylbutan-2-amine (0.028 g, 0.32 mmol). Purification via silica gel column chromatography (0−30% EtOAc in hexanes) provided the title compound as a white powder (0.049 g, 0.14 mmol, 87%). ^{1}H NMR (600 MHz, $CDCl_3$): δ 8.32 (s, 1H), 7.54−7.49 (m, 1H), 7.09−7.06 (m, 2H), 6.34 (br s, 1H), 3.12 (br s, 1H), 1.61 (oct, J = 6 Hz, 1H), 1.03 (d, J = 6 Hz, 3H), 0.77 (d, J = 6 Hz, 3H), 0.74 (d, J = 6 Hz, 3H) ppm; ^{13}C NMR (150 MHz, $CDCl_3$): δ 160.77 (dt, J = 250.66, 5.3 Hz), 158.04, 154.89 (d, J = 4.5 Hz), 153.65, 145.94, 132.38−132.22 (m), 110.93 (t, J = 21.1 Hz), 112.08−111.81 (m), 89.78, 54.76, 33.65, 33.63, 18.21 (q, 3 Hz), 18.00 (q, J = 7.6 Hz), 17.80 (q, J = 3 Hz) ppm; HRMS (ES$^+$): calcd for $C_{18}H_{17}ClFN_6$ [M + H]$^+$, 352.1135; found, 352.1135.

(*R*)-5-Chloro-6-(2-fluorophenyl)-*N*-(3-methylbutan-2-yl)-[1,2,4]triazolo[1,5-*a*]pyrimidin-7-amine (65). General procedure C was followed using 5,7-dichloro-6-(2-fluorophenyl)-[1,2,4]triazolo-[1,5-*a*]pyrimidine (0.046 g, 0.16 mmol) (**95**) and (*R*)-3-methylbutan-2-amine (0.028 g, 0.32 mmol). Purification via silica gel column chromatography (0−30% EtOAc in hexanes) provided the title compound as a white powder (0.017 g, 0.051 mmol, 31%). ^{1}H NMR (600 MHz, $CDCl_3$): mixture of diastereomers δ 8.33 (s, 1H), 7.52 (q, J = 6 Hz, 1H), 7.36−7.29 (m, 2H), 7.24 (t, J = 6 Hz, 1H), 6.19 (br s, 1H), 3.15 (br s, 1H), 1.02 (d, J = 6 Hz, 1.5H), 0.96 (d, J = 6 Hz, 1.5H), 0.77 (t, J = 6 Hz, 3H), 0.74 (d, J = 6 Hz, 1.5H), 0.72 (d, J = 6 Hz, 1.5H) ppm; ^{13}C NMR (150 MHz, $CDCl_3$): δ 160.83 (dd, J = 250.66, 9 Hz), 158.26 (d, J = 12.1 Hz), 153.91, 152.70, 146.02, 133.61, 133.61, 132.98, 132.06 (t, J = 8.3 Hz), 124.94 (d, J = 4.5 Hz), 124.89 (d, J = 3.0 Hz), 120.96 (d, J = 25.7 Hz), 120.85 (dd, J = 21.9, 1.6 Hz), 97.14, 96.99, 54.75, 54.59, 33.77, 33.47, 18.28, 17.98, 17.81, 17.73, 17.62 ppm; HRMS (ES$^+$): calcd for $C_{18}H_{17}ClFN_6$ [M + H]$^+$, 334.1229; found, 334.1227.

(*R*)-4-(5-Chloro-7-((3-methylbutan-2-yl)amino)-[1,2,4]-triazolo[1,5-*a*]pyrimidin-6-yl)-3,5-difluorobenzonitrile (66). General procedure C was followed using 4-(5,7-dichloro-[1,2,4]-triazolo[1,5-*a*]pyrimidin-6-yl)-3,5-difluorobenzonitrile (0.030 g, 0.09

https://dx.doi.org/10.1021/acs.jmedchem.0c01605
J. Med. Chem. 2021, 64, 1073−1102

mmol) (**106**) and (*R*)-3-methylbutan-2-amine (0.017 g, 0.19 mmol). Purification by reverse-phase HPLC provided the title compound as a white powder (0.028 g, 0.07 mmol, 81%). ^{1}H NMR (600 MHz, DMSO-d_6): δ 8.62 (s, 1H), 8.11 (t, J = 7.8 Hz, 2H), 7.88 (s, 1H), 1.78 (dq, J = 13.9, 6.8 Hz, 1H), 1.10 (d, J = 6.6 Hz, 3H), 0.74 (dd, J = 6.8, 2.9 Hz, 6H) ppm; ^{13}C NMR (151 MHz, DMSO-d_6): δ 160.71 (dd, J = 249.2, 6.8 Hz), 160.38 (dd, J = 249.5, 6.3 Hz), 155.02, 146.81, 117.00 (ddd, J = 26.3, 12.6, 3.9 Hz), 116.48 (d, J = 3.5 Hz), 114.83 (t, J = 12.8 Hz) ppm; ^{19}F NMR (469 MHz): δ −103.93 (d, J = 9.9 Hz), −104.42 (d, J = 9.9 Hz) ppm; IR (film) ν: 2966, 2220, 1690, 1562, 1422, 1204 cm^{-1}; HRMS (ES$^+$): calcd for $C_{17}H_{16}ClF_2N_6$ [M + H]$^+$, 377.1088; found, 377.1089.

(*R*)-4-(5-Chloro-7-((3-methylbutan-2-yl)amino)-[1,2,4]-triazolo[1,5-*a*]pyrimidin-6-yl)-3-fluorobenzonitrile (67) and (68). General procedure C was followed using 4-(5,7-dichloro-[1,2,4]triazolo[1,5-*a*]pyrimidin-6-yl)-3-fluorobenzonitrile (0.048 g, 0.15 mmol) (**107**) and (*R*)-3-methylbutan-2-amine (0.037 g, 0.42 mmol). Purification via silica gel column chromatography provided atropoisomer **67** as a white solid (0.029 g, 0.08 mmol, 39%) and atropoisomer **68** (0.023 g, 0.06 mmol, 30%). Recrystallization of **68** from CH2Cl2 followed by single crystal diffraction (mp 143.7−145.2) permitted the structural assignment of the two atropoisomers (see Supporting Information). **68** ^{1}H NMR (600 MHz, $CDCl_3$): δ 8.35 (s, 1H), 7.63 (dd, J = 12.0, 3.0 Hz, 1H), 7.56 (dd, J = 12.0, 3.0 Hz, 1H), 7.53 (t, J = 9.0 Hz, 1H), 6.29 (d, J = 12.0 Hz, 1H), 3.00 (br s, 1H), 1.64 (oct, J = 6.0 Hz, 1H), 0.99 (d, J = 6 Hz, 3H), 0.80 (d, J = 6 Hz, 3H), 0.77 (d, J = 6 Hz, 3H) ppm; ^{13}C NMR (150 MHz, $CDCl_3$): δ 161.37, 159.70, 156.91, 155.15, 153.15, 145.67, 134.39, 128.71, 128.69, 127.13 (d, J = 16.6 Hz), 120.02 (d, J = 25.7 Hz), 116.98, 115.50 (d, J = 9.1 Hz), 94.53, 55.04, 33.48, 18.16, 17.80, 17.14 ppm. **67** ^{1}H NMR (600 MHz, $CDCl_3$): δ 8.35 (s, 1H), 7.63 (dd, J = 12.0, 3.0 Hz, 1H), 7.56 (dd, J = 12.0, 3.0 Hz, 1H), 7.52 (t, J = 9.0 Hz, 1H), 6.30 (br s, 1H), 3.05 (br s, 1H), 1.61 (oct, J = 6.0 Hz, 1H), 1.05 (d, J = 6 Hz, 3H), 0.79 (d, J = 6 Hz, 3H), 0.75 (d, J = 6 Hz, 3H) ppm; ^{13}C NMR (150 MHz, $CDCl_3$): δ 161.40, 159.73, 156.90, 155.19, 153.57, 145.67, 135.08, 134.40 (d, J = 3.0 Hz), 128.55 (d, J = 4.5 Hz), 127.03 (d, J = 15.1 Hz), 120.22 (d, J = 25.7 Hz), 117.01, 115.45 (d, J = 9.1 Hz), 94.37, 54.85, 33.80, 18.20, 17.90, 17.82 ppm; IR (film) ν: 2963, 2220, 1608, 1570, 1260, 1156 cm^{-1}; HRMS (ES$^+$): calcd for $C_{18}H_{17}ClFN_6$ [M + H]$^+$, 359.1182; found, 359.1184.

(*R*)-4-(5-Chloro-7-((3,3-dimethylbutan-2-yl)amino)-[1,2,4]-triazolo[1,5-*a*]pyrimidin-6-yl)-3,5-difluorobenzonitrile (69). General procedure C was followed using 4-(5,7-dichloro-[1,2,4]-triazolo[1,5-*a*]pyrimidin-6-yl)-3,5-difluorobenzonitrile (0.020 g, 0.06 mmol) (**106**) and (*R*)-3,3-dimethylbutan-2-amine (0.013 g, 0.13 mmol). Purification by reverse-phase HPLC provided the title compound as a white powder (0.018 g, 0.05 mmol, 75%). ^{1}H NMR (600 MHz, $CDCl_3$): δ 8.36 (s, 1H), 7.45−7.41 (m, 2H), 6.52 (d, J = 10.8 Hz, 1H), 2.94 (s, 1H), 1.02 (d, J = 6.7 Hz, 3H), 0.84 (s, 9H) ppm; ^{13}C NMR (150 MHz, $CDCl_3$): δ 161.33 (dd, J = 253.8, 6.2 Hz), 161.05 (dd, J = 253.8, 6.2 Hz), 157.12, 155.22, 146.03, 116.22 (d, J = 4.0 Hz), 116.13−115.95 (m), 115.95−115.82 (m), 58.57, 34.93, 25.86, 16.56 ppm; ^{19}F NMR (469 MHz): δ −103.70 (d, J = 4.7 Hz), −104.31 (d, J = 4.7 Hz) ppm; HRMS (ES$^+$): calcd for $C_{18}H_{18}ClF_2N_6$ [M + H]$^+$, 391.1244; found, 391.1241.

(*R*)-4-(5-Chloro-7-((3,3-dimethylbutan-2-yl)amino)-[1,2,4]-triazolo[1,5-*a*]pyrimidin-6-yl)-3-fluorobenzonitrile (70). General procedure C was followed using 4-(5,7-dichloro-[1,2,4]triazolo[1,5-*a*]pyrimidin-6-yl)-3-fluorobenzonitrile (0.040 g, 0.13 mmol) (**107**) and (*R*)-3,3-dimethylbutan-2-amine (0.028 g, 0.27 mmol). Purification by reverse-phase HPLC provided the title compound as a white powder (0.027 g, 0.07 mmol, 56%). ^{1}H NMR (600 MHz, $CDCl_3$): mixture of diastereomers δ 8.41−8.34 (m, 1H), 7.67−7.61 (m, 1H), 7.60−7.55 (m, 1H), 7.55−7.49 (m, 1H), 6.37 (s, 1H), 2.94−2.89 (m, 1H), 1.01 (d, J = 6.7 Hz, 1H), 0.94 (d, J = 6.7 Hz, 2H), 0.82 (s, 5H), 0.81 (s, 4H) ppm; ^{13}C NMR (150 MHz, $CDCl_3$): δ 161.71−159.28 (m), 156.76, 156.67, 145.96, 135.28 (d, J = 2.4 Hz), 133.96 (d, J = 2.3 Hz), 128.65 (d, J = 4.1 Hz), 128.43 (d, J = 4.1 Hz), 119.96 (dd, J = 37.6, 25.4 Hz), 116.86 (d, J = 2.8 Hz), 115.42 (dd, J = 16.7, 9.3 Hz), 94.27, 94.14, 58.27, 58.07, 35.01, 34.82, 25.77 (d, J = 1.9 Hz), 16.42 (d, J = 2.2 Hz) ppm; HRMS (ES$^+$): calcd for $C_{18}H_{19}ClFN_6$ [M + H]$^+$, 373.1338; found, 373.1338.

4-(5-Chloro-7-((1*R*,3*s*,5*S*)-3-methoxy-8-azabicyclo[3.2.1]-octan-8-yl)-[1,2,4]triazolo[1,5-*a*]pyrimidin-6-yl)-3,5-difluorobenzonitrile (71). General procedure C was followed using 4-(5,7-dichloro-[1,2,4]triazolo[1,5-*a*]pyrimidin-6-yl)-3,5-difluorobenzonitrile (0.100 g, 0.31 mmol) (**106**), (1*R*,3*R*,5*S*)-3-methoxy-8-azabicyclo-[3.2.1]octane hydrochloride (0.082 g, 0.46 mmol) and Et_3N (0.094 g, 0.92 mmol). Purification by reverse-phase HPLC provided the title compound as a white powder (0.112 g, 0.26 mmol, 85%). ^{1}H NMR (600 MHz, $CDCl_3$): δ 8.28 (s, 1H), 7.39 (d, J = 5.9 Hz, 2H), 4.57 (s, 2H), 3.45 (s, 1H), 3.23 (s, 3H), 2.13 (d, J = 7.4 Hz, 2H), 2.00 (d, J = 14.9 Hz, 2H), 1.92 (d, J = 14.7 Hz, 2H), 1.80−1.74 (m, 2H) ppm; ^{13}C NMR (150 MHz, $CDCl_3$): δ 161.66 (d, J = 6.6 Hz), 159.98 (d, J = 6.6 Hz), 156.99, 155.05, 146.39, 118.79, 116.34, 116.30, 116.18, 116.15, 116.11, 115.16 (t, J = 11.8 Hz), 92.08, 73.33, 62.34, 59.30, 56.53, 36.34, 27.98 ppm; HRMS (ES$^+$): calcd for $C_{20}H_{18}ClF_2N_6O$ [M + H]$^+$, 431.1188; found, 431.1193.

4-(7-(Azepan-1-yl)-5-chloro-[1,2,4]triazolo[1,5-*a*]pyrimidin-6-yl)-3,5-difluorobenzonitrile (72). General procedure C was followed using 4-(5,7-dichloro-[1,2,4]triazolo[1,5-*a*]pyrimidin-6-yl)-3,5-difluorobenzonitrile (0.020 g, 0.06 mmol) (**106**) and azepane (0.013 g, 0.13 mmol). Purification by reverse-phase HPLC provided the title compound as a white powder (0.015 g, 0.04 mmol, 63%). ^{1}H NMR (600 MHz, $CDCl_3$): δ 8.38 (s, 1H), 7.40 (d, J = 6.0 Hz, 2H), 3.45−3.39 (m, 4H), 1.78−1.70 (m, 4H), 1.64−1.60 (m, 4H) ppm; ^{13}C NMR (150 MHz, $CDCl_3$): δ 160.74 (dd, J = 253.4, 6.6 Hz), 157.14, 155.26, 152.10, 118.61 (t, J = 19.7 Hz), 116.30−115.97 (m), 115.12 (t, J = 11.9 Hz), 97.32, 53.99, 51.22, 28.27, 28.17, 27.28, 27.07 ppm; ^{19}F NMR (469 MHz): δ −105.22 ppm; IR (film) ν: 2928, 2857, 2238, 1589, 1515, 1422 cm^{-1}; HRMS (ES$^+$): calcd for $C_{18}H_{16}ClF_2N_6$ [M + H]$^+$, 389.1088; found, 389.1085.

4-(7-(Azepan-1-yl)-5-chloro-[1,2,4]triazolo[1,5-*a*]pyrimidin-6-yl)-3-fluorobenzonitrile (73). General procedure C was followed using 4-(5,7-dichloro-[1,2,4]triazolo[1,5-*a*]pyrimidin-6-yl)-3-fluorobenzonitrile (0.040 g, 0.13 mmol) (**107**) and azepane (0.027 g, 0.27 mmol). Purification by reverse-phase HPLC provided the title compound as a white powder (0.027 g, 0.07 mmol, 56%). ^{1}H NMR (600 MHz, $CDCl_3$): δ 8.34 (s, 1H), 7.61 (dd, J = 7.9, 1.6 Hz, 1H), 7.53 (dd, J = 8.7, 1.6 Hz, 1H), 7.48 (t, J = 7.5 Hz, 1H), 3.38−3.33 (m, 4H), 1.71 (dq, J = 8.0, 4.2 Hz, 4H), 1.60 (p, J = 3.0 Hz, 4H) ppm; ^{13}C NMR (150 MHz, $CDCl_3$): δ 160.85, 159.18, 156.93, 155.27, 155.18, 151.61, 134.44 (d, J = 2.8 Hz), 128.60 (d, J = 3.9 Hz), 128.48, 120.11, 119.94, 117.09 (d, J = 2.8 Hz), 114.68 (d, J = 9.2 Hz), 103.59, 54.05, 28.27, 28.03 ppm; IR (film) ν: 2926, 2235, 1589, 1519, 1446 cm^{-1}; HRMS (ES$^+$): calcd for $C_{18}H_{17}ClFN_6$ [M + H]$^+$, 371.1182; found, 371.1180.

4-(7-(Azocan-1-yl)-5-chloro-[1,2,4]triazolo[1,5-*a*]pyrimidin-6-yl)-3,5-difluorobenzonitrile (74). General procedure C was followed using 4-(5,7-dichloro-[1,2,4]triazolo[1,5-*a*]pyrimidin-6-yl)-3,5-difluorobenzonitrile (0.054 g, 0.17 mmol) (**106**) and azocane (0.019 g, 0.17 mmol). Purification via silica gel column chromatography provided the title compound as a white solid (0.031 g, 0.08 mmol, 46%). ^{1}H NMR (600 MHz, $CDCl_3$): δ 8.29 (s, 1H), 7.30 (d, J = 6.0 Hz, 2H), 3.36 (t, J = 5.7 Hz, 5H), 1.62 (t, J = 5.8 Hz, 5H), 1.52 (t, J = 5.5 Hz, 6H), 1.44 (d, J = 6.0 Hz, 2H) ppm; ^{13}C NMR (151 MHz, $CDCl_3$): δ 160.68 (dd, J = 253.6, 6.5 Hz), 157.23, 155.73, 155.12, 151.06, 118.55 (t, J = 19.8 Hz), 116.38, 116.34, 116.23, 116.19, 115.23 (t, J = 11.8 Hz), 97.29, 52.24, 27.72, 26.80, 24.44 ppm; HRMS (ES$^+$): calcd for $C_{18}H_{17}ClFN_6$ [M + H]$^+$, 403.1244; found, 403.1240.

4-(7-(Azocan-1-yl)-5-chloro-[1,2,4]triazolo[1,5-*a*]pyrimidin-6-yl)-3-fluorobenzonitrile (75). General procedure C was followed using 4-(5,7-dichloro-[1,2,4]triazolo[1,5-*a*]pyrimidin-6-yl)-3-fluorobenzonitrile (0.048 g, 0.15 mmol) (**107**) and azocane (0.035 g, 0.30 mmol). Purification via silica gel column chromatography provided the title compound as a white solid (0.032 g, 0.08 mmol, 53%). ^{1}H NMR (600 MHz, $CDCl_3$): mixture of diastereomers δ 8.59 (s, 0.4H), 8.42 (s, 0.3H), 7.80−7.77 (m, 0.6H), 7.30 (d, J = 6 Hz, 0.3H), 7.16 (d, J = 12 Hz, 0.4H), 3.41 (t, J = 6 Hz, 1.2H), 3.32 (br s,

https://dx.doi.org/10.1021/acs.jmedchem.0c01605
J. Med. Chem. 2021, 64, 1073−1102

1.8H), 3.04 (br s, 1.8H), 1.70−1.41 (m, 10H) ppm; HRMS (ES^+): calcd for $C_{18}H_{17}ClFN_6$ $[M + H]^+$, 385.1338; found, 385.1332.

Diethyl 2-Phenylmalonate (76). General procedure A was followed using diethyl malonate (6.122 g, 38.20 mmol) and bromobenzene (2.002 g, 12.70 mmol). Purification via silica gel column chromatography (0−8% EtOAc in hexanes) provided the title compound as a colorless oil (0.833 g, 3.53 mmol, 28%). ^1H NMR (500 MHz, $CDCl_3$): δ 7.50−7.31 (m, 5H), 4.61 (s, 1H), 4.45−4.01 (m, 4H), 1.26 (t, J = 7.1 Hz, 6H); ^{13}C NMR (126 MHz, $CDCl_3$): δ 168.30, 132.94, 129.40, 128.73, 128.33, 61.94, 58.12, 14.16 ppm; IR (film) ν: 3450, 1731, 1638, 1455, 1368, 1305, 1217, 1147, 1029, 700 cm^{-1}; HRMS (ES^+): calcd for $C_{13}H_{16}NaO_4$ $[M + Na]^+$, 259.0946; found, 259.0952.

Diethyl 2-(4-Fluorophenyl)malonate (77). General procedure A was followed using diethyl malonate (5.491 g, 34.30 mmol) and 1-bromo-4-fluorobenzene (2.000 g, 11.40 mmol). Purification via silica gel column chromatography (8/8/84 EtOAc/CH_2Cl_2/hexanes) provided the title compound as a colorless oil (0.818 g, 3.22 mmol, 28%). ^1H NMR (500 MHz, $CDCl_3$): δ 7.41−7.36 (m, 2H), 7.07−7.01 (m, 2H), 4.59 (s, 1H), 4.27−4.14 (m, 4H), 1.25 (t, J = 7.1 Hz, 6H) ppm; ^{13}C NMR (126 MHz, $CDCl_3$): δ 168.10, 162.72 (d, J = 246.9 Hz), 131.11 (d, J = 8.3 Hz), 128.70 (d, J = 3.4 Hz), 115.59 (d, J = 21.6 Hz), 61.99, 57.18, 14.07 ppm; IR (film) ν: 3451, 2985, 2940, 1733, 1607, 1467, 1447, 1369, 1302, 1223, 1157, 1096, 1031, 841, 806, 753 cm^{-1}; HRMS (ES^+): calcd for $C_{13}H_{15}FNaO_4$ $[M + Na]^+$, 277.0852; found, 277.0861.

Diethyl 2-(2-Fluorophenyl)malonate (78). General procedure A was followed using diethyl malonate (5.491 g, 34.30 mmol) and 1-bromo-2-fluorobenzene (2.000 g, 11.40 mmol). Purification via silica gel column chromatography (0−8% EtOAc in hexanes) provided the title compound as a colorless oil (1.411 g, 5.55 mmol, 49%). ^1H NMR (500 MHz, $CDCl_3$): δ 7.47 (td, J = 7.6, 1.8 Hz, 1H), 7.34−7.28 (m, 1H), 7.16 (t, J = 7.6 Hz, 1H), 7.07 (t, J = 9.1 Hz, 1H), 4.98 (s, 1H), 4.23 (p, J = 7.0 Hz, 4H), 1.27 (t, J = 7.1 Hz, 6H) ppm; ^{13}C NMR (126 MHz, $CDCl_3$): δ 167.66, 160.59 (d, J = 247.6 Hz), 130.54 (d, J = 3.0 Hz), 130.04 (d, J = 8.3 Hz), 124.34 (d, J = 3.7 Hz), 120.51 (d, J = 14.5 Hz), 115.51 (d, J = 22.2 Hz), 62.09, 50.61 (d, J = 3.3 Hz), 14.07 ppm; IR (film) ν: 3458, 2984, 2940, 2907, 1737, 1617, 1589, 1494, 1458, 1369, 1303, 1232, 1149, 1094, 1030, 952, 860, 815, 756, 697 cm^{-1}; HRMS (ES^+): calcd for $C_{13}H_{15}FNaO_4$ $[M + Na]^+$, 277.0852; found, 277.0858.

Diethyl 2-(2,4-Difluorophenyl)malonate (79). General procedure A was followed using diethyl malonate (5.000 g, 31.10 mmol) and 1-bromo-2,4-difluorobenzene (2.000 g, 10.30 mmol). Purification via silica gel column chromatography (0−5% EtOAc in hexanes) provided the title compound as a colorless oil (1.907 g, 6.98 mmol, 68%). ^1H NMR (500 MHz, $CDCl_3$): δ 7.47 (td, J = 8.5, 6.3 Hz, 1H), 6.89 (td, J = 7.4, 3.8 Hz, 1H), 6.82 (td, J = 8.5, 2.5 Hz, 1H), 4.91 (s, 1H), 4.29−4.15 (m, 4H), 1.25 (t, J = 7.1 Hz, 6H) ppm; ^{13}C NMR (126 MHz, $CDCl_3$): δ 167.46, 162.83 (dd, J = 249.9, 12.2 Hz), 160.68 (dd, J = 250.0, 12.1 Hz), 131.58 (dd, J = 9.8, 4.5 Hz), 116.52 (dd, J = 14.6, 4.0 Hz), 111.64 (dd, J = 21.4, 3.7 Hz), 103.88 (t, J = 25.8 Hz), 62.17, 49.97 (d, J = 2.7 Hz), 14.01 ppm; IR (film) ν: 3449, 1737, 1624, 1508, 1291, 1220, 1144, 1031, 970, 851 cm^{-1}; HRMS (ES^+): calcd for $C_{13}H_{15}F_2O_4$ $[M + H]^+$, 273.0938; found, 273.0946.

Diethyl 2-(2,6-Difluorophenyl)malonate (80). General procedure A was followed using diethyl malonate (4.981 g, 31.10 mmol) and 2-bromo-1,3-difluorobenzene (2.000 g, 10.30 mmol). Purification via preparative reverse-phase HPLC provided the title compound as a colorless oil (2.082 g, 7.64 mmol, 74%). ^1H NMR (500 MHz, $CDCl_3$): δ 7.34−7.27 (m, 1H), 6.93 (t, J = 8.1 Hz, 2H), 4.97 (s, 1H), 4.26 (q, J = 7.1 Hz, 4H), 1.27 (t, J = 7.1 Hz, 6H) ppm; ^{13}C NMR (126 MHz, $CDCl_3$): δ 167.05, 161.29 (dd, J = 250.6, 7.1 Hz), 130.27 (t, J = 11.9 Hz), 111.75 (t, J = 25.6 Hz), 111.65 (dd, J = 20.6, 4.6 Hz), 62.38, 47.32, 14.05 ppm; IR (film) ν: 3460, 2985, 1746, 1628, 1595, 1471, 1370, 1303, 1274, 1236, 1157, 1096, 1035, 1003, 788, 698 cm^{-1}; HRMS (ES^+): calcd for $C_{13}H_{14}F_2NaO_4$ $[M + Na]^+$, 295.0758; found, 295.0757.

Diethyl 2-(3,5-Difluorophenyl)malonate (81). General procedure A was followed using diethyl malonate (5.000 g, 31.10 mmol) and 1-bromo-3,5-difluorobenzene (2.000 g, 10.30 mmol). Purification via silica gel column chromatography (0−5% EtOAc in hexanes) provided the title compound as a colorless oil (1.462 g, 5.36 mmol, 52%). ^1H NMR (500 MHz, $CDCl_3$): δ 6.99−6.93 (m, 2H), 6.76 (tt, J = 8.9, 2.4 Hz, 1H), 4.57 (s, 1H), 4.28−4.13 (m, 4H), 1.25 (t, J = 7.1 Hz, 6H) ppm; ^{13}C NMR (126 MHz, $CDCl_3$): δ 167.20, 162.86 (dd, J = 248.7, 12.9 Hz), 136.08 (t, J = 9.9 Hz), 112.63 (dd, J = 20.7, 6.0 Hz), 103.87 (t, J = 25.2 Hz), 62.26, 57.35 (t, J = 1.9 Hz), 14.00 ppm; IR (film) ν: 3450, 2986, 1736, 1626, 1601, 1465, 1369, 1305, 1234, 1154, 1121, 1037, 995, 867, 738, 675 cm^{-1}; HRMS (ES^+): calcd for $C_{13}H_{14}F_2NaO_4$ $[M + Na]^+$, 295.0758; found, 295.0745.

Diethyl 2-(2,5-Difluorophenyl)malonate (82). General procedure A was followed using diethyl malonate (5.000 g, 31.10 mmol) and 2-bromo-1,4-difluorobenzene (2.000 g, 10.30 mmol). Purification via silica gel column chromatography (0−10% EtOAc in hexanes) provided the title compound as a colorless oil (1.767 g, 6.46 mmol, 62%). ^1H NMR (500 MHz, $CDCl_3$): δ 7.25−7.19 (m, 1H), 7.06−6.95 (m, 2H), 4.94 (s, 1H), 4.29−4.17 (m, 4H), 1.26 (t, J = 7.1 Hz, 6H) ppm; ^{13}C NMR (126 MHz, $CDCl_3$): δ 167.10, 158.54 (dd, J = 242.3, 2.5 Hz), 156.62 (dd, J = 243.9, 2.5 Hz), 121.84 (dd, J = 17.0, 8.4 Hz), 117.20 (dd, J = 25.5, 3.2 Hz), 116.59 (dd, J = 15.0, 8.8 Hz), 116.39 (dd, J = 16.3, 8.6 Hz), 62.29, 50.35 (d, J = 2.7 Hz), 14.02 ppm; IR (film) ν: 3452, 2986, 1737, 1631, 1499, 1369, 1303, 1226, 1154, 1031, 877, 819, 739 cm^{-1}; HRMS (ES^+): calcd for $C_{13}H_{14}F_2NaO_4$ $[M + Na]^+$, 295.0758; found, 295.0755.

Diethyl 2-(3,4-Difluorophenyl)malonate (83). General procedure A was followed using diethyl malonate (5.002 g, 31.10 mmol) and 4-bromo-1,2-difluorobenzene (2.001 g, 10.30 mmol). Purification via preparative reverse-phase HPLC provided the title compound as an orange oil (0.530 g, 1.95 mmol, 19%). ^1H NMR (500 MHz, $CDCl_3$): δ 7.33−7.28 (m, 1H), 7.18−7.07 (m, 2H), 4.56 (d, J = 2.9 Hz, 1H), 4.28−4.17 (m, 4H), 1.27 (td, J = 7.3, 2.2 Hz, 6H) ppm; ^{13}C NMR (126 MHz, $CDCl_3$): δ 167.67, 150.35 (dd, J = 272.8, 12.7 Hz), 150.35 (dd, J = 224.7, 12.6 Hz), 129.67 (dd, J = 6.2, 4.0 Hz), 125.77 (dd, J = 6.5, 3.7 Hz), 118.63 (d, J = 18.4 Hz), 117.34 (d, J = 17.4 Hz), 62.24, 57.00, 14.05 ppm; IR (film) ν: 3450, 2986, 1734, 1613, 1520, 1441, 1369, 1287, 1154, 1032, 773 cm^{-1}; HRMS (ES^+): calcd for $C_{13}H_{15}F_2O_4$ $[M + H]^+$, 273.0938; found, 273.0941.

Diethyl 2-(2,3,4-Trifluorophenyl)malonate (84). General procedure A was followed using diethyl malonate (4.560 g, 28.44 mmol) and 1-bromo-2,3,4-trifluorobenzene (2.000 g, 9.48 mmol). Purification via silica gel column chromatography (0−8% EtOAc in hexanes) provided the title compound as a colorless oil (1.621 g, 5.58 mmol, 59%). ^1H NMR (500 MHz, $CDCl_3$): δ 7.28−7.19 (m, 1H), 7.00 (tdd, J = 9.2, 7.0, 2.1 Hz, 1H), 4.90 (s, 1H), 4.29−4.19 (m, 4H), 1.28 (t, J = 7.1 Hz, 6H) ppm; ^{13}C NMR (126 MHz, $CDCl_3$): δ 166.98, 151.11 (ddd, J = 251.2, 9.8, 3.2 Hz), 149.78 (ddd, J = 251.2, 10.7, 3.4 Hz), 139.90 (dt, J = 251.5, 15.5 Hz), 124.30 (dt, J = 7.9, 3.9 Hz), 118.08 (dd, J = 11.8, 4.0 Hz), 112.31 (dd, J = 17.6, 3.9 Hz), 62.40, 50.06, 14.01 ppm; IR (film) ν: 3405, 2986, 1738, 1617, 1513, 1490, 1370, 1305, 1243, 1151, 1033, 992, 865, 810, 672 cm^{-1}; HRMS (ES^+): calcd for $C_{13}H_{13}F_3NaO_4$ $[M + Na]^+$, 313.0664; found, 313.0663.

Diethyl 2-(2,4,6-Trifluorophenyl)malonate (85). General procedure A was followed using diethyl malonate (8.408 g, 52.5 mmol) and 2-bromo-1,3,5-trifluorobenzene (3.692 g, 17.5 mmol). Purification via silica gel column chromatography (0−8% EtOAc in hexanes) provided the title compound as a white powder (2.542 g, 8.75 mmol, 50% yield). ^1H NMR (500 MHz; $CDCl_3$): δ 6.74−6.68 (m, 2H), 4.89 (s, 1H), 4.29−4.23 (m, 4H), 1.28 (t, J = 7.1 Hz, 6H) ppm; ^{13}C NMR (126 MHz, $CDCl_3$): δ 166.68, 162.78 (dt, J = 250.7, 15.1 Hz), 161.5 (dd, J = 250.7, 15.1 Hz), 161.44 (dd, J = 252.2, 15.1 Hz), 107.25 (dt, J = 18.1, 4.5 Hz), 100.81−100.43 (m), 62.41, 46.95, 14.04 ppm; LCMS: $[M + H]^+$, 291.

Diethyl 2-(2,4,6-Trifluorobenzyl)malonate (86). To a suspension of NaH (60 wt % in mineral oil) (0.462 g, 11.56 mmol, 1.30 equiv) in anhydrous DMF (8.5 mL) at 0 °C under N_2 was slowly added diethyl malonate (1.712 g, 10.67 mmol, 1.20 equiv). After addition, the reaction was stirred at 0 °C for 10 min. Then, 2-(bromomethyl)-1,3,5-trifluorobenzene (2.001 g, 8.89 mmol, 1.00

https://dx.doi.org/10.1021/acs.jmedchem.0c01605
J. Med. Chem. 2021, 64, 1073−1102

equiv) in solution in anhydrous DMF (8.5 mL) was slowly added and the reaction was stirred at 0 °C for 1 h. Then, the reaction was quenched with a saturated solution of NH_4Cl and H_2O (85 mL) was added. The mixture was extracted with EtOAc (×3). The combined organic extracts were washed with brine, then dried over $MgSO_4$, filtered, and concentrated under reduced pressure. Purification via silica gel column chromatography (0−5% EtOAc in hexanes) provided the title compound as a colorless oil (2.43 g, 7.99 mmol, 90%). ^{1}H NMR (500 MHz, $CDCl_3$): δ 7.28−7.19 (m, 1H), 7.04−6.95 (m, 1H), 4.90 (s, 1H), 4.29−4.19 (m, 4H), 1.28 (t, J = 7.1 Hz, 6H) ppm; ^{13}C NMR (126 MHz, $CDCl_3$): δ 168.33, 161.72 (dd, J = 248.9, 11.3 Hz), 161.70 (dt, J = 248.9, 16.0, 15.5 Hz), 161.60 (dd, J = 249.0, 11.2 Hz), 109.78 (td, J = 20.1, 4.7 Hz), 100.35−99.84 (m), 61.63, 51.10, 21.45 (t, J = 2.3 Hz), 13.90 ppm; IR (film) ν: 3437, 1733, 1639, 1499, 1444, 1371, 1304, 1239, 1153, 1048, 838, 617 cm^{-1}; HRMS (ES$^+$): calcd for $C_{14}H_{15}F_3NaO_4$ $[M + Na]^+$, 327.0820; found, 327.0818.

Diethyl 2-(2,6-Difluoro-4-methylphenyl)malonate (87). General procedure A was followed using diethyl malonate (4.180 g, 26.10 mmol) and 2-bromo-1,3-difluoro-5-methylbenzene (1.800 g, 8.69 mmol). Purification via silica gel column chromatography (0−8% EtOAc in hexanes) provided the title compound as a colorless oil (2.005 g, 6.99 mmol, 80%). ^{1}H NMR (600 MHz, $CDCl_3$): δ 6.67−6.65 (m, 2H), 4.83 (d, J = 3.0 Hz, 1H), 4.20−4.14 (m, 4H), 2.27 (d, J = 3.2 Hz, 3H), 1.22−1.17 (m, 6H) ppm; ^{13}C NMR (150 MHz, $CDCl_3$): δ 166.89, 160.75 (dd, J = 249.1, 8.1 Hz), 141.32, 115.89−110.83 (m), 107.42 (t, J = 18.8 Hz), 61.99, 46.98, 21.23 (d, J = 1.9 Hz), 13.87 ppm; IR (film) ν: 3000, 1678, 1106, 1017 cm^{-1}. LCMS: $[M + H]^+$, 287.

Diethyl 2-(2,6-Difluoro-4-(trifluoromethyl)phenyl)malonate (88). General procedure A was followed using diethyl malonate (2.160 g, 13.50 mmol) and 1,2,3-trifluoro-5-(trifluoromethyl)benzene (0.900 g, 4.50 mmol). Purification via silica gel column chromatography (0−5% EtOAc in hexanes) provided the title compound as a colorless oil (0.620 g, 1.82 mmol, 40%). ^{1}H NMR (500 MHz, $CDCl_3$): δ 7.23 (d, J = 7.3 Hz, 2H), 4.99 (s, 1H), 4.27 (dt, J = 7.4, 6.5 Hz, 4H), 1.29 (t, J = 7.1 Hz, 6H) ppm; ^{13}C NMR (126 MHz, $CDCl_3$): δ 166.12, 161.21 (dd, J = 252.9, 7.4 Hz), 132.89 (qt, J = 34.8, 10.3 Hz), 122.63 (qt, J = 272.6, 3.3 Hz), 114.85 (t, J = 18.5 Hz), 109.41 (ddt, J = 26.3, 7.4, 3.8 Hz), 62.69, 47.34, 14.07 ppm; IR (film) ν: 3083, 2987, 1755, 1061, 1442, 1365, 1306, 1240, 1177, 1138, 1080, 1031, 910, 867, 719, 702 cm^{-1}; HRMS (ES$^+$): calcd for $C_{14}H_{13}F_5NaO_4$ $[M + Na]^+$, 363.0632; found, 363.0631.

Diethyl 2-(4-Cyano-2,6-difluorophenyl)malonate (89). A mixture of 3,4,5-trifluorobenzonitrile (1.000 g, 6.37 mmol, 1 equiv), potassium carbonate (1.760 g, 12.70 mmol, 2.00 equiv), and diethyl malonate (1.031 g, 6.43 mmol, 1.01 equiv) in DMF (6.37 mL) under N_2 was stirred at 65 °C until the starting material was consumed as determined by TLC. The reaction mixture was cooled to rt, washed with 1 M HCl (50 mL), and extracted with EtOAc (×3). The organic layers were combined, washed with satd. aq NaCl, dried over Na_2SO_4, filtered, and concentrated under reduced pressure. Purification via silica gel column chromatography (0−30% EtOAc in hexanes) provided the title compound as a white solid (1.408 g, 4.69 mmol, 73%). ^{1}H NMR (600 MHz, $CDCl_3$): δ 7.30 (d, J = 7.0 Hz, 2H), 5.01 (s, 1H), 4.31−4.24 (m, 4H), 1.29 (t, J = 7.4 Hz, 6H) ppm; ^{13}C NMR (150 MHz, $CDCl_3$): δ 165.54, 161.02 (dd, J = 254.0, 7.8 Hz), 116.78 (t, J = 18.5 Hz), 116.20 (t, J = 3.4 Hz), 115.94−115.48 (m), 113.88 (t, J = 12.4 Hz), 62.60, 47.24, 13.87 ppm; IR (film) ν: 2856, 2178, 1695 cm^{-1}; LCMS: $[M + H]^+$, 298.

Diethyl 2-(4-Cyano-2-fluorophenyl)malonate (90). To a dry flask, under nitrogen, was added 3,4-difluorobenzonitrile (4.000 g, 28.81 mmol, 1 equiv), K_2CO_3 (7.954 g, 57.51 mmol, 2.00 equiv), diethyl malonate (4.660 g, 29.10 mmol, 1.01 equiv), and anhydrous DMF (24 mL) and it was heated at 65 °C until the starting material was consumed based on TLC. The reaction mixture was cooled to rt and added to a separatory funnel containing 50 mL of 1 N HCl. The mixture was extracted with EtOAc (×3), and the combined organic layers were washed with H_2O and satd. aq NaCl. The organic layer was dried over anh. Na_2SO_4, filtered, and concentrated under reduced pressure. Purification via silica gel column chromatography (0−30% EtOAc in hexanes) provided the title compound as a colorless oil (6.734 g, 24.10 mmol, 84%). ^{1}H NMR (600 MHz, $CDCl_3$): δ 7.64 (t, J = 7.6 Hz, 1H), 7.47 (dd, J = 8.0, 1.6 Hz, 1H), 7.38 (dd, J = 9.2, 1.6 Hz, 1H), 4.98 (s, 1H), 4.28−4.18 (m, 4H), 1.26 (t, J = 7.2 Hz, 6H) ppm; ^{13}C NMR (150 MHz, $CDCl_3$): δ 166.55, 160.04 (d, J = 252.0 Hz), 131.98 (d, J = 3.5 Hz), 128.26 (d, J = 4.0 Hz), 126.21 (d, J = 14.4 Hz), 119.23 (d, J = 26.0 Hz), 117.28 (d, J = 2.9 Hz), 113.71 (d, J = 9.8 Hz), 62.55, 50.44 (d, J = 2.9 Hz), 14.00 ppm; IR (film) ν: 2984, 2236, 1733, 1219 cm^{-1}; LCMS: $[M + H]^+$, 280.

Diethyl 2-(4-Chloro-2,6-difluorophenyl)malonate (91). General procedure A was followed using diethyl malonate (6.390 g, 39.57 mmol) and 2-bromo-5-chloro-1,3-difluorobenzene (3.000 g, 13.19 mmol). Purification via silica gel column chromatography (0−8% EtOAc in hexanes) provided the title compound as a colorless oil (1.424 g, 4.63 mmol, 35%). ^{1}H NMR (600 MHz, $CDCl_3$): δ 6.96−6.93 (m, 2H), 4.89 (s, 1H), 4.24 (q, J = 7.2 Hz, 4H), 1.28−1.24 (m, 6H) ppm; ^{13}C NMR (150 MHz, $CDCl_3$): δ 166.40, 161.05 (dd, J = 252.7, 8.8 Hz), 135.40 (t, J = 13.4 Hz), 113.18−112.42 (m), 109.85 (t, J = 18.8 Hz), 62.4, 47.07, 14.01 ppm; IR (film) ν: 2838, 1678, 1642, 1249 cm^{-1}; LCMS: $[M + H]^+$, 308.

Diethyl 2-(2,6-Difluoro-4-nitrophenyl)malonate (92). A mixture of 1,2,3-trifluoro-5-nitrobenzene (1.000 g, 5.65 mmol, 1 equiv), potassium carbonate (1.562 g, 11.29 mmol, 2.00 equiv), and diethyl malonate (0.914 g, 5.71 mmol, 1.01 equiv) in DMF (6.37 mL) under N_2 was stirred at 65 °C until the starting material was consumed as indicated by TLC. The reaction mixture was cooled to rt, washed with 1 N HCl (50 mL), and extracted with EtOAc (×3). The organic layers were combined, washed with satd. aq NaCl, dried over Na_2SO_4, filtered, and concentrated under reduced pressure. Purification via silica gel column chromatography (0−30% EtOAc in hexanes) provided the title compound as a white solid (1.536 g, 4.85 mmol, 86%). ^{1}H NMR (600 MHz, $CDCl_3$): δ 7.84 (d, J = 7.2 Hz, 2H), 5.00 (s, 1H), 4.27 (q, J = 7.1 Hz, 4H), 1.28 (t, J = 7.2 Hz, 6H) ppm; ^{13}C NMR (150 MHz, $CDCl_3$): δ 165.55, 160.93 (dd, J = 254.8, 7.7 Hz), 148.60 (t, J = 11.2 Hz), 118.05 (t, J = 18.7 Hz), 108.15−107.61 (m), 62.84, 47.49, 14.04 ppm.

5,7-Dichloro-6-phenyl-[1,2,4]triazolo[1,5-*a*]pyrimidine (93). General procedure B was followed using diethyl 2-phenylmalonate (0.780 g, 3.30 mmol) (**76**) and 3-amino-1,2,4-triazole (0.292 g, 3.47 mmol). Then, the intermediate sodium 6-phenyl-[1,2,4]triazolo[1,5-*a*]pyrimidine-5,7-bis(olate) (0.740 g, 2.71 mmol) and $POCl_3$ (7.410 g, 48.46 mmol) were used to obtain the title compound as a brown solid (0.527 g, 1.99 mmol, 73%). ^{1}H NMR (500 MHz, $CDCl_3$): δ 8.56 (s, 1H), 7.58−7.51 (m, 3H), 7.38−7.34 (m, 2H) ppm; ^{13}C NMR (126 MHz, $CDCl_3$): δ 156.93, 156.65, 153.35, 139.90, 131.72, 130.07, 129.95, 129.16, 124.01 ppm; IR (film) ν: 3437, 1637, 1458, 1383, 1267, 1205, 1180, 867, 802, 764, 740, 698, 652 cm^{-1}; HRMS (ES$^+$): calcd for $C_{11}H_7Cl_2N_4$ $[M + H]^+$, 265.0042; found, 265.0043.

5,7-Dichloro-6-(4-fluorophenyl)-[1,2,4]triazolo[1,5-*a*]pyrimidine (94). General procedure B was followed using diethyl 2-(4-fluorophenyl)malonate (0.700 g, 2.75 mmol) (**77**) and 3-amino-1,2,4-triazole (0.242 g, 2.89 mmol). Then, the intermediate sodium 6-(4-fluorophenyl)-[1,2,4]triazolo[1,5-*a*]pyrimidine-5,7-bis(olate) (0.760 g, 2.61 mmol) and $POCl_3$ (7.150 g, 46.45 mmol) were used to obtain the title compound as a brown solid (0.481 g, 1.70 mmol, 67%). ^{1}H NMR (500 MHz, $CDCl_3$): δ 8.53 (s, 1H), 7.36 (dd, J = 8.4, 5.2 Hz, 2H), 7.29−7.20 (m, 2H) ppm; ^{13}C NMR (126 MHz, $CDCl_3$): δ 163.47 (d, J = 250.9 Hz), 156.95, 156.53, 153.29, 140.05, 132.18 (d, J = 8.6 Hz), 127.59 (d, J = 3.7 Hz), 123.03, 116.43 (d, J = 21.9 Hz) ppm; IR (film) ν: 3421, 1600, 1529, 1504, 1460, 1330, 1267, 1229, 1203, 1183, 1160, 1089, 1024, 899, 837, 790 cm^{-1}; HRMS (ES$^+$): calcd for $C_{11}H_6Cl_2FN_4$ $[M + H]^+$, 282.9948; found, 282.9945.

5,7-Dichloro-6-(2-fluorophenyl)-[1,2,4]triazolo[1,5-*a*]pyrimidine (95). General procedure B was followed using diethyl 2-(2-fluorophenyl)malonate (0.700 g, 2.75 mmol) (**78**) and 3-amino-1,2,4-triazole (0.242 g, 2.89 mmol). Then, the intermediate sodium 6-(2-fluorophenyl)-[1,2,4]triazolo[1,5-*a*]pyrimidine-5,7-bis(olate) (0.760 g, 2.61 mmol) and $POCl_3$ (7.150 g, 46.45 mmol) were used to

https://dx.doi.org/10.1021/acs.jmedchem.0c01605
J. Med. Chem. 2021, 64, 1073−1102

obtain the title compound as a brown solid (0.572 g, 2.02 mmol, 77%). ^{1}H NMR (500 MHz, $CDCl_3$): δ 8.54 (t, J = 3.3 Hz, 1H), 7.59−7.51 (m, 1H), 7.38−7.29 (m, 2H), 7.28−7.20 (m, 1H) ppm; ^{13}C NMR (126 MHz, $CDCl_3$): δ 159.79 (d, J = 249.6 Hz), 156.94, 156.57, 153.53, 140.57, 132.48 (d, J = 8.2 Hz), 131.78 (d, J = 1.8 Hz), 124.85 (d, J = 3.7 Hz), 119.39 (d, J = 15.9 Hz), 118.45, 116.38 (d, J = 21.1 Hz) ppm; IR (film) ν: 3436, 1598, 1492, 1463, 1425, 1366, 1330, 1263, 1221, 1196, 1131, 1099, 1033, 900, 822, 792, 755, 652 cm^{-1}; HRMS (ES$^+$): calcd for $C_{11}H_5Cl_2FN_4Na$ [M + Na]$^+$, 304.9768; found, 304.9772.

5,7-Dichloro-6-(2,4-difluorophenyl)-[1,2,4]triazolo[1,5-*a*]-pyrimidine (96). General procedure B was followed using diethyl 2-(2,4-difluorophenyl)malonate (0.800 g, 2.94 mmol) (**79**) and 3-amino-1,2,4-triazole (0.260 g, 3.09 mmol). Then, the intermediate sodium 6-(2,4-difluorophenyl)-[1,2,4]triazolo[1,5-*a*]pyrimidine-5,7-bis(olate) (0.800 g, 2.60 mmol) and $POCl_3$ (7.080 g, 46.23 mmol) were used to obtain the title compound as a brown solid (0.455 g, 1.51 mmol, 58%). ^{1}H NMR (500 MHz, $CDCl_3$): δ 8.50 (s, 1H), 7.39−7.32 (m, 1H), 7.06 (td, J = 8.3, 2.5 Hz, 1H), 6.99 (td, J = 9.1, 2.5 Hz, 1H) ppm; ^{13}C NMR (126 MHz, $CDCl_3$): δ 164.23 (dd, J = 253.6, 11.8 Hz), 160.18 (dd, J = 252.2, 12.3 Hz), 156.94, 156.47, 153.47, 140.79, 132.91 (dd, J = 10.1, 3.4 Hz), 117.55, 115.54 (dd, J = 16.1, 4.1 Hz), 112.47 (dd, J = 21.9, 3.7 Hz), 104.96 (t, J = 25.4 Hz) ppm; IR (film) ν: 3451, 1600, 1503, 1464, 1424, 1368, 1335, 1267, 1196, 1143, 1128, 1092, 1022, 969, 890, 851, 796, 765, 735, 652, 631 cm^{-1}; HRMS (ES$^+$): calcd for $C_{11}H_5Cl_2F_2N_4$ [M + H]$^+$, 300.9854; found, 300.9850.

5,7-Dichloro-6-(2,6-difluorophenyl)-[1,2,4]triazolo[1,5-*a*]-pyrimidine (97). General procedure B was followed using diethyl 2-(2,6-difluorophenyl)malonate (0.800 g, 2.94 mmol) (**80**) and 3-amino-1,2,4-triazole (0.260 g, 3.09 mmol). Then, the intermediate sodium 6-(2,6-difluorophenyl)-[1,2,4]triazolo[1,5-*a*]pyrimidine-5,7-bis(olate) (0.600 g, 1.90 mmol) and $POCl_3$ (5.310 g, 34.70 mmol) were used to obtain the title compound as a brown solid (0.290 g, 0.96 mmol, 49%). ^{1}H NMR (500 MHz, $CDCl_3$): δ 8.59 (d, J = 1.4 Hz, 1H), 7.61−7.52 (m, 1H), 7.11 (t, J = 7.9 Hz, 2H) ppm; ^{13}C NMR (126 MHz, $CDCl_3$): δ 160.23 (dd, J = 252.0, 5.7 Hz), 157.17, 156.65, 153.87, 141.38, 133.06 (t, J = 10.2 Hz), 113.14, 112.16 (dd, J = 20.4, 4.2 Hz), 109.07 (t, J = 19.9 Hz) ppm; IR (film) ν: 3427, 1629, 1602, 1460, 1384, 1266, 1194, 1003, 899, 806, 765, 652 cm^{-1}; HRMS (ES$^+$): calcd for $C_{11}H_5Cl_2F_2N_4$ [M + H]$^+$, 300.9854; found, 300.9866.

5,7-Dichloro-6-(3,5-difluorophenyl)-[1,2,4]triazolo[1,5-*a*]-pyrimidine (98). General procedure B was followed using diethyl 2-(3,5-difluorophenyl)malonate (0.700 g, 2.57 mmol) (**81**) and 3-amino-1,2,4-triazole (0.227 g, 2.70 mmol). Then, the intermediate sodium 6-(3,5-difluorophenyl)-[1,2,4]triazolo[1,5-*a*]pyrimidine-5,7-bis(olate) (0.700 g, 2.27 mmol) and $POCl_3$ (6.200 g, 40.51 mmol) were used to obtain the title compound as a brown solid (0.422 g, 1.40 mmol, 62%). ^{1}H NMR (500 MHz, $CDCl_3$): δ 8.60 (s, 1H), 7.02 (tt, J = 8.8, 2.4 Hz, 1H), 6.97−6.89 (m, 2H) ppm; ^{13}C NMR (126 MHz, $CDCl_3$): δ 163.29 (dd, J = 251.5, 12.6 Hz), 157.31, 155.74, 153.47, 140.16, 134.33 (t, J = 10.3 Hz), 121.84, 113.71 (dd, J = 19.6, 6.9 Hz), 105.89 (t, J = 25.0 Hz) ppm; IR (film) ν: 3434, 1628, 1595, 1460, 1435, 1121, 987, 833 cm^{-1}; HRMS (ES$^+$): calcd for $C_{11}H_5Cl_2F_2N_4$ [M + H]$^+$, 300.9854; found, 300.9871.

5,7-Dichloro-6-(2,5-difluorophenyl)-[1,2,4]triazolo[1,5-*a*]-pyrimidine (99). General procedure B was followed using diethyl 2-(2,5-difluorophenyl)malonate (0.800 g, 2.94 mmol) (**82**) and 3-amino-1,2,4-triazole (0.259 g, 3.09 mmol). Then, the intermediate sodium 6-(2,5-difluorophenyl)-[1,2,4]triazolo[1,5-*a*]pyrimidine-5,7-bis(olate) (0.800 g, 2.60 mmol) and $POCl_3$ (7.080 g, 46.23 mmol) were used to obtain the title compound as a brown solid (0.443 g, 1.47 mmol, 57%). ^{1}H NMR (500 MHz, $CDCl_3$): δ 8.58 (s, 1H), 7.28−7.23 (m, 2H), 7.11−7.07 (m, 1H) ppm; ^{13}C NMR (126 MHz, $CDCl_3$): δ 158.60 (dd, J = 245.1, 2.5 Hz), 157.24, 156.21, 156.03 (dd, J = 245.9, 2.7 Hz), 153.68, 140.80, 120.50 (dd, J = 18.7, 8.8 Hz), 119.24 (dd, J = 23.9, 8.4 Hz), 118.42 (dd, J = 25.1, 2.2 Hz), 117.80 (dd, J = 24.2, 8.7 Hz), 117.43 ppm; IR (film) ν: 3421, 1642, 1492, 1458, 1432, 1383, 1253, 1203, 1092, 1025, 858, 822, 775, 699, 651 cm^{-1}; HRMS (ES$^+$): calcd for $C_{11}H_5Cl_2F_2N_4$ [M + H]$^+$, 300.9854; found, 300.9857.

5,7-Dichloro-6-(3,4-difluorophenyl)-[1,2,4]triazolo[1,5-*a*]-pyrimidine (100). General procedure B was followed using diethyl 2-(3,4-difluorophenyl)malonate (0.456 g, 1.67 mmol) (**83**) and 3-amino-1,2,4-triazole (0.147 g, 1.73 mmol). Then, the intermediate sodium 6-(3,4-difluorophenyl)-[1,2,4]triazolo[1,5-*a*]pyrimidine-5,7-bis(olate) (0.400 g, 1.30 mmol) and $POCl_3$ (2.982 g, 23.11 mmol) were used to obtain the title compound as a brown solid (0.183 g, 0.61 mmol, 40%). ^{1}H NMR (500 MHz, $CDCl_3$): δ 8.57 (s, 1H), 7.41−7.32 (m, 1H), 7.26−7.21 (m, 1H), 7.16−7.11 (m, 1H) ppm; ^{13}C NMR (126 MHz, $CDCl_3$): δ 157.20, 156.17, 153.39, 151.41 (dd, J = 252.7, 11.8 Hz), 150.60 (dd, J = 251.2, 12.8 Hz), 140.27, 128.21 (dd, J = 6.6, 4.6 Hz), 126.97 (dd, J = 6.7, 3.9 Hz), 122.03, 119.74 (d, J = 18.4 Hz), 118.49 (d, J = 17.9 Hz) ppm; IR (film) ν: 3377, 2918, 1606, 1460, 1383, 1269, 1180, 1120, 861, 793, 652 cm^{-1}; HRMS (ES$^+$): calcd for $C_{11}H_5Cl_2F_2N_4$ [M + H]$^+$, 300.9854; found, 300.9859.

5,7-Dichloro-6-(2,3,4-trifluorophenyl)-[1,2,4]triazolo[1,5-*a*]-pyrimidine (101). General procedure B was followed using diethyl 2-(2,3,4-trifluorophenyl)malonate (0.800 g, 2.75 mmol) (**84**) and 3-amino-1,2,4-triazole (0.242 g, 2.89 mmol). Then, the intermediate sodium 6-(2,3,4-trifluorophenyl)-[1,2,4]triazolo[1,5-*a*]pyrimidine-5,7-bis(olate) (0.740 g, 2.67 mmol) and $POCl_3$ (6.151 g, 40.33 mmol) were used to obtain the title compound as a brown solid (0.367 g, 1.15 mmol, 43%). ^{1}H NMR (500 MHz, $CDCl_3$): δ 8.59 (s, 1H), 7.24−7.16 (m, 1H), 7.16−7.09 (m, 1H) ppm; ^{13}C NMR (126 MHz, $CDCl_3$): δ 157.39, 156.24, 153.75, 152.71 (ddd, J = 254.7, 9.8, 3.0 Hz), 149.54 (ddd, J = 253.6, 10.9, 3.6 Hz), 141.10, 140.64 (dt, J = 254.7, 15.1 Hz), 125.78 (ddd, J = 8.0, 4.4, 1.7 Hz), 117.08 (dd, J = 12.9, 4.0 Hz), 116.70 (d, J = 2.3 Hz), 113.42 (dd, J = 18.0, 3.9 Hz) ppm; IR (film) ν: 3387, 1601, 1485, 1458, 1383, 1343, 1274, 12010, 1180, 1053, 1024, 963, 915, 859, 820, 790, 761, 689, 650 cm^{-1}; HRMS (ES$^+$): calcd for $C_{11}H_4Cl_2F_3N_4$ [M + H]$^+$, 318.9760; found, 319.9764.

5,7-Dichloro-6-(2,4,6-trifluorophenyl)-[1,2,4]triazolo[1,5-*a*]-pyrimidine (102). General procedure B was followed using diethyl 2-(2,4,6-trifluorophenyl)malonate (3.66 g, 12.58 mmol) (**85**) and 3-amino-1,2,4-triazole (1.07 g, 12.83 mmol). Then, the intermediate sodium 6-(2,3,4-trifluorophenyl)-[1,2,4]triazolo[1,5-*a*]pyrimidine-5,7-bis(olate) (2.000 g, 6.29 mmol) and $POCl_3$ (17.20 g, 112.0 mmol) were used to obtain the title compound as a brown solid (1.00 g, 3.14 mmol, 50%). ^{1}H NMR (500 MHz, $CDCl_3$): δ 8.62 (s, 1H), 6.91 (t, J = 6.0 Hz, 2H) ppm; ^{13}C NMR (126 MHz, $CDCl_3$): δ 164.60 (dt, J = 253.7, 16.6 Hz), 160.77 (dd, J = 252.9, 9.1 Hz), 160.67 (dd, J = 252.9, 9.1 Hz), 157.36, 156.69, 141.67, 112.36, 105.67 (dt, J = 19.6, 4.5 Hz), 101.63−101.26 (m) ppm.

5,7-Dichloro-6-(2,4,6-trifluorobenzyl)-[1,2,4]triazolo[1,5-*a*]-pyrimidine (103). General procedure B was followed using diethyl 2-(2,4,6-trifluorobenzyl)malonate (0.800 g, 2.63 mmol) (**86**) and 3-amino-1,2,4-triazole (0.232 g, 2.76 mmol). Then, the intermediate sodium 6-(2,4,6-trifluorobenzyl)-[1,2,4]triazolo[1,5-*a*]pyrimidine-5,7-bis(olate) (0.700 g, 2.06 mmol) and $POCl_3$ (5.610 g, 36.60 mmol) were used to obtain the title compound as a brown solid (0.355 g, 1.07 mmol, 52%). ^{1}H NMR (500 MHz, $CDCl_3$): δ 8.40 (s, 1H), 6.59 (t, J = 8.5 Hz, 2H), 4.27 (s, 2H) ppm; ^{13}C NMR (126 MHz, $CDCl_3$): δ 161.93 (dt, J = 250.5, 16.0 Hz), 161.44 (dd, J = 249.9, 10.6 Hz), 161.33 (dd, J = 249.8, 10.7 Hz), 156.68, 156.48, 152.67, 140.34, 118.92, 108.12 (td, J = 18.5, 4.8 Hz), 102.62−96.83 (m), 23.49 (t, J = 2.4 Hz) ppm; IR (film) ν: 3408, 1633, 1471, 1266, 1118, 1038 cm^{-1}; HRMS (ES$^+$): calcd for $C_{12}H_6Cl_2F_3N_4$ [M + H]$^+$, 332.9916; found, 332.9906.

5,7-Dichloro-6-(2,6-difluoro-4-methylphenyl)-[1,2,4]-triazolo[1,5-*a*]pyrimidine (104). General procedure B was followed using diethyl 2-(2,6-difluoro-4-methylphenyl)malonate (0.800 g, 2.79 mmol) (**87**) and 3-amino-1,2,4-triazole (0.247 g, 2.93 mmol). Then, the intermediate sodium 6-(2,6-difluoro-4-methylphenyl)-[1,2,4]triazolo[1,5-*a*]pyrimidine-5,7-bis(olate) (0.500 g, 1.55 mmol) and $POCl_3$ (4.240 g, 27.60 mmol) were used to obtain the title compound as a brown solid (0.334 g, 1.06 mmol, 68%). ^{1}H NMR (600 MHz, $CDCl_3$): δ 8.59 (s, 1H), 6.92 (d, J = 8.5 Hz, 2H),

https://dx.doi.org/10.1021/acs.jmedchem.0c01605
J. Med. Chem. 2021, 64, 1073−1102

2.46 (s, 3H) ppm; ^{13}C NMR (150 MHz, $CDCl_3$): δ 159.92 (dd, J = 251.1, 6.6 Hz), 157.07, 157.01, 153.85, 144.81 (d, J = 19.7 Hz), 141.44, 113.44, 112.74 (dd, J = 20.7, 3.5 Hz), 106.01 (d, J = 39.9 Hz), 21.88 (d, J = 1.9 Hz) ppm; IR (film) ν: 3071, 1606, 1571, 1356 cm^{-1}; LCMS: $[M + H]^+$, 317.

5,7-Dichloro-6-(2,6-difluoro-4-(trifluoromethyl)phenyl)-[1,2,4]triazolo[1,5-*a*]pyrimidine (105). General procedure B was followed using diethyl 2-(2,6-difluoro-4-(trifluoromethyl)phenyl)-malonate (0.600 g, 1.76 mmol) (**88**) and 3-amino-1,2,4-triazole (0.156 g, 1.85 mmol). Then, the intermediate sodium 6-(2,6-difluoro-4-(trifluoromethyl)phenyl)-[1,2,4]triazolo[1,5-*a*]pyrimidine-5,7-bis-(olate) (0.600 g, 1.60 mmol) and $POCl_3$ (4.350 g, 28.41 mmol) were used to obtain the title compound as a brown solid (0.392 g, 1.07 mmol, 66%). ^{1}H NMR (500 MHz, $CDCl_3$): δ 8.62 (s, 1H), 7.47 (d, J = 7.2 Hz, 2H) ppm; ^{13}C NMR (126 MHz, $CDCl_3$): δ 160.16 (dd, J = 254.8, 5.8 Hz), 157.22, 155.50, 153.81, 141.35, 135.19 (qt, J = 35.3, 34.6, 9.5 Hz), 122.14 (qt, J = 273.3, 3.2 Hz), 112.72 (t, J = 19.7 Hz), 111.49, 110.18−109.25 (m) ppm; IR (film) ν: 3435, 1633, 1603, 1466, 1437, 1364, 1266, 1250, 1179, 1137, 1038, 916, 868, 801, 766, 705, 653 cm^{-1}; HRMS (ES^-) calcd for $C_{12}H_3Cl_2F_4N_4$ $[M - F]^-$, 348.9676; found, 348.9662.

4-(5,7-Dichloro-[1,2,4]triazolo[1,5-*a*]pyrimidin-6-yl)-3,5-difluorobenzonitrile (106). General procedure B was followed using diethyl 2-(4-cyano-2,6-difluorophenyl)malonate (0.500 g, 1.68 mmol) (**89**) and 3-amino-1,2,4-triazole (0.148 g, 1.77 mmol). Then, the intermediate sodium 6-(4-cyano-2,6-difluorophenyl)-[1,2,4]triazolo-[1,5-*a*]pyrimidine-5,7-bis(olate) (0.400 g, 1.20 mmol) and $POCl_3$ (3.280 g, 21.41 mmol) were used to obtain the title compound as a brown solid (0.210 g, 1.20 mmol, 53%). ^{1}H NMR (600 MHz, $CDCl_3$): δ 8.65 (s, 1H), 7.47 (d, J = 6.2 Hz, 2H) ppm; ^{13}C NMR (150 MHz, $CDCl_3$): δ 161.21 (d, J = 6.4 Hz), 159.51 (d, J = 6.2 Hz), 157.66, 155.57, 116.85, 116.62−116.30 (m), 115.86 (t, J = 3.5 Hz), 114.64 (t, J = 19.6 Hz) ppm; IR (film) ν: 3087, 2195, 1571, 1338, 1195 cm^{-1}; LCMS: $[M + H]^+$, 327.

4-(5,7-Dichloro-[1,2,4]triazolo[1,5-*a*]pyrimidin-6-yl)-3-fluorobenzonitrile (107). General procedure B was followed using diethyl 2-(4-cyano-2,6-difluorophenyl)malonate (0.500 g, 1.68 mmol) (**90**) and 3-amino-1,2,4-triazole (0.148 g, 1.77 mmol). Then, the intermediate sodium 6-(4-cyano-2-fluorophenyl)-[1,2,4]triazolo[1,5-*a*]pyrimidine-5,7-bis(olate) (3.000 g, 9.52 mmol) and $POCl_3$ (26.000 g, 169.00 mmol) were used to obtain the title compound as a brown solid (1.970 g, 9.52 mmol, 67%). ^{1}H NMR (600 MHz, $CDCl_3$): δ 8.61 (s, 1H), 7.68 (dd, J = 7.9, 1.5 Hz, 1H), 7.61 (dd, J = 8.6, 1.5 Hz, 1H), 7.54 (t, J = 7.4 Hz, 1H) ppm; ^{13}C NMR (150 MHz, $CDCl_3$): δ 160.47, 158.79, 157.48, 155.52, 153.79, 140.73, 133.32, 128.86 (d, J = 4.6 Hz), 124.68 (d, J = 15.7 Hz), 120.42 (d, J = 24.9 Hz), 116.76 (d, J = 2.9 Hz), 116.69, 116.36 (d, J = 9.3 Hz) ppm.

5,7-Dichloro-6-(4-chloro-2,6-difluorophenyl)-[1,2,4]-triazolo[1,5-*a*]pyrimidine (108). General procedure B was followed using diethyl 2-(4-chloro-2,6-difluorophenyl)malonate (1.2 g, 3.91 mmol) (**91**) and 3-amino-1,2,4-triazole (0.350 g, 4.10 mmol). Then, the intermediate sodium 6-(4-chloro-2,6-difluorophenyl)-[1,2,4]triazolo[1,5-*a*]pyrimidine-5,7-bis(olate) (1.000 g, 2.92 mmol) and $POCl_3$ (7.970 g, 52.00 mmol) were used to obtain the title compound as a brown solid (0.710 g, 2.12 mmol, 73%). ^{1}H NMR (600 MHz, $CDCl_3$): δ 8.62 (s, 1H), 7.18 (d, J = 7.1 Hz, 2H) ppm; ^{13}C NMR (150 MHz, $CDCl_3$): δ 161.29−159.09 (m), 157.36, 156.45, 153.95, 141.55, 138.63 (t, J = 13.0 Hz), 113.78−113.35 (m), 112.29, 108.08 (t, J = 20.0 Hz) ppm; IR (film) ν: 3106, 1642, 1427, 1391, 1071 cm^{-1}; LCMS: $[M + H]^+$, 336.

5,7-Dichloro-6-(2,6-difluoro-4-nitrophenyl)-[1,2,4]triazolo-[1,5-*a*]pyrimidine (109). General procedure B was followed using diethyl 2-(2,6-difluoro-4-nitrophenyl)malonate (0.500 g, 1.58 mmol) (**92**) and 3-amino-1,2,4-triazole (0.139 g, 1.65 mmol). Then, the intermediate sodium 6-(2,6-difluoro-4-nitrophenyl)-[1,2,4]triazolo-[1,5-*a*]pyrimidine-5,7-bis(olate) (0.150 g, 0.43 mmol) and $POCl_3$ (1.160 g, 7.56 mmol) were used to obtain the title compound as a brown solid (0.100 g, 0.29 mmol, 68%). ^{1}H NMR (600 MHz, $CDCl_3$): δ 8.64 (s, 1H), 8.04 (d, J = 6.8 Hz, 2H) ppm; ^{13}C NMR (150 MHz, $CDCl_3$): δ 160.22 (dd), 157.70, 156.90, 155.39, 154.08, 150.51 (d, J = 10.5 Hz), 141.48, 116.12−115.19 (m), 111.63, 108.69−108.36 (m) ppm; IR (film) ν: 2916, 2848, 1698, 1601, 1532 cm^{-1}; LCMS: $[M + H]^+$, 347.

Methyl 2-(5-Chloro-6-(2,4,6-trifluorophenyl)-[1,2,4]triazolo-[1,5-*a*]pyrimidin-7-yl)-4,4,4-trifluoro-3-methylbutanoate (110). To a solution of HMDS (0.101 g, 0.63 mmol, 1 equiv) in THF (0.632 mL) at −78 °C was added *n*-butyllithium (0.369 mL, 0.63 mmol, 1 equiv) and the mixture was stirred at 0 °C for 1 h. Then, methyl 4,4,4-trifluoro-3-methylbutanoate (0.117 g, 0.69 mmol, 1.1 equiv) was added dropwise at −78 °C and the reaction mixture was stirred for 1 h. Then, a solution of 5,7-dichloro-6-(2,4,6-trifluorophenyl)-[1,2,4]triazolo[1,5-*a*]pyrimidine (0.200 g, 0.63 mmol, 1 equiv) (**102**) in THF (0.500 mL) was added at −78 °C and the resulting mixture was stirred for 2.5 h prior to quenching of the reaction with 1 M HCl. The aqueous layer was then extracted using EtOAc (×2) and washed with sat. aq NaCl, dried, and concentrated under reduced pressure. Purification via silica gel chromatography using hexanes/EtOAc (5−20%) provided the product (0.200 g, 0.44 mmol, 70%) as a white solid. ^{1}H NMR (600 MHz, $CDCl_3$): mixture of diastereomers δ 8.53 (d, J = 6.6 Hz, 1H), 6.94−6.86 (m, 2H), 4.04 (d, J = 7.4 Hz, 1H), 3.92−3.85 (m, 1H), 3.62 (d, J = 10.4 Hz, 3H), 1.38 (d, J = 6.6 Hz, 1H), 0.80 (d, J = 7.4 Hz, 2H) ppm; HRMS (ES^+): calcd for $C_{17}H_{12}ClF_6N_4O_2$ $[M + H]^+$, 453.0547; found, 453.0542.

7,9-Difluoro-10-(3,3,3-trifluoro-2-methylpropyl)benzofuro-[2,3-d][1,2,4]triazolo[1,5-*a*]pyrimidine (111). Methyl 2-(5-chloro-6-(2,4,6-trifluorophenyl)-[1,2,4]triazolo[1,5-*a*]pyrimidin-7-yl)-4,4,4-trifluoro-3-methylbutanoate (0.020 g, 0.04 mmol, 1 equiv) (**110**), LiCl (0.002 g, 0.04 mmol, 1 equiv), and DMSO (0.100 mL) were stirred at 130 °C for 3 h (microwave irradiation). The reaction mixture was then diluted in water and extracted with EtOAc (×3) and the combined organic layers were washed with brine (×2), dried over $MgSO_4$, filtered, and concentrated. Purification by reverse-phase HPLC provided the title compound as a white solid (0.012 g, 0.03 mmol, 76%). X-ray quality crystals were obtained by slow evaporation from a CH_2Cl_2/pentane solution: mp (CH_2Cl_2/pentane) 103.4−107.4. ^{1}H NMR (600 MHz, $CDCl_3$): δ 8.55 (s, 1H), 8.01 (s, 1H), 7.01 (ddd, J = 11.0, 9.3, 2.2 Hz, 1H), 6.86−6.79 (m, 3H), 4.11−4.05 (m, 2H), 3.88−3.78 (m, 2H), 3.30 (p, J = 7.3 Hz, 1H), 3.20 (dd, J = 13.9, 5.8 Hz, 2H), 3.05 (dt, J = 15.1, 7.6 Hz, 2H), 2.79 (dd, J = 14.0, 8.7 Hz, 2H), 1.20 (d, J = 7.0 Hz, 3H), 1.02 (d, J = 7.0 Hz, 3H) ppm; ^{13}C NMR (150 MHz, $CDCl_3$): δ 165.15−164.48 (m), 163.01 (d, J = 15.1 Hz), 162.26−160.00 (m), 158.41, 156.38, 152.47, 150.91, 145.88, 143.80, 127.47 (dd, J = 279.5, 28.1 Hz), 108.69, 106.96, 106.21−104.64 (m), 102.08−100.00 (m), 97.85 (dd, J = 27.4, 4.6 Hz), 36.01 (q, J = 28.3, 27.6 Hz), 30.84, 29.86 ppm; HRMS (ES^+): calcd for $C_{15}H_9F_5N_4O$ $[M + H]^+$, 357.0769; found, 357.0768.

***tert*-Butyl-2-(5-chloro-6-(2,4,6-trifluorophenyl)-[1,2,4]-triazolo[1,5-*a*]pyrimidin-7-yl)-4,4,4-trifluoro-3-methylbutanoate (112).** To a solution of HMDS (0.054 g, 0.33 mmol, 1.6 equiv) in THF (3 mL) at −78 °C was added *n*-butyllithium (0.180 mL, 0.33 mmol, 1.6 equiv) and the mixture was stirred at 0 °C for 30 min. Then, *tert*-butyl 4,4,4-trifluoro-3-methylbutanoate (0.066 g, 0.31 mmol, 1.5 equiv) was added dropwise at −78 °C and the mixture was stirred at this temperature for 1 h. Finally, a solution of 5,7-dichloro-6-(2,4,6-trifluorophenyl)-[1,2,4]triazolo[1,5-*a*]pyrimidine (0.066 g, 0.21 mmol, 1 equiv) (**102**) in THF (0.500 mL) was added at −78 °C. After stirring for 2.5 h at this temperature, the reaction was quenched with a 1 M HCl solution. The aqueous layer was then extracted twice with EtOAc and the combined organic layers were washed with brine, dried, and concentrated under reduced pressure. Purification via silica gel chromatography using a hexanes/EtOAc gradient (95/05 to 80/20) provided *tert*-butyl 2-(5-chloro-6-(2,4,6-trifluorophenyl)-[1,2,4]triazolo[1,5-*a*]pyrimidin-7-yl)-4,4,4-trifluoro-3-methylbutanoate (0.026 g, 0.05 mmol, 25%) as a white solid. ^{1}H NMR (600 MHz, $CDCl_3$): mixture of diastereomers δ 8.56 (s, 0.6H), 8.55 (s, 0.4H), 6.91−6.87 (m, 2H), 4.14−4.04 (m, 0.4H), 3.95−3.83 (m, 1.2H), 3.72 (d, 0.4H), 1.38 (d, J = 6.7 Hz, 1.3H), 1.27 (s, 3.5H), 1.25 (s, 6.8H), 0.80 (d, J = 7.0 Hz, 2H) ppm; IR (film) ν: 2922, 2852, 1598, 1736, 1493, 1460, 1441, 1371, 1271, 1252, 1201, 1182, 1173,

https://dx.doi.org/10.1021/acs.jmedchem.0c01605
J. Med. Chem. 2021, 64, 1073−1102

1142, 1040 cm^{-1}; HRMS (ES^+): calcd for $C_{20}H_{18}ClF_6N_4O_2$ $[M + H]^+$, 495.1017; found, 495.1010.

Computational Studies. The X-ray crystal structure of the tubulin in complex with a triazolopyrimidine was downloaded from the Protein Data Bank and completed with MAESTRO (Schrödinger Release 2019-3),[32] waters, and other co-crystallized molecules were removed, except for the ligand and GDP. Predicting protonation states of protein residues were calculated considering a temperature of 300 K and a pH of 7, while the molecules were prepared considering the ionization states at pH 7 ± 2. A 12 Å docking grid (inner-box 10 Å and outer-box 20 Å) was prepared using as centroid the cocrystallized ligand. The docking studies were performed using Glide SP precision keeping the default parameters and setting, and it was combined with "molecular mechanics generalized Born surface area" (MMGBSA), implemented in the Prime module from Maestro, to re-score the three output docking poses of each compound. Only the best MMGBSA score and pose for each compound were plotted in the graph and correlated with the normalized activity, expressed as the log of the average of the activity at 1 and 10 μM in the AcTub assay, relative to the positive control (**5**).

The 3D-QSAR field-based and activity atlas models were constructed using Forge software (Cresset Inc., Cambridgeshire, UK).[33] First, the molecular structures of each compound were subjected to a field-based alignment to the cocrystallized compound, which was used as the reference structure. This method is based on the 3D-shape and electrostatic potential similarity calculated by the alignment and superposition between the reference compound and the compounds in the database according to their electrostatic distribution and volume occupied. Field point-based descriptors were used for building the 3D-QSAR model after the alignment of 52 Class I compounds with the known activity. The activity was computed using the log of the average of the activity at 1 and 10 μM in the AcTub assay and defined as the dependent variable. The derived QSAR model was assessed by the LOO technique to optimize the activity-prediction model. Activity atlas was used to acquire qualitative information of the field and steric contributions significant for the activity.

Molecular Operating Environment (MOE) 2019.10 was used to visualize the structures and acquire the images,[34] while GraphPad software[35] and DataWarrior[36] were used for the statistical analysis.

QBI293 Cell and Neuronal Acetyl-Tubulin and α-Tub Determinations. Compound-induced changes in acetylated-tubulin and α-Tub in QBI293 cells or primary mouse neurons were as previously described.[5,11] Briefly, QBI293 cells were maintained in Dulbecco's modified Eagle's medium containing 10% fetal bovine serum, 2 mM L-glutamine (Mediatech), 50 units/mL penicillin, and 50 μg/mL streptomycin. For compound testing, cells were dissociated with trypsin/EDTA and plated at a density of 6×10^5 cells/well in six-well plates. After overnight incubation, the medium was aspirated and fresh medium containing a vehicle or a test compound was added. After 4 h of incubation, whole-cell extracts were prepared from the QBI293 cells as described.[5,11] The supernatant fraction from each sample was collected and analyzed for protein content by BCA assay.[11] The acetyl-tubulin and α-Tub enzyme-linked immunosorbent assays (ELISA) were performed on the supernatant fraction as previously described.[11] The amount of acetyl- and α-Tub protein in each sample was extrapolated using standard curves generated from serial dilutions with acetyl- or α-Tub preparations of known concentrations. Acetyl-tubulin levels were determined in a similar fashion in mouse cortical neuron cultures plated at 6×10^5 cells/well in six-well plates, essentially as previously described for rat cortical neurons.[11] After 10 days of growth, the neurons were treated for 8 h with 15 nM OA in the presence of the test compound (1 or 10 μM) or vehicle (0.25% DMSO), and homogenates were prepared for determination of acetyl-tubulin levels as previously described.[11]

Acetyl-Tubulin Staining of Rat Cortical Neuron Cultures Treated with Test Compounds in the Absence or Presence of OA. Rat cortical neurons were grown in 24-well plates on coverslips for 10 days as previously described.[11] The cultures were then treated for 8 h with or without 15 nM OA in the presence or absence of test compound (1 μM), with methods as described.[11] Finally, the cultures were prepared for acetyl-tubulin staining as previously discussed.[11]

Determination of Plasma and Brain Drug Concentrations. All animal protocols were approved by the University of Pennsylvania Institutional Animal Care and Use Committee (IACUC). Test compounds were administered to groups of three 2−3-month-old CD-1 mice (Charles River). For standard single time-point brain and plasma determinations, the mice were injected i.p. with a single dose of 5 mg/kg compound dissolved in DMSO. In some instances, the mice were cassette-dosed via i.p. administration with 2−3 compounds concurrently, each at 2.5 mg/kg. One hour following compound administration, the mice were euthanized following an IACUC-approved protocol. For multiple time-point studies, groups of 3 CD-1 mice injected i.p. with compound at 5 mg/kg were sacrificed at varying times after compound administration. Whole-brain hemispheres were homogenized in 10 mM ammonium acetate, pH 5.7 (50%, w/v), using a hand-held sonic homogenizer. Plasma was obtained from blood collected in 0.5 M EDTA solution and centrifuged for 10 min at 4500*g* at 4 °C. Compound levels with plasma and brain homogenates were determined essentially as previously described[10,11,37] either in-house or at a contract laboratory (Inotiv, Inc.).

■ ASSOCIATED CONTENT

Supporting Information

The Supporting Information is available free of charge at https://pubs.acs.org/doi/10.1021/acs.jmedchem.0c01605.

NMR spectra of test compounds; X-ray crystal structures of compounds **68** (CCDC 1995770) and **111** (CCDC 2003391); the authors will release the atomic coordinates and experimental data upon article publication (PDF)

SMILES string structures and the full data (CSV)

Chemical file format of compound **3** (PDB)

Chemical file format of compound **30** (PDB)

Chemical file format of compound **54** (PDB)

Chemical file format of compound **72** (PDB)

■ AUTHOR INFORMATION

Corresponding Authors

Kurt R. Brunden − *Center for Neurodegenerative Disease Research, Perelman School of Medicine, University of Pennsylvania, Philadelphia, Pennsylvania 19104, United States*; Email: kbrunden@upenn.edu

Carlo Ballatore − *Skaggs School of Pharmacy and Pharmaceutical Sciences, University of California, San Diego, La Jolla, California 92093, United States*; orcid.org/0000-0002-2718-3850; Email: cballatore@health.ucsd.edu

Authors

Killian Oukoloff − *Skaggs School of Pharmacy and Pharmaceutical Sciences, University of California, San Diego, La Jolla, California 92093, United States*

Goodwell Nzou − *Center for Neurodegenerative Disease Research, Perelman School of Medicine, University of Pennsylvania, Philadelphia, Pennsylvania 19104, United States*

Carmine Varricchio − *Cardiff School of Pharmacy and Pharmaceutical Sciences, Cardiff University, Cardiff CF103NB, U.K.*; orcid.org/0000-0002-1673-4768

Bobby Lucero − *Department of Chemistry & Biochemistry, University of California San Diego, La Jolla, California 92093, United States*

Thibault Alle − *Skaggs School of Pharmacy and Pharmaceutical Sciences, University of California, San Diego,*

https://dx.doi.org/10.1021/acs.jmedchem.0c01605
J. Med. Chem. 2021, 64, 1073−1102

La Jolla, California 92093, United States; orcid.org/0000-0001-8459-6443

Jane Kovalevich − *Center for Neurodegenerative Disease Research, Perelman School of Medicine, University of Pennsylvania, Philadelphia, Pennsylvania 19104, United States*

Ludovica Monti − *Skaggs School of Pharmacy and Pharmaceutical Sciences, University of California, San Diego, La Jolla, California 92093, United States*

Anne-Sophie Cornec − *Department of Chemistry, School of Arts and Sciences, University of Pennsylvania, Philadelphia, Pennsylvania 19104-6323, United States*

Yuemang Yao − *Center for Neurodegenerative Disease Research, Perelman School of Medicine, University of Pennsylvania, Philadelphia, Pennsylvania 19104, United States*

Michael J. James − *Center for Neurodegenerative Disease Research, Perelman School of Medicine, University of Pennsylvania, Philadelphia, Pennsylvania 19104, United States*

John Q. Trojanowski − *Center for Neurodegenerative Disease Research, Perelman School of Medicine, University of Pennsylvania, Philadelphia, Pennsylvania 19104, United States*

Virginia M.-Y. Lee − *Center for Neurodegenerative Disease Research, Perelman School of Medicine, University of Pennsylvania, Philadelphia, Pennsylvania 19104, United States*

Amos B. Smith, III − *Department of Chemistry, School of Arts and Sciences, University of Pennsylvania, Philadelphia, Pennsylvania 19104-6323, United States;* orcid.org/0000-0002-1712-8567

Andrea Brancale − *Cardiff School of Pharmacy and Pharmaceutical Sciences, Cardiff University, Cardiff CF103NB, U.K.;* orcid.org/0000-0002-9728-3419

Complete contact information is available at: https://pubs.acs.org/10.1021/acs.jmedchem.0c01605

Notes

The authors declare no competing financial interest.

■ ACKNOWLEDGMENTS

Financial support for this work has been provided by the NIH/NIA (AG061173, AG044332).

■ ABBREVIATIONS

AcTub, acetylated α-tubulin; *m*-CPBA, *meta*-chloroperbenzoic acid; MMGBSA,, molecular mechanics generalized Born surface-area; MT, microtubule; NFTs, neurofibrillary tangles; NTs, neuropil threads; Tg, transgenic

■ REFERENCES

(1) Lee, V. M.-Y.; Goedert, M.; Trojanowski, J. Q. Neurodegenerative tauopathies. *Annu. Rev. Neurosci.* **2001**, *24*, 1121−1159.

(2) Ballatore, C.; Lee, V. M.-Y.; Trojanowski, J. Q. Tau-mediated neurodegeneration in Alzheimer's disease and related disorders. *Nat. Rev. Neurosci.* **2007**, *8*, 663−672.

(3) Sadleir, K. R.; Kandalepas, P. C.; Buggia-Prévot, V.; Nicholson, D. A.; Thinakaran, G.; Vassar, R. Presynaptic dystrophic neurites surrounding amyloid plaques are sites of microtubule disruption, BACE1 elevation, and increased Abeta generation in Alzheimer's disease. *Acta Neuropathol.* **2016**, *132*, 235−256.

(4) Lee, V. M. Y.; Daughenbaugh, R.; Trojanowski, J. Q. Microtubule stabilizing drugs for the treatment of Alzheimers-disease. *Neurobiol. Aging* **1994**, *15*, 87−89.

(5) Brunden, K. R.; Zhang, B.; Carroll, J.; Yao, Y.; Potuzak, J. S.; Hogan, A.-M. L.; Iba, M.; James, M. J.; Xie, S. X.; Ballatore, C.; Smith, A. B., III; Lee, V. M. Y.; Trojanowski, J. Q. Epothilone D improves microtubule density, axonal integrity, and cognition in a transgenic mouse model of tauopathy. *J. Neurosci.* **2010**, *30*, 13861−13866.

(6) Makani, V.; Zhang, B.; Han, H.; Yao, Y.; Lassalas, P.; Lou, K.; Paterson, I.; Lee, V. M. Y.; Trojanowski, J. Q.; Ballatore, C.; Smith, A. B., III; Brunden, K. R. Evaluation of the brain-penetrant microtubule-stabilizing agent, dictyostatin, in the PS19 tau transgenic mouse model of tauopathy. *Acta Neuropathol. Commun.* **2016**, *4*, 106.

(7) Zhang, B.; Carroll, J.; Trojanowski, J. Q.; Yao, Y.; Iba, M.; Potuzak, J. S.; Hogan, A.-M. L.; Xie, S. X.; Ballatore, C.; Smith, A. B., III; Lee, V. M. Y.; Brunden, K. R. The microtubule-stabilizing agent, epothilone D, reduces axonal dysfunction, neurotoxicity, cognitive deficits, and Alzheimer-like pathology in an interventional study with aged tau transgenic mice. *J. Neurosci.* **2012**, *32*, 3601−3611.

(8) Barten, D. M.; Fanara, P.; Andorfer, C.; Hoque, N.; Wong, P. Y. A.; Husted, K. H.; Cadelina, G. W.; DeCarr, L. B.; Yang, L.; Liu, V.; Fessler, C.; Protassio, J.; Riff, T.; Turner, H.; Janus, C. G.; Sankaranarayanan, S.; Polson, C.; Meredith, J. E.; Gray, G.; Hanna, A.; Olson, R. E.; Kim, S.-H.; Vite, G. D.; Lee, F. Y.; Albright, C. F. Hyperdynamic microtubules, cognitive deficits, and pathology are improved in tau transgenic mice with low doses of the microtubule-stabilizing agent BMS-241027. *J. Neurosci.* **2012**, *32*, 7137−7145.

(9) Ballatore, C.; Brunden, K. R.; Trojanowski, J. Q.; Lee, V. M.-Y.; Smith, A. B., III. Non-naturally occurring small molecule microtubule-stabilizing agents: a potential tactic for CNS-directed therapies. *ACS Chem. Neurosci.* **2017**, *8*, 5−7.

(10) Lou, K.; Yao, Y.; Hoye, A. T.; James, M. J.; Cornec, A.-S.; Hyde, E.; Gay, B.; Lee, V. M.-Y.; Trojanowski, J. Q.; Smith, A. B., III; Brunden, K. R.; Ballatore, C. Brain-penetrant, orally bioavailable microtubule-stabilizing small molecules are potential candidate therapeutics for Alzheimer's disease and related tauopathies. *J. Med. Chem.* **2014**, *57*, 6116−6127.

(11) Kovalevich, J.; Cornec, A.-S.; Yao, Y.; James, M.; Crowe, A.; Lee, V. M. Y.; Trojanowski, J. Q.; Smith, A. B., III; Ballatore, C.; Brunden, K. R. Characterization of brain-penetrant pyrimidine-containing molecules with differential microtubule-stabilizing activities developed as potential therapeutic agents for Alzheimer's disease and related tauopathies. *J. Pharmacol. Exp. Ther.* **2016**, *357*, 432−450.

(12) Zhang, B.; Yao, Y.; Cornec, A.-S.; Oukoloff, K.; James, M. J.; Koivula, P.; Trojanowski, J. Q.; Smith, A. B., III; Lee, V. M.-Y.; Ballatore, C.; Brunden, K. R. A brain-penetrant triazolopyrimidine enhances microtubule-stability, reduces axonal dysfunction and decreases tau pathology in a mouse tauopathy model. *Mol. Neurodegener.* **2018**, *13*, 59.

(13) Sáez-Calvo, G.; Sharma, A.; Balaguer, F. d. A.; Barasoain, I.; Rodríguez-Salarichs, J.; Olieric, N.; Muñoz-Hernández, H.; Berbís, M. Á.; Wendeborn, S.; Peñalva, M. A.; Matesanz, R.; Canales, Á.; Prota, A. E.; Jímenez-Barbero, J.; Andreu, J. M.; Lamberth, C.; Steinmetz, M. O.; Díaz, J. F. Triazolopyrimidines are microtubule-stabilizing agents that bind the vinca inhibitor site of tubulin. *Cell Chem. Biol.* **2017**, *24*, 737−750.

(14) Yao, Y.; Nzou, G.; Alle, T.; Tsering, W.; Maimaiti, S.; Trojanowski, J. Q.; Lee, V. M. Y.; Ballatore, C.; Brunden, K. R. Correction of microtubule defects within Aβ plaque-associated dystrophic axons results in lowered Aβ release and plaque deposition. *Alzheimer's Dementia* **2020**, *16*, 1345−1357.

(15) Zhang, N.; Ayral-Kaloustian, S.; Nguyen, T.; Afragola, J.; Hernandez, R.; Lucas, J.; Gibbons, J.; Beyer, C. Synthesis and SAR of [1,2,4]triazolo[1,5-a]pyrimidines, a class of anticancer agents with a unique mechanism of tubulin inhibition. *J. Med. Chem.* **2007**, *50*, 319−327.

(16) Zhang, N.; Ayral-Kaloustian, S.; Nguyen, T.; Hernandez, R.; Lucas, J.; Discafani, C.; Beyer, C. Synthesis and SAR of 6-chloro-4-

fluoroalkylamino-2-heteroaryl-5-(substituted)phenylpyrimidines as anti-cancer agents. *Bioorg. Med. Chem.* **2009**, *17*, 111−118.
(17) Ayral-Kaloustian, S.; Zhang, N.; Beyer, C. Cevipabulin (TTI-237): preclinical and clinical results for a novel antimicrotubule agent. *Methods Find. Exp. Clin. Pharmacol.* **2009**, *31*, 443−447.
(18) Wang-Gillam, A.; Arnold, S. M.; Bukowski, R. M.; Rothenberg, M. L.; Cooper, W.; Wang, K. K.; Gauthier, E.; Lockhart, A. C. A phase I dose escalation study of TTI-237 in patients with advanced malignant solid tumors. *Invest. New Drugs* **2012**, *30*, 266−272.
(19) Fukushima, N.; Furuta, D.; Hidaka, Y.; Moriyama, R.; Tsujiuchi, T. Post-translational modifications of tubulin in the nervous system. *J. Neurochem.* **2009**, *109*, 683−693.
(20) Cornec, A.-S.; James, M. J.; Kovalevich, J.; Trojanowski, J. Q.; Lee, V. M.-Y.; Smith, A. B., III; Ballatore, C.; Brunden, K. R. Pharmacokinetic, pharmacodynamic and metabolic characterization of a brain retentive microtubule (MT)-stabilizing triazolopyrimidine. *Bioorg. Med. Chem. Lett.* **2015**, *25*, 4980−4982.
(21) Gomez, L.; Massari, M. E.; Vickers, T.; Freestone, G.; Vernier, W.; Ly, K.; Xu, R.; McCarrick, M.; Marrone, T.; Metz, M.; Yan, Y. G.; Yoder, Z. W.; Lemus, R.; Broadbent, N. J.; Barido, R.; Warren, N.; Schmelzer, K.; Neul, D.; Lee, D.; Andersen, C. B.; Sebring, K.; Aertgeerts, K.; Zhou, X.; Tabatabaei, A.; Peters, M.; Breitenbucher, J. G. Design and synthesis of novel and selective phosphodiesterase 2 (PDE2a) inhibitors for the treatment of memory disorders. *J. Med. Chem.* **2017**, *60*, 2037−2051.
(22) Krapcho, P. A.; Ciganek, E. The Krapcho Dealkoxycarbonylation Reaction of Esters with α-Electron-Withdrawing Substituents. *Organic Reactions*; American Cancer Society, 2013; pp 1−536.
(23) Oukoloff, K.; Kovalevich, J.; Cornec, A.-S.; Yao, Y.; Owyang, Z. A.; James, M.; Trojanowski, J. Q.; Lee, V. M.-Y.; Smith, A. B., III; Brunden, K. R.; Ballatore, C. Design, synthesis and evaluation of photoactivatable derivatives of microtubule (MT)-active [1,2,4]-triazolo[1,5-a]pyrimidines. *Bioorg. Med. Chem. Lett.* **2018**, *28*, 2180−2183.
(24) Wang, E.; Sun, H.; Wang, J.; Wang, Z.; Liu, H.; Zhang, J. Z. H.; Hou, T. End-point binding free energy calculation with MM/PBSA and MM/GBSA: strategies and applications in drug design. *Chem. Rev.* **2019**, *119*, 9478−9508.
(25) Tosco, P.; Mackey, M. Lessons and Successes in the Use of Molecular Fields. In *Comprehensive Medicinal Chemistry III*; Chackalamannil, S., Rotella, D., Ward, S. E., Eds.; Elsevier, 2017; Vol. 3−8, p 253−296.
(26) Ballatore, C.; Brunden, K. R.; Huryn, D. M.; Trojanowski, J. Q.; Lee, V. M.-Y.; Smith, A. B., III Microtubule Stabilizing Agents as Potential Treatment for Alzheimer's Disease and Related Neurodegenerative Tauopathies. *J. Med. Chem.* **2012**, *55*, 8979−8996.
(27) Beyer, C. F.; Zhang, N.; Hernandez, R.; Vitale, D.; Lucas, J.; Nguyen, T.; Discafani, C.; Ayral-Kaloustian, S.; Gibbons, J. J. TTI-237: a novel microtubule-active compound with in vivo antitumor activity. *Cancer Res.* **2008**, *68*, 2292−2300.
(28) Hansch, C.; Leo, A.; Taft, R. W. A survey of Hammett substituent constants and resonance and field parameters. *Chem. Rev.* **1991**, *91*, 165−195.
(29) Activity Atlas, Forge, Version 10.6.0; Cresset: Litlington, Cambridgeshire, https://www.cresset-group.com/software/forge/ (accessed November 17, 2020).
(30) Stumpfe, D.; Bajorath, J. Exploring activity cliffs in medicinal chemistry. *J. Med. Chem.* **2012**, *55*, 2932−2942.
(31) Fleming, F. F.; Yao, L.; Ravikumar, P. C.; Funk, L.; Shook, B. C. Nitrile-containing pharmaceuticals: efficacious roles of the nitrile pharmacophore. *J. Med. Chem.* **2010**, *53*, 7902−7917.
(32) Schrödinger, LLC, Schrödinger, LLC: New York, NY, 2019. https://www.schrodinger.com (accessed Nov 17, 2020).
(33) 3D QSAR, Forge, Version 10.6.0; Cresset: Litlington, Cambridgeshire. https://www.cresset-group.com/software/forge/ (accessed Nov 17, 2020).
(34) Molecular Operating Environment (MOE), Montreal, QC, Canada, H3A 2R7, 2019. http://www.chemcomp.com (acessed Nov 17, 2020).
(35) GraphPad Prism Version 8.00 for Windows; GraphPad Software: La Jolla California USA. https://www.graphpad.com (acessed Nov 17, 2020).
(36) Sander, T.; Freyss, J.; Von Korff, M.; Rufener, C. DataWarrior: an open-source program for chemistry aware data visualization and analysis. *J. Chem. Inf. Model.* **2015**, *55*, 460−473.
(37) Brunden, K. R.; Yao, Y.; Potuzak, J. S.; Ferrer, N. I.; Ballatore, C.; James, M. J.; Hogan, A.-M. L.; Trojanowski, J. Q.; Smith, A. B., III; Lee, V. M.-Y. The characterization of microtubule-stabilizing drugs as possible therapeutic agents for Alzheimer's disease and related tauopathies. *Pharmacol. Res.* **2011**, *63*, 341−351.

https://dx.doi.org/10.1021/acs.jmedchem.0c01605
J. Med. Chem. 2021, 64, 1073−1102